

**GEOPHYSICAL INVESTIGATION FOR GROUNDWATER IN
THE GUSHIEGU-KARAGA AND ZABZUGU-TATALE
DISTRICTS OF THE NORTHERN REGION OF GHANA USING
THE ELECTROMAGNETIC METHOD**

By

Blessing Kwasi Tsikudo B.Sc. Physics (Hons.)

**A Thesis Submitted to the Department of Physics,
Kwame Nkrumah University of Science and Technology
in partial fulfillment of the requirements for the degree
of**

MASTER OF SCIENCE

College of Science

April, 2009

DECLARATION

I hereby declare that this submission is my own work towards the MSc and that, to the best of my knowledge, it contains no material previously published by another person nor material which has been accepted for the award of any other degree of the University, except where due acknowledgment has been made in text.

.....
Student Name and ID Signature Date

Certified by:

.....
Supervisor(s) Name Signature Date

Certified by:

.....
Head of Dept.Name Signature Date

ABSTRACT

Due to the lack of access to potable drinking water in the Gushiegu-Karaga and Zabzugu-Tatale Districts of the Northern Region of Ghana, Geophysical investigation has been carried out with the aim of mapping out potential groundwater sites for boreholes to be drilled for these communities. Electromagnetic profiling using the Geonics EM-34 conductivity meter was carried out in 15 communities; seven in the Gushiegu-Karaga and eight in the Zabzugu-Tatale District. The EM equipment was operated in the horizontal (HD) and vertical dipole (V.D) modes with a 20 m intercoil spacing, probing depths of 15 and 30 m respectively. Analysis and interpretation of the field results in the two districts revealed that potential aquifers within the various communities could be located with respect to two distinct features namely, weathered and fractured zones. Three lithologic logs for each District obtained for the points recommended have been presented and compared with profiling results in order to provide a scientific basis for siting of similar boreholes in virgin areas. The results also show a response, which is significantly different from that of the weathered and fractured zones. It indicates a nearly symmetrical negative response, with values as low as 5 mS/m in some communities. This was interpreted to be due to dike-like structures or a highly conductive material that has been masked, which could contain water. The lithologic logs of the communities in the Gushiegu-Karaga District revealed that the topmost part consists of brown loose laterite with the subsurface underlain with hard fresh fractured siltstone with at times, sandstone intercalations. The yield of the boreholes drilled within these communities was between 21 and 73 litres/min and the aquifer horizon averagely between 30-60 m. On the other hand, the logs of the communities in Zabzugu-Tatale

District revealed that the topmost layer consists of brown sandy laterite with the subsurface underlain with grey hard quartzite with at times, siltstone intercalations. The yield of the boreholes drilled within these communities were between 10 and 117 litres/min and the aquifer horizon averagely between 30 and 70 m. The result of the study yielded a 75% success rate which confirms that the Electromagnetic Method is very suitable for sitting boreholes in these communities. To increase this success rate, it is recommended that the combination of two or more geophysical techniques such the Vertical Electrical Sounding and other EM methods be considered in the future to ensure a more accurate selection of potential drilling sites.

CONTENTS

DECLARATION.....	i
ABSTRACT.....	ii
LIST OF FIGURES.....	viii
TABLES.....	xii
ACKNOWLEDGEMENT.....	xiii

CHAPTER ONE

1. 1 Introduction.....	1
1. 2 Objective.....	5
1. 3 Scope of Work.....	6
1. 4 Methodology.....	6

CHAPTER TWO

2.0 Groundwater.....	8
2. 1 Occurrence.....	8
2.2.0 Aquifer.....	15
2.2. 1 Tropical African Regolith.....	17
2.2. 2 Crystalline Aquifers.....	17
2.2. 3 Sandstone-shale Aquifers.....	18
2. 3 Prospecting for Groundwater.....	19
2.3.1 Geological and Hydrological Studies.....	20

CHAPTER THREE

3.0 The Project Area.....	22
3.1 Location, Climate and Vegetation.....	22

3.2 Geology and Hydrogeology.....	25
3.3. Socio-Economic Condition.....	30

CHAPTER FOUR

4.0 The Electromagnetic (EM) Method and it's Principle.....	32
4.1. Elementary Electromagnetic Theory.....	32
4.2. Fundamental Physical Quantities and Field Equations.....	32
4.2.1 Electromagnetic Field Attenuation.....	33
4.2.2 Depth of Penetration of Electromagnetic Fields.....	35
4.3. Principle of the Geophysical Electromagnetic Method.....	37
4.3.1 Theory of the Geophysical Electromagnetic Method.....	38
4.3.2 Field Parameters Measured.....	40
4.4. Conductivity in Rocks.....	41
4. 4. 1. Factors affecting terrain conductivity.....	42
4.5 The Geonics EM 34-3 Surveying Equipment.....	42
4.5.1 Instrument Hardware.....	42
4.6 Field Procedures.....	42
4.6.1 Terrain Evaluation.....	44
4.6.2 Electromagnetic Traversing Method.....	44

CHAPTER FIVE

5.0 Qualitative Interpretation of the Field Results.....	47
5.1 Geophysical Criteria for the Selection of Drilling Points.....	48
5.2 Interpretation of Field Results.....	51
5.3.1 Nakpoligu In The Gushiegu-Karaga District.....	51
5.3.2 Yibeyili in the Gushiegu-Karaga District.....	54
5.3.3 Pishigu In The Gushiegu-Karaga District.....	56
5.3.4 Tindang In The Gushiegu-Karaga District.....	59
5.3.5 Zulogu In The Gushiegu-Karaga District.....	62
5.3.6 Gorgu In The Gushiegu-Karaga District.....	64
5.3.7 Nanduli In The Gushiegu-Karaga District.....	68
5.3.8 Nakpale In The Zabzugu-Tatale District.....	71
5.3.9 Bencharignadom in the Zabzugu-Tatale District.....	74
5.3.10 Jatodor in the Zabzugu-Tatale District.....	78
5.3.11 Benatabe East in the Zabzugu-Tatale District.....	82
5.3.12 Gor Kukani in the Zabzugu-Tatale District.....	85
5.3.13 Batigmado in the Zabzugu-Tatale District.....	87
5.3.14 Bikpanjib in the Zabzugu-Tatale District.....	91

CHAPTER SIX

6.0 Conclusions and Recommendation.....96

6.0 Conclusions.....96

6.1 Recommendations.....97

REFERENCE.....98

APPENDICES

Appendix A Elementary Electromagnetic (EM) Theory.....102

Appendix B Solution of the diffusion equation.....108

Appendix C Theory of Operation of EM-34-3 at Low induction numbers..112

Appendix D Field Results.....117

LIST OF FIGURES

FIGURE	PAGE
Fig 2.1. The Water Table during Rainfall.....	9
Fig 2.2 The Water Table in the Desert.....	9
Fig 2.3 The Hydrologic Cycle.....	10
Fig 3.1a Map of Gushiegu-Karaga District.....	23
Fig 3.1b Map of the Zabzugu-Tatale District.....	24
Fig 3.2a Hydrological provinces and river systems of Ghana	26
Fig 3.2b. Geological map of Ghana (After Kesse, 1985).....	29
Fig 3.2c. Geological map of the Northern Region of Ghana(After Kesse, 1985).....	30
Fig 4.1. General Principle of EM surveying. (Keary and Brooks, 1987).....	37
Fig 4.2 Induced current flow in homogenous half space	38
Fig 5.1 Geophysical Model: fractured zone and weathered zone.....	49
Fig. 5.2. Geophysical model: Vertical dike.....	50
Fig 5.3. Terrain Conductivity measurements along profile 1 using a 20 m coil at Nakpoligu.....	51
Fig 5.4. Terrain Conductivity measurements along profile 2 using the 20 m coil at Nakpoligu.....	52

Fig 5.5. Terrain Conductivity measurements along profile 1 using the 20 m coil at Yibeyili.....	54
Fig 5.6. Terrain Conductivity measurements along profile 2 using the 20 m coil at Yibeyili.....	55
Fig 5.7. Terrain Conductivity measurements along profile 1 using the 20 m coil at Pishigu.....	56
Fig 5.8. Terrain Conductivity measurements along profile 2 using the 20 m coil at Pishigu.....	57
Fig 5.9a. Terrain Conductivity measurements along profile 1 using the 20 m coil at Tindang.....	59
Fig 5.9b. Lithologic Log of point 30 m on profile 1 at Tindang.....	59
Fig 5.10. Terrain Conductivity measurements along profile 2 using the 20 m coil at Tindang.....	61
Fig 5.11. Terrain Conductivity measurements along profile 1 using the 20 m coil at Zulogu.....	62
Fig 5.12. Terrain Conductivity measurements along profile 2 using the 20 m coil at Zulogu.....	63
Fig 5.13a. Terrain Conductivity measurements along profile 2 using the 20 m coil at Gorgu.....	65

Fig 5.13b. Lithologic log of point 30 m on the profile 1 at Gorgu.....	66
Fig 5.14a. Terrain Conductivity measurements along profile 1 using the 20 m coil at Gorgu.....	67
Fig 5.14b. Lithologic log of Point 90 m on the profile 2 at Gorgu.....	67
Fig 5.15a. Terrain Conductivity measurements along profile 1 using the 20 m coil at Nanduli.....	68
Fig 5.15b. Lithologic Log of Point 110 m of profile 1 at Nanduli.....	69
Fig 5.16. Terrain Conductivity measurements along profile 1 using a 20 m coil at Nakpale.....	71
Fig 5.17. Terrain Conductivity measurements along profile 2 using the 20 m coil at Nakpale.....	72
Fig 5.18. Terrain Conductivity measurements along profile 3 using the 20 m coil at Nakpale.....	73
Fig 5.19a. Terrain Conductivity measurements along profile 3 using the 20 m coil at Bencharignado.....	74
Fig 5.19b. Lithologic Log of the 20m point of the Profile at Bencharignadom....	76
Fig 5.20. Terrain Conductivity measurements along profile 2 using the 20 m coil at Bencharignadom.....	76
Fig 5.21. Terrain Conductivity measurements along profile 1 using the 20 m coil at Jatodor.....	78
Fig 5.22. Terrain Conductivity measurements along profile 2 using the 20 m coil at Jatodor.....	79

Fig 5.23. Terrain Conductivity measurements along profile 3 using the 20 m coil at Jatodor.....	80
Fig 5.24. Terrain Conductivity measurements along profile 4 using the 20 m coil at Jatodor.....	81
Fig 5.25a. Terrain Conductivity measurements along profile 1 using the 20 m coil at Benatabe East.....	82
Fig 5.25b. Lithologic Log of the 100 m point at profile 1 at Benatabe East..	83
Fig 5.26. Terrain Conductivity measurements along profile 2 using the 20 m coil at Benatabe East.....	85
Fig 5.27. Terrain Conductivity measurements along profile 1 using the 20 m coil at Gor Kukani.....	86
Fig 5.28 Terrain Conductivity measurements along profile 2 using the 20 m coil at Gor Kukani.....	87
Fig 5.29 Terrain Conductivity measurements along profile 1 using the 20 m coil at Batigmado.....	88
Fig 5.30. Terrain Conductivity measurements along profile 2 using the 20 m coil at Batigmado.....	89
Fig 5.31. Terrain Conductivity measurements along profile 3 using the 20 m coil at Batigmado.....	90
Fig 6.32. Terrain Conductivity measurements along profile 1 using the 20 m coil at Bikpanjib.....	91
Fig 6.33. Terrain Conductivity measurements along profile 2 using the 20 m coil at Bikpanjib.....	92

Fig 6.34. Terrain Conductivity measurements along profile 3 using the 20 m coil at Bikpanjib.....93

Fig 6.35. Terrain Conductivity measurements along profile 4 using the 20 m coil at Bikpanjib.....94

LIST OF TABLES

TABLE	PAGE
Table 2.1. Usual mode of water occurrence.....	13
Table 2.2 Porosity and hydraulic permeability for some common ground material....	14
Table 2.3 Showing aquifers and their types.....	16
Table 4.1 Exploration depths for Geonics EM 34-3 at various intercoil spacing.....	44
Table 5.1 Summary of log results for both districts.....	95
Table 5.2 Summary of Test Drilling and Success Rates of Both Districts.....	95

ACKNOWLEDGEMENT

Thanks be to God for the wisdom He has given me to write this Master of Science thesis report.

I wish to express my heartfelt gratitude and appreciation to my supervisor, Dr. S.K Danuor for all the efforts and contribution he made to see this work as a success. His patience, understanding, encouragement and technical advice were pivotal to the success of this work.

I am grateful to all the geophysics lecturers at the Physics Department: Messrs Asare Vandyke, Kofi Ampong and Acheampong Enin for their assistance, motivation and encouragement.

I am also grateful to the management and staff of World Vision International- Ghana Rural Water Project (GRWP) for granting me permission to use the EM data to publish the thesis.

Finally, I thank my colleagues' Postgraduate students at the Physics Department, Kumasi for diverse assistance in making this work a reality.

CHAPTER ONE

1.0 INTRODUCTION

Water is an indispensable asset to man, animals and plants, without which life on earth would be unbearable. From the very inception of human civilization, people have settled close to water sources, along rivers, besides lakes or natural springs. Indeed where people live, some water is normally available for drinking, domestic use, and possibly for watering of plants and the drinking of animals. This does not imply, however, that the available source of water is convenient and is of sufficient quantity, nor that the water is safe and wholesome. On the contrary, in many countries people live in areas where water is scarce.

In fact, more than nine million people in Ghana have no access to safe drinking water (Water Aid-Ghana, 2007). In many rural communities, water, which constitutes about 70% of the human body according to scientists, is one of the scarcest commodities (Water Aid-Ghana, 2007). During the wet season, unsafe sources of water get more contaminated by runoff water from polluted sites. In the dry season, even contaminated water becomes scarce since the streams usually dry up.

This compels especially women and children to walk over long distances to look for water for all domestic chores and drinking. They usually carry very big pans and containers to enable them carry as much water as possible. The heavy load on their heads, the long distance to walk, and other chores to perform during the day compound their already fragile health problems and reduce their productivity.

There are so many water and sanitation related diseases prevalent in Ghana. At the moment, Ghana ranks second worldwide in guinea worm cases. The Northern Region alone, as at October 2002

represented more than 70% of Ghana's total guinea worm cases that year. Nationwide, there were 4,101 reported cases. Other water and sanitation related diseases include diarrhea, trachoma, cholera, hepatitis A, bilharzias, typhoid, malaria, polio, hookworm, and tapeworm (Water Aid-Ghana, 2007). When plagued by Guinea worm for instance, whole communities suffer, not just the individuals with the disease. Children with the disease cannot attend school because they, and other victims, are incapacitated for an average of two months after a worm has begun to emerge from a person's body. Communities suffer food shortages when their residents are unable to work (The Carter Centre, 2007).

It is also observed from the climate of Ghana that the rainfall is not uniform in terms of its temporal and spatial distributions. This means that there is a period of surplus water and a period of water deficit in the streams and rivers. The annual rainfall decreases towards the north and south-east of the country. These factors point to the fact that many streams, particularly, in the north and south-east may not be perennial. Most small streams which feed many rural communities apart from the possibility of being polluted cannot even do so on sustainable basis throughout the year. Likewise, rainfall harvesting cannot be done all year round due to the rainfall pattern. This is a serious limitation since the storage facility required for harvesting rainfall for use by a rural family throughout the year is economically not affordable.

It therefore appears that the solution to the problems of traditional rural water supply systems lies basically in the efficient utilization of groundwater and efficient management of aquifers, hand-dug wells and boreholes. Groundwater has been found to be sufficient both in quantity and quality for most rural communities. The advantages of groundwater as the main anchor or pillar of Ghana's rural water supply development project are numerous.

Firstly, there are aquifers which underlie geographically large areas of the country which can be tapped at shallow depths close to the demand centers in response to the dispersed nature of the rural settlements. Some of these aquifers have modestly been assessed and their characteristics are fairly well known (WVI-GRWP, 2001).

Secondly, water stored in aquifers is almost protected naturally from evaporation, and well yields are in many cases adequate, offering water security in regions prone to protracted droughts as experienced in the northern parts of the country. Thirdly, with aquifer protection, groundwater has excellent microbiological and chemical quality which require minimal or no treatment. Lastly, the capital cost of groundwater development as opposed to conventional treatment of surface waters is relatively modest and the resource lends itself to flexible development capable of being faced with rising demand (WVI-GRWP, 2001).

The tapping of groundwater resources, both for drinking water supply and for irrigation purposes, date back to ancient times. In China, wells were drilled at least 3,000 years ago with hand operated churn drills, to depths as deep as 100 m and lined with bamboo casings. Hand-dug wells have been sunk since times immemorial, sometimes to a considerable depth, and such wells continue to be made in several parts of the world. The technology for tapping groundwater at great depth through tube wells is of recent date (International Centre for Community Water Supply and Sanitation, 1981).

When groundwater is present at a shallow depth (e.g. less than 10 m) it may be polluted from sources of faecal contamination such as pit latrines or septic tanks. Pathogenic bacteria and viruses from such sources can be carried by the groundwater, although they tend to attach themselves by adsorption to the solid particles. When assessing the possible health hazards of groundwater

sources, one should pay attention to the travel-time of the water through the ground strata than to the distance the water has to flow to the point of withdrawal. In limestone karstic formations and fissured rocks, human contamination may be carried over a distance of several kilometers. In sand formations, groundwater flow is much slower so that only contamination from nearby sources needs to be considered when selecting the point of groundwater withdrawal (International Centre of Community Water Supply and Sanitation, 1981).

Frequently, the available data on groundwater resources are grossly inadequate. Successful development of groundwater supplies may then be promoted by prospecting. These would also bring to light the physical and chemical characteristics of the groundwater. Considering the numerous advantages of groundwater prospecting addressed earlier, it is therefore not surprising that the percentage of the rural communities which depend on boreholes and wells has increased substantially since 1984 as the Government and the Non-Governmental Organizations (NGOs) such as World Vision International (WVI), Ghana have embarked on large scale drilling of more boreholes and wells.

Now, considering the area of study, many geophysical surveys for borehole selection have been carried out in the Middle Voltaian Sedimentary Basin of the Northern Region of Ghana with little or average successful results. This has been attributed partly to the use of inappropriate field methods and techniques of the geophysical data (WVI-GRWP, 2001).

The EM-34 Ground Conductivity equipment from Geonics Ltd has been used for a long time for ground water prospecting. Although certain good results have been obtained in the past, research shows that with the right and appropriate interpretation of geophysical data acquired, the results obtained would increase significantly, meeting the safe water requirement in these areas to prevent

water- borne diseases and in the long round, improve the socio-economic standard of life of the people living the Gushiegu-Karaga and Zabzugu-Tatale Districts of the Northern Region of Ghana.

The geology of the Voltaian is very complex and therefore striking groundwater in the Basin has been a difficult issue for past researchers as reported by the Ghana Rural Water Project of the World Vision International.

The EM-34 equipment has proven very successful in delineating groundwater potential zones in some parts of the Voltaian as reported by the Ghana Rural Water Project of the World Vision International. An average success rate of 55% has been recorded. It is therefore hoped that with the electromagnetic method based on the EM-34 equipment, good quality and reliable data will be obtained. Hence, this research would go a long way to minimize the water problem of most communities in the region in the Gushiegu-Karaga and Zabzugu-Tatale Districts of the Northern Region of Ghana and serve as a guideline for groundwater exploration. Thus, groundwater exploration will be less cumbersome and guided with prior information about the terrain under study.

1.1 OBJECTIVE

The objective of this project work is to carry out geophysical investigations in the field using electromagnetic methods that are based on the Geonics EM-34 equipment to determine groundwater potential zones in the Gushiegu-Karaga and Zabzugu-Tatale Districts of the Northern Region of Ghana.

1.2 SCOPE OF THE WORK

This project involves a geophysical survey using the electromagnetic method for investigating ground conductivity to delineate groundwater potential zone within the Gushiegu-Karaga and Zabzugu-Tatale Districts of the Northern Region of Ghana. The project work was carried out as part of the World Vision International (WVI) groundwater survey project of the Northern Region. The work involved the use of geophysical techniques to identify potential groundwater sites in the communities. This was followed by drilling of some of the selected sites. My project work is therefore made up of the geophysical field survey work in the communities in the study area, analysis and interpretation of the results and in some cases, comparison with drilling results, where some selected sites were drilled.

1.3 METHODOLOGY

The methodology considered in the geophysical exploration and interpretation procedure included;

- a. Desk Study; which includes assessment of existing hydrogeological and water resources information in and around the beneficiary communities. The establishment of current knowledge about the lineament patterns and fractures, the presence of suitable aquifers and their thickness, the mean depth to aquifer and water table and the expected lithological sequences. All baseline information covering at least 2km around each beneficiary community was assembled and studied. Climatic information pertaining to the area of operation was sought from the meteorological services. This information help assess the recharge of aquifer.
- b. Reconnaissance Survey of beneficiary communities and its immediate neighbourhood to update baseline information, location of target areas for geophysical surveys,

hydrogeological survey of the area, terrain assessment, and cutting of available traverse line(s) whose bearing are noted with the GPS instrument.

- c. Electromagnetic survey using Geonics EM-34 Conductivity meter. The equipment consists of a battery operated transmitter and receiver unit, a transmitter and receiver coil or loop of about 800 mm in diameter. It uses three frequency/coils spacing pairs. The coil spacing are 10, 20 and 40 m, using frequencies of 6400, 1600, 400 Hz. The coils are placed at a known distance apart and coplanar, either both horizontal on the ground or both vertical. The transmitter is turned on and the distance between the transmitter and receiver is adjusted. The apparent terrain conductivity is then read from the receiver directly. When both coils are placed horizontally on the ground, the transmitter generates an electric field with a vertical dipole, thus this is called the vertical dipole mode. The vertical dipole mode has a greater penetration depth than the horizontal dipole mode. Where the vertical dipole conductivity exceeds the horizontal dipole mode reading, the main attribution to the ground conductivity is coming from deeper than 39% of the spacing between the coils. This fact allows the instrument to be used quantitatively to interpret the variation of ground conductivity with depth.(Payne,1990)
- d. Processing, Analysis and Interpretation of Data. These involve field measurements and interpretation of the results with regards to selection of potential sites for boreholes. It takes a combination of geological, hydrogeological, geophysical, and socio-cultural, experience, right judgment and other considerations to select the most suitable site for drill a well for the abstraction of groundwater. Community participation is crucial to the sustainability of wells located within the community as such it must form an essential component of the processing leading to the final selection of well sites for drilling.

CHAPTER TWO

2.0 GROUNDWATER

2.1 OCCURRENCE

Groundwater is water that exists in the pore spaces and fractures in rock and sediment beneath the Earth's surface. It originates as rainfall or snow, and then moves through the soil into the groundwater system, where it eventually makes its way back to surface streams, lakes, or oceans.

Groundwater makes up about 1% of the water on Earth (most water is in oceans).

But, groundwater makes up about 35 times the amount of water in lakes and streams.

Groundwater occurs everywhere beneath the Earth's surface, but is usually restricted to depths less than about 750 meters. The volume of groundwater is equivalent to a 55 meter thick layer spread out over the entire surface of the Earth.

The surface below which all rocks are saturated with groundwater is the water table.

Rain that falls on the surface seeps down through the soil and into a zone called the zone of aeration or unsaturated zone where most of the pore spaces are filled with air. As it penetrates deeper it eventually enters a zone where all pore spaces and fractures are filled with water. This zone is called the saturated zone. The surface below which all openings in the rock are filled with water (the top of the saturated zone) is called the water table as shown in fig 2.1.

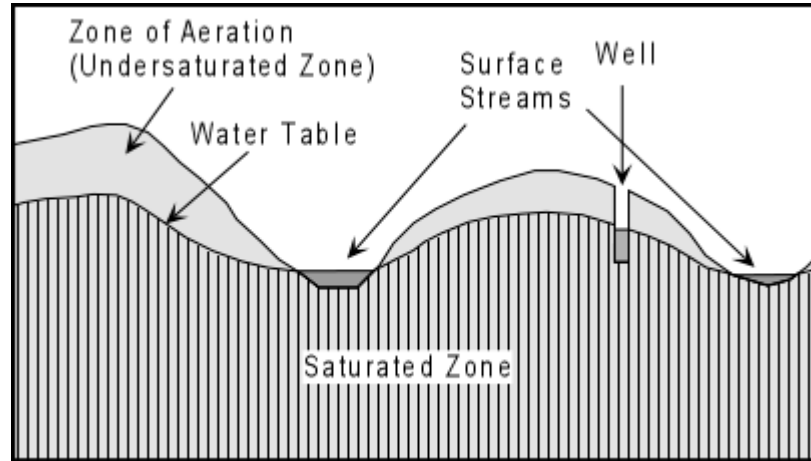


Fig 2.1. The Water Table during Rainfall (Santosh,1996)

The water table occurs everywhere beneath the Earth's surface. In desert regions it is always present, but rarely intersects the surface.

In more humid regions it reaches the surface at streams and lakes, and generally tends to follow surface topography. The depth to the water table may change, however, as the amount of water flowing into and out of the saturated zone changes. During dry seasons, the depth to the water table increases. During wet seasons, the depth to the water table decreases as shown in fig 2.2.

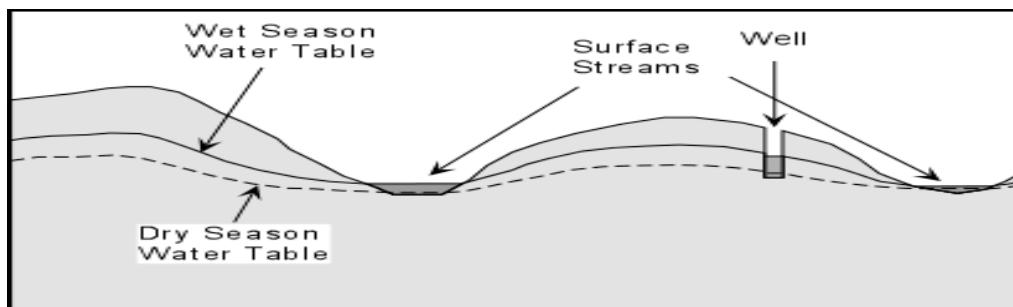


Fig 2.2 The Water Table in the Desert (Santosh, 1996)

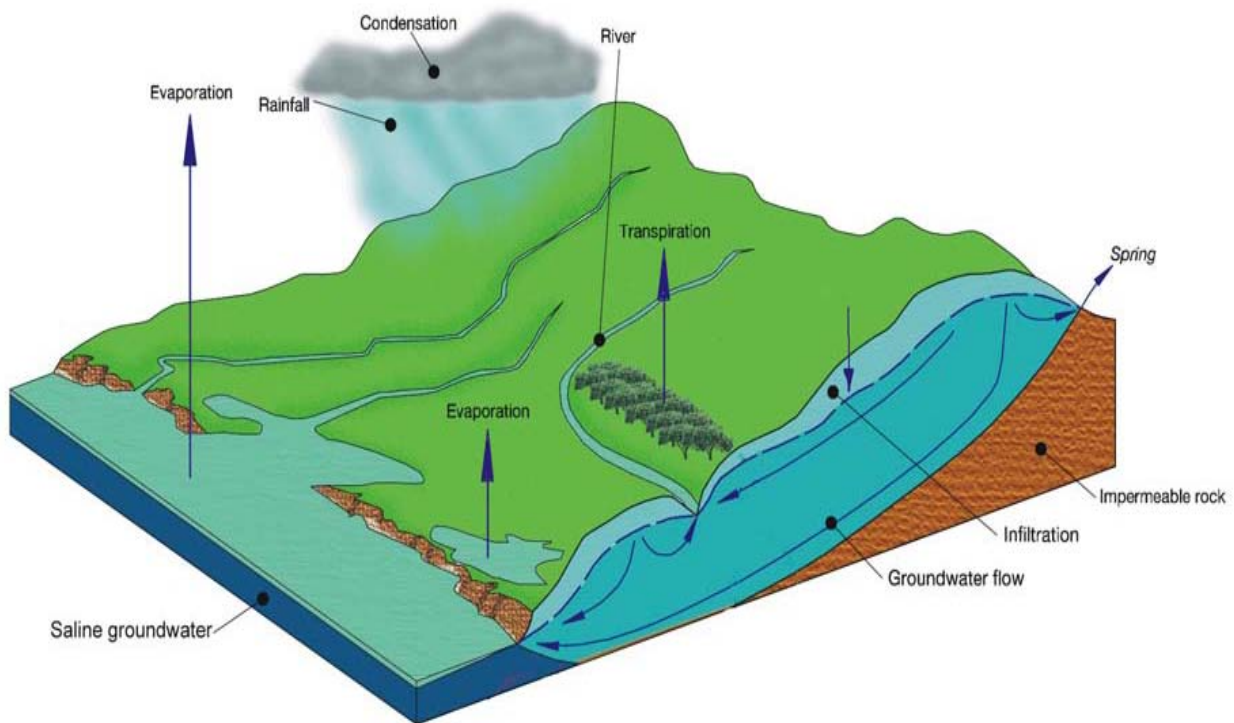


Fig 2.3 The Hydrologic Cycle (Santosh, 1996)

The distribution of water on the land is dependent upon the complex interaction between atmosphere and oceans that we call climate. The circular path of the hydrologic cycle links evaporation, condensation, run-off, infiltration, percolation, and transpiration. This is shown in fig 2.3 above. These processes cause water to change state (vapor, liquid, solid) as it moves between different elements of the earth system (Santosh,1996).

The oceans are the ultimate source for all water on or below the land surface. The average residence time - the length of time water remains in a given location - for oceanic water is 3,000-4,000 years. The bulk of evaporation (85%) occurs over oceans and is greatest in areas of warm climates at low latitudes. Water vapor cools and relative humidity of the air increases as it rises in the atmosphere. Condensation (water

vapor converted to liquid) forms tiny moisture droplets that may coalesce to form clouds form when the air becomes saturated with water vapor (100% humidity). Atmospheric circulation patterns may redistribute the saturated air prior to precipitation (Santosh,1996).

Precipitation is concentrated over areas of rising air (e.g. along equator or above mountains) and is least in areas of descending air (e.g. along the tropics). The volume of moisture in the atmosphere is equivalent to ~25 mm of precipitation. It is estimated that moisture in the atmosphere is recharged 40 times a year (residence time ~9 days) as the average annual precipitation for the world is approximately 1000 mm. Nearly a third of all water falling as precipitation completes the circuit to the oceans by surface run-off in streams (average residence time 14 days). Most of the rest returns to the atmosphere by evaporation or through the transpiration of plants (Santosh,1996).

A slim fraction of water falling as precipitation infiltrates below the surface through bedrock or soils to form groundwater. Some of the soil moisture is lost to evaporation or taken up by vegetation and the remainder recharges the groundwater system. Groundwater flow is termed percolation and occurs at rates from meters per day to millimeters per year. Consequently the residence time for groundwater may be measured in intervals of weeks or thousands of years. Even the slowest flow rates will eventually return the groundwater to the ocean, completing the hydrologic cycle (Santosh,1996).

Evidently, the mode of occurrence of groundwater depends largely upon the type of formation, and hence upon the geology of the area.

Groundwater is stored in rocks or sediments that act as storage reservoirs for groundwater which are called Aquifers. The volume of water contained in the aquifers in a localized area that is the storage capacity of the groundwater is dependent upon:

The porosity and permeability of the rocks

The rate at which water is added to it by infiltration and

The rate at which water is lost from it by evaporation, seepage to surface courses and withdrawal by man

(Santosh, 1996).

Prospecting for water requires a basic knowledge of the various kinds of groundwater-bearing formations that can be found in the earth's crust. From this, the approach to their exploration for water purposes should be developed.

Groundwater occurs in pores, voids or fissures of ground formations (Tab 2.1). Pores are the spaces between the mineral grains in sedimentary ground layers and in decomposed rocks. The amount of pore space in a ground formation depends upon such factors as grain size, shape, packing and the presence of cementing material. Porosity of the soil, which is the major geological criteria for the occurrence of groundwater, is the quantitative measurement of the interstices or voids in a given volume of soil aggregate. Mathematically porosity is expressed as (η) (Santosh, 1996).

$$\eta = \frac{V_v}{V} \times 100\%$$

Where V_v = Total volume of voids in the soil aggregate and V = Total volume of soil aggregate.

The porosity determines the amount of water that a rock can contain. In sediments or sedimentary rocks the porosity depends on grain size, the shapes of the grains, and the degree of sorting, and the degree of cementation. Well-rounded coarse-grained sediments usually have higher porosity than fine-grained sediments, because the grains do not fit together well. Poorly sorted sediments usually have lower porosity because the fine-grained fragments tend to fill in the open space. In igneous and metamorphic rocks porosity is usually low because the minerals tend to be intergrown, leaving little free space. Highly

fractured igneous and metamorphic rocks, however, could have high porosity (Santosh,1996).

Table 2.1. Usual mode of water occurrence

Ground Type	Quality Water occurring in:
Sand and Gravel	Pores
Sandstone	Pores and fissures
Limestone	Fissures often expanding into caves
Chalk	Pores and fissures
Clay	Very small pores
Massive Igneous	Fissures with pores in weathered zones
Lava	Fissures with pores in igneous zones
Metamorphic	Fissures with spores in weathered zones

Source: International Centre of Community Water Supply and Sanitation, 1981

The ease with which water can flow through a ground formation under a hydraulic head is the hydraulic permeability which is expressed as the velocity of flow of water through the ground per unit of hydraulic gradient, e.g. mm/sec, m/day. Permeability is a measure of the degree to which the pore spaces are interconnected, and the size of the interconnections. Low porosity usually results in low permeability, but high porosity does not necessarily imply high permeability. It is possible to have a highly porous rock with little or no interconnections between pores. A good example of a rock with high porosity and low permeability is a vesicular volcanic rock, where the bubbles that once contained gas give the rock a high porosity, but since these holes are not connected to one another the rock has low permeability. (Aning,

2000) Permeability depends on the porosity, the average pore size and the distribution of the fissures.

This is shown in Table 2.2.

2.2 Porosity and hydraulic permeability for some common ground materials

Material	Porosity (%)	Hydraulic Permeability Coefficient in mm/sec
Clay	45-55	10^{-3} - 10^{-9}
Silt	40-50	10^{-2} - 10^{-6}
Sand	35-40	10^{-2} - 10^{-1}
Clean Gravel	40-45	10^{-3} - 10^{-1}
Sandy Gravel	25-40	10^{-1} - 10^{-2}
Sandstone	10-20 (Pores)	10^{-4} - 10^{-6}
Material	Porosity (%)	Hydraulic Permeability Coefficient in mm/sec
Sandstone	(fissures)	10^{-1}
Limestone	1-10 (Pores)	10^{-6} - 10^{-8}
	(Fissures)	10^{-2}
Granite	(Fissures)	10^{-10}
		10^{-2}

Source: International Centre of Community Water Supply and Sanitation, 1981.

Ground layers with a very low hydraulic permeability (less than 10^{-6} mm/sec) are said to be impermeable and those with higher hydraulic permeability are regarded as permeable.

2.2.0 Aquifers

Aquifers are rock or sediment that act as storage reservoirs for groundwater and are typically characterized by high porosity and permeability. In contrast, an aquiclude is composed of a low permeability rock or sediment that essentially acts as a barrier to groundwater flow. Water has been found in wells that have penetrated as deep as 9 km (over 5 miles) into the earth's crust. Most useable fresh groundwater is relatively shallow (less than 100 meters [330 feet]). Deeper waters are more expensive to retrieve and often contain high concentrations of minerals. Aquifers (and aquicludes) are typically in sediments or sedimentary rocks as the sediments and sedimentary rocks are found at the earth's surface more frequently than the relatively impermeable igneous and metamorphic rocks (Mc-Graw Hill, 2001).

Aquifers can be divided into open (unconfined) aquifers and closed (artesian or confined) aquifers. In an open aquifer, water infiltrates through permeable soil and rock or sediment that make up the unsaturated zone (where pore spaces are only partially filled with water) into the saturated zone of the aquifer (where all the pore spaces are filled with water) A closed (artesian) aquifer is confined by an overlying aquiclude that prevents water simply infiltrating down into the aquifer. Instead, water enters the tilted aquifer layer through a recharge area where the aquifer rock is exposed at higher elevations (Mc-Graw Hill, 2001)

Aquifer layers can be continuous, discontinuous, or mixed with the continuous being the most important in many respect: potential, extension, renewal, and discharge whilst the discontinuous are localized and linked to the fracturation systems in both arid and semi-arid zones as well as tropical humid zones. Table

2.3 below shows the different types of aquifers.

Table 2.3 Showing aquifers and their types

Type of aquifer layer	Formation
Continuous	Sand
	Clayed sand
	Sandy-clayed sand
	Clay and marl
	Limy Clay
Mixed	Clayed sandstone
	Sandstone
	Limy sandstone
	Limestone
	Marly sandstone
	Dolomite
Discontinuous or Local	Shist
	Quartzite
	Conglomerate
	Volcanic Rock
	Dolerite
	Crystallophyllian Rock
	Granite

Source: Diagana, 1996

2.2.1 Tropical African Regoliths

The tectonically inactive African shield consists mostly of Pre-Cambrian Basement Complex rocks, which, because of their crystalline nature, are poor aquifers. Deep chemical weathering has, however, produced from the rock relatively thick regoliths (overburden) in which extractable groundwater resources abound. However, regional differences in climate and marked spatial variations in weathering depth are reflected in the characteristics of regolith aquifers. The effects of these factors on the mode of the relationship between saturated zone thickness and weathering depth have been specifically reported (Enslin, 1943; Faniran & Omoribola, 1980a; Omoribola, 1982). For example, while isolated groundwater compartments occurring in discrete basins of decomposition, tend to characterize regolith aquifers in semiarid areas (Enslin, 1943), the zone of saturation in the regolith overburden is generally widespread or spatially continuous in the more humid low relief areas (Omoribola, 1982, 1983a). Even the humid areas, local rainfall variations can be used to explain difference in the values of weathering depth threshold for the formation of a groundwater zone in tropical regolith (Omoribola, 1982).

Additionally the hydrogeological significance and characteristics of tropical regoliths have also been reported by Sikes (1934) for parts of Kenya, Ruddock (1964) for the Kumasi district in Ghana, and Asseez (1972) for the Basement Complex of southwestern Nigeria.

Probably the greatest challenge posed by the hydrogeology of tropical Africa is to obtain reliable estimates of the groundwater resources in the regoliths (Challenges in African Hydrology, 1996).

2.2.2 Crystalline Aquifers

Aquifers in crystalline rocks are heterogeneous and have irregular configuration with variable hydraulic characteristics over short distances. Locally, they constitute isolated groundwater basins with little or no inter-basin exchange. It is thus uncommon that two interconnected boreholes can be found. Considering

the wide distribution of boreholes in rural communities in many developing countries, it is imperative that appropriate measures are found to monitor the behaviour of aquifers in this peculiar situation. This raises issues of how best the boreholes should be monitored for the effective management of aquifers, in order to safeguard the capital benefits to the rural population (Challenges in African Hydrology, 1996).

2.2.3 Sandstone-Shale Aquifers

Sequences of alternating sand, or sandstone, shale and clay are characteristics of many sedimentary successions. Deposition of such sequences takes place in the marine, delta, littoral, and arid-continental environment. The main difference between such sequences and similar rock associations shown on geologic maps under the definition alluvium or recent deposits is the greater age and hence the more advanced stage of consolidation. In contrast to alluvial sediments, sandstone-shale sequences usually exhibit a rather persistent stratigraphy. The primary porosity of a layer of sandstone is often strongly reduced by compaction and cementation. Zones of secondary porosity are usually aligned along bedding planes, fractures and joints. Near the surface sandstones are often underrated by almost impermeable crusts (Challenges in African Hydrology, 1996).

Alternating sandstone-shale formations occur under a great variety of geologic conditions. On some of the continental platforms they fill vast bowl-shaped depressions or basins and constitute large regional, often confined aquifers. In strongly deformed regions, however, intense tectonic forces often compact the rocks, or even transform them through metamorphic processes into quartzite-slate formations, so that the original water-bearing properties are lost. In addition, tectonic movements disrupt the continuity of aquiferous strata (Challenges in African Hydrology, 1996).

In gently folded and dissected regions, a fairly complete image of the sandstone-shale formations can be

obtained from surface observations. In plane regions, however, with more or less horizontal strata, where outcrops are rare, interpolation or extrapolation based on distant information points may be misleading (Challenges in African Hydrology, 1996).

2.3. PROSPECTING FOR GROUNDWATER

Many wells are drilled or dug without any effort to locate a promising area of groundwater flow. Successful prospecting for groundwater requires knowledge of the manner in which water exists in the water-bearing ground formation. Without this knowledge, effective and efficient water exploration is impossible and well drilling then becomes like a game of chance. The aim of the prospecting work must be clearly defined. Is it for providing a small local supply or is it to determine aquifer characteristics for the development of the groundwater resources of an entire area? (Aning, 2000)

The available hydrological information about the study area should be collected and collated. This includes geological maps and reports; geological reconnaissance, meteorological records, and hydrological data.

To assist in the collection of information, a survey of the study area should be made, preferably towards the end of the dry season. In some cases this may be all that is needed for an experienced hydrogeologist to define water resources for small community supplies and no further investigation would be required. If essential data were lacking, some fieldwork would be necessary. In a previous field work carried out in the study area it was found out that the area has a 60% success rate which shows great groundwater potential. (Prospecting for Groundwater using the Electromagnetic Method in the middle Voltaian Sedimentary Basin of the Northern Region of Ghana-A case study of Gushiegu-Karaga District, Menye et al, December 2005)

2.3.1 Geological and hydrogeological Studies

Geological boundaries define the volume of an aquifer and hydrological boundaries; especially the water table defines the volume of water stored within it. Commonly encountered geological boundaries are stratification of aquifers against aquicludes, the termination of aquifers by faults, unconformity and igneous intrusions. (Blyth et al., 1974).

Hydrological boundaries include the water table and spring line, coastal and shorelines, rivers, lakes and reservoirs. Such boundaries usually fluctuate in elevation and are dynamic. The spring line is an important boundary that marks the intersection of the water table with the ground level. Groundwater discharges from ground below the spring line thus preventing infiltration from occurring over this area (Blyth et al., 1974).

Hydrogeological and hydrological investigations that enable predictions to be made either of the influence of groundwater upon engineering works, or its potential as a source for water supply, should be designed to assess the following:

Geological field reconnaissance,

The location and thickness of aquifer horizons and zones, their confinement and their hydrogeological boundaries

The levels of water in the ground, their variation over an area and their fluctuation with time;

The storage and transmissive characters of the ground; and

The quality of the groundwater.

Taking inventory of existing wells and boreholes

Study and analysis of meteorological factors: precipitation and evaporation transpiration.

Geophysical surveys. To obtain this information investigations must be conducted at the surface and below ground level (Blyth et al, 1974; Michael et al., 1999).

CHAPTER THREE

3.0 THE PROJECT AREA

3.1 LOCATION, CLIMATE AND VEGETATION

The Gushiegu-Karaga District is located in the North-Eastern side of the Northern Region, roughly between latitudes 9°30' and 10°30' North and longitudes 0° and 45' West. Karaga is the administrative capital. The District is 94 km from Tamale, the Regional Capital (Fig 3.1a).

The Zabzugu/Tatale District is situated on the eastern flank of the Northern Region. It shares boundaries with the Republic of Togo to the East; Yendi District to the West; Nanumba and Nkwanta Districts to the South; and the Saboba/Chereponi District to the North. Zabzugu, the district capital, is about 160 km from Tamale (Fig 3.1b).

The climate of the Gushiegu-Karaga and Zabzugu-Tatale Districts are relatively dry, with a single rainy season that begins in May and ends in October. The amount of rainfall recorded annually varies between 750 mm and 1050 mm. The dry season starts in November and ends in March/April with maximum temperatures occurring towards the end of the dry season (March-April) and minimum temperatures in December and January. The harmattan winds, which occur during the months of December to early February, have considerable effect on the temperatures in the region, which may vary between 14°C at night and 40°C during the day. Humidity, however, which is very low, mitigates the effect of the daytime heat. The rather harsh climatic condition makes the cerebrospinal meningitis thrive, almost to endemic proportions, and adversely affects economic activity in the region.

The main vegetation is classified as vast areas of grassland, interspersed with the guinea savannah

woodland, characterised by drought-resistant trees such as the acacia, baobab, shea nut, dawadawa, mango, neem.

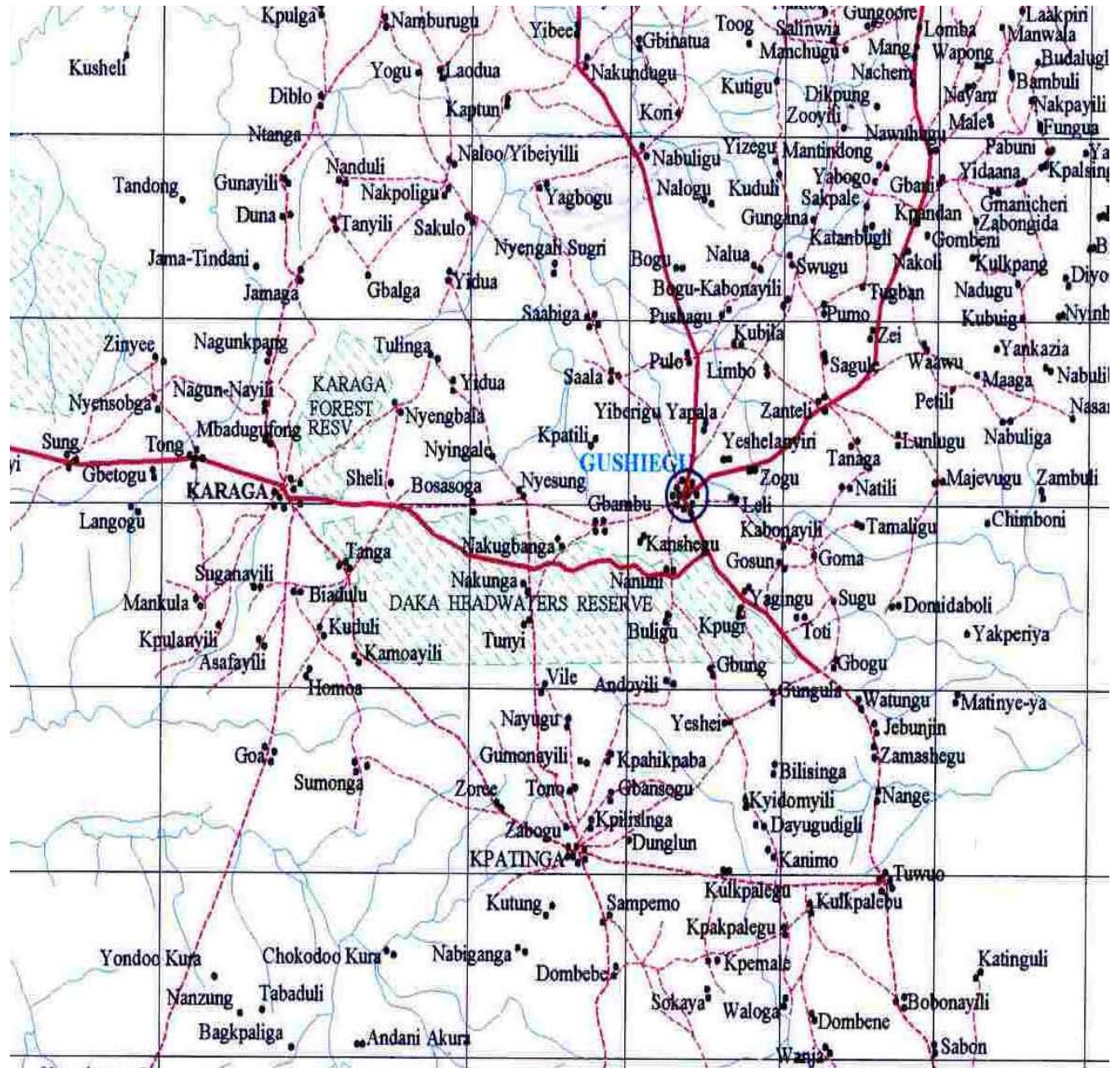


Fig 3.1a Map of Gushiegu-Karaga District (WVI-GWRP, 2001)

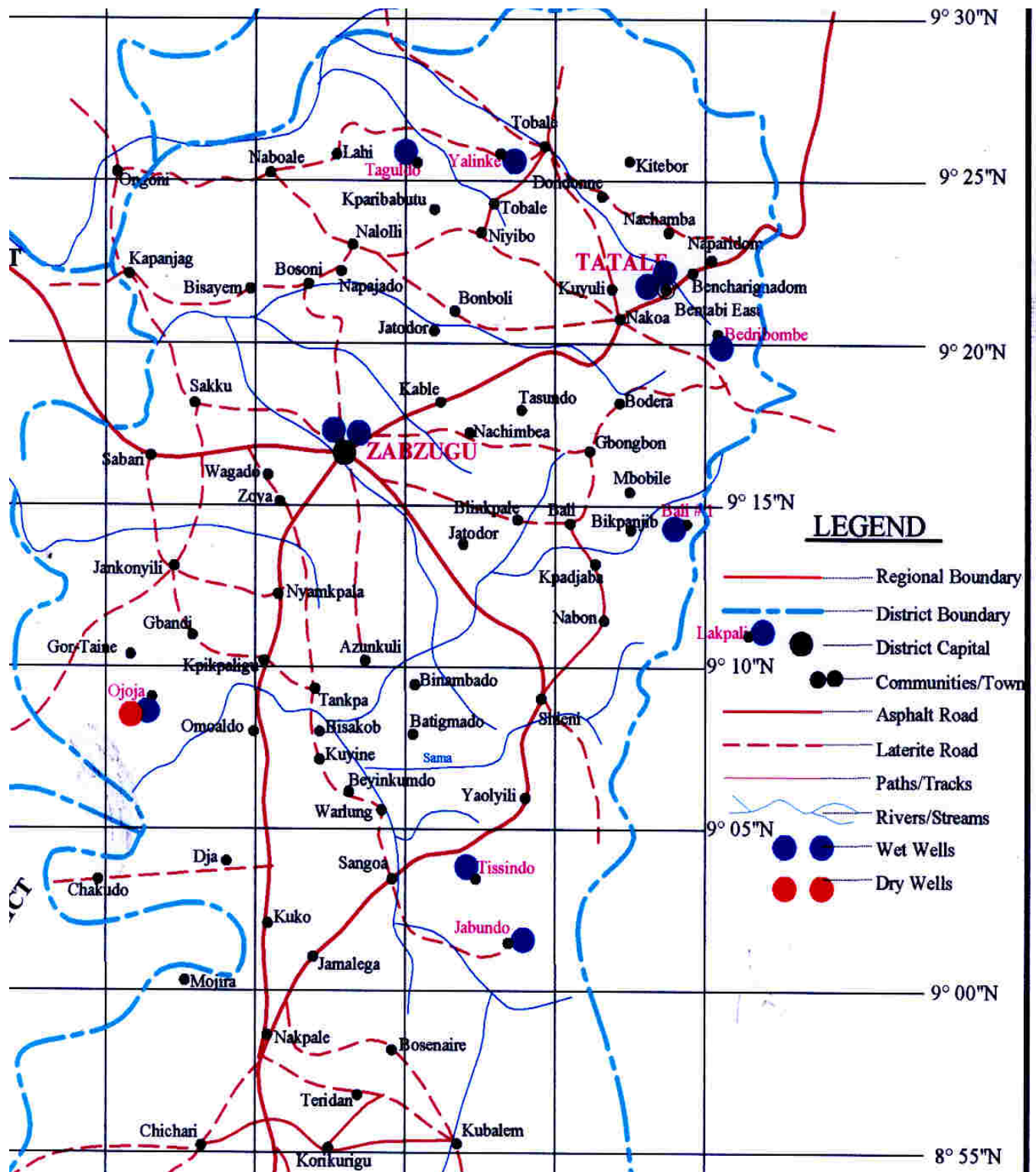


Fig 3.1b Map of the Zabzugu-Tatale District (WVI-GWRP, 2001)

3.2 GEOLOGY AND HYDROGEOLOGY

Geologically, the area lies within the middle Voltaian Basin. The Voltaian system (Fig. 3.2a) is one of two main hydro-geological terrains in Ghana. It underlies about 45% of the total landmass (the total landmass of Ghana is 238,539 km²) and covers most of the poverty endemic rural settlements with water supply problems. According to statistics from the Community Water and Sanitation Agency, less than 30% of these communities have access to safe drinking water (International Reference Centre for Community Water Supply and Sanitation, 1981).

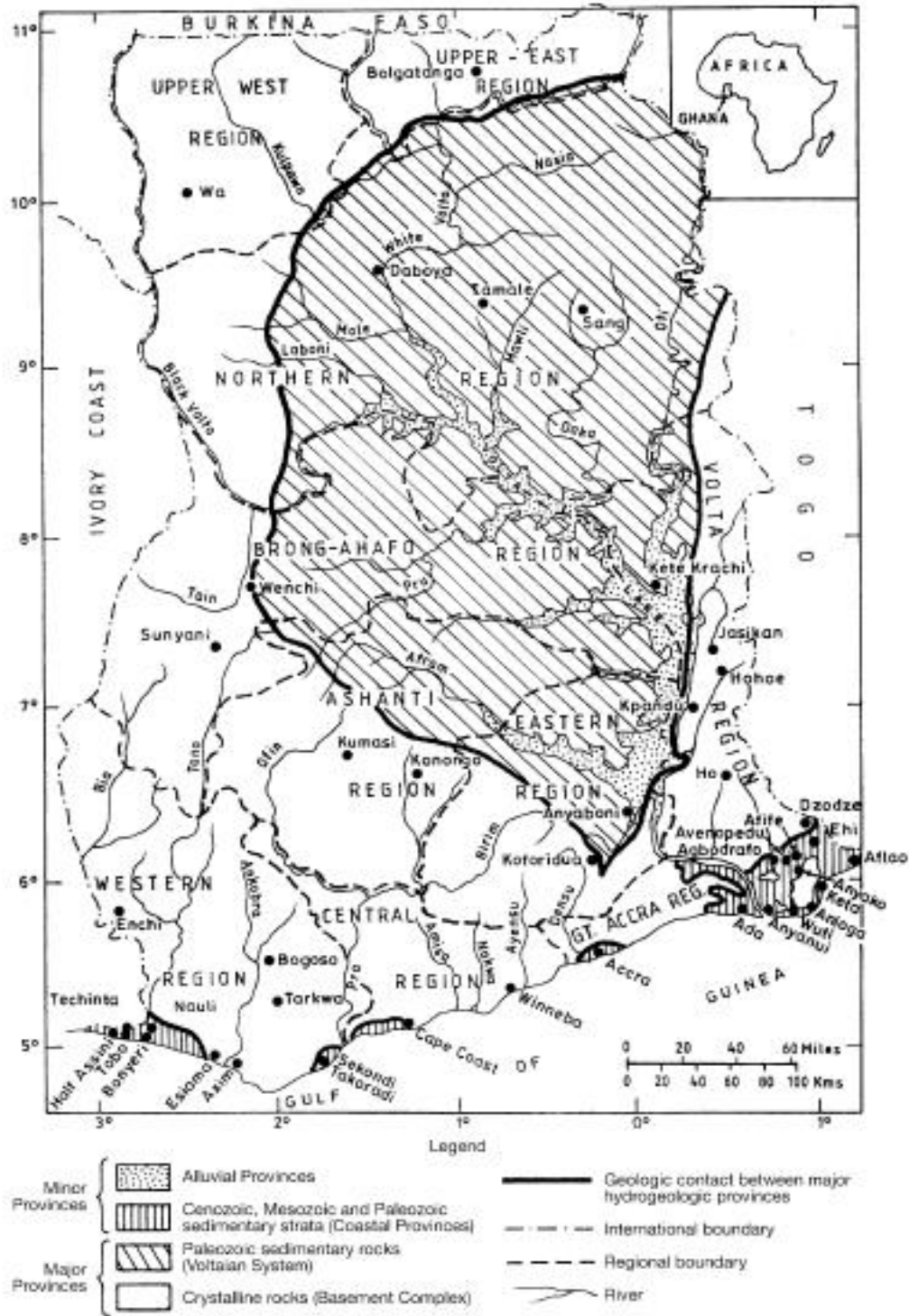


Fig 3.2a Hydrological provinces and river systems of Ghana (Geological Survey of Ghana 1969).

A paleozoic sedimentary terrain, the Voltaian system is highly heterogeneous consisting of mudstones, sandstones, conglomerate, sandy and pebbly beds and limestones (Dapaah-Siakwan and Gyan Boakye, 2000). Data on the hydrogeology of the Voltaian system is well documented though the terrain is not evenly covered due mainly to the dispersed nature of settlements on it. The groundwater fortunes of this terrain have been extensively investigated by Junner and Service (1936), Junner and Hirst (1946), Gill(1968), Buckley (1986), Bannerman (1988), Minor et al (1995) and Acheampong (1996). Results of a two year (1993-1994) hydro-geologic investigation (Minor et al. 1995) indicate that a semi-confined aquifer capable of yielding sufficient quantities of water for the rural folk exists in the area. The hydrogeology of the terrain is predominantly controlled by secondary porosity in the form of fractures developed in sedimentary units in which the primary porosity has been destroyed through compaction and slight metamorphism (Bannerman, 1988). Analysis of the available lithologic data from wells drilled in the area (Prakla Seismos, 1984; Minor et al. 1995) indicates that fractured aquifer provides most of the well water. This formation has been further subdivided into 3 hydro-geological sub provinces on the basis of lithology, field relationships and groundwater fortunes (Junner and Hirst, 1946, Soviet Geological Survey Team 1964-66). These are

- (1) Upper Voltaian (massive sandstone and thin bedded sandstone);
- (2) Middle Voltaian (Obosum and Oti beds, i.e. the regions where Gushegu-Karaga and Zabzugu-Tatale can be located). The geology of which is indicated on the geological map of Ghana in fig 3.2b;
- (3) Lower Voltaian (quartz-sandstone and pebbly grits).

The topography is basically flat to slightly undulating. Due to the impervious nature of the rock surface runoff is generally very high. This fact, combined with the high temperatures, low vegetation cover and low humidity of about 20% in the basin facilitate evaporation of rainwater before it infiltrates to recharge

aquifers. As a result, the fraction of rainwater that finally finds its way into the groundwater system is only about 5%.

In spite of numerous drilling projects undertaken by both governmental and Non Governmental Organizations within the basin, the development of groundwater resources during the past decade has produced mixed results (World Vision, 1993; Prakla Seismos 1984). The high failure rates in drilling successful wells and the high variability of well yields of aquifers within the basin (World Vision, 1993) show the need for greater understanding of the hydrogeological properties of the formation.

GEOLOGICAL MAP OF GHANA

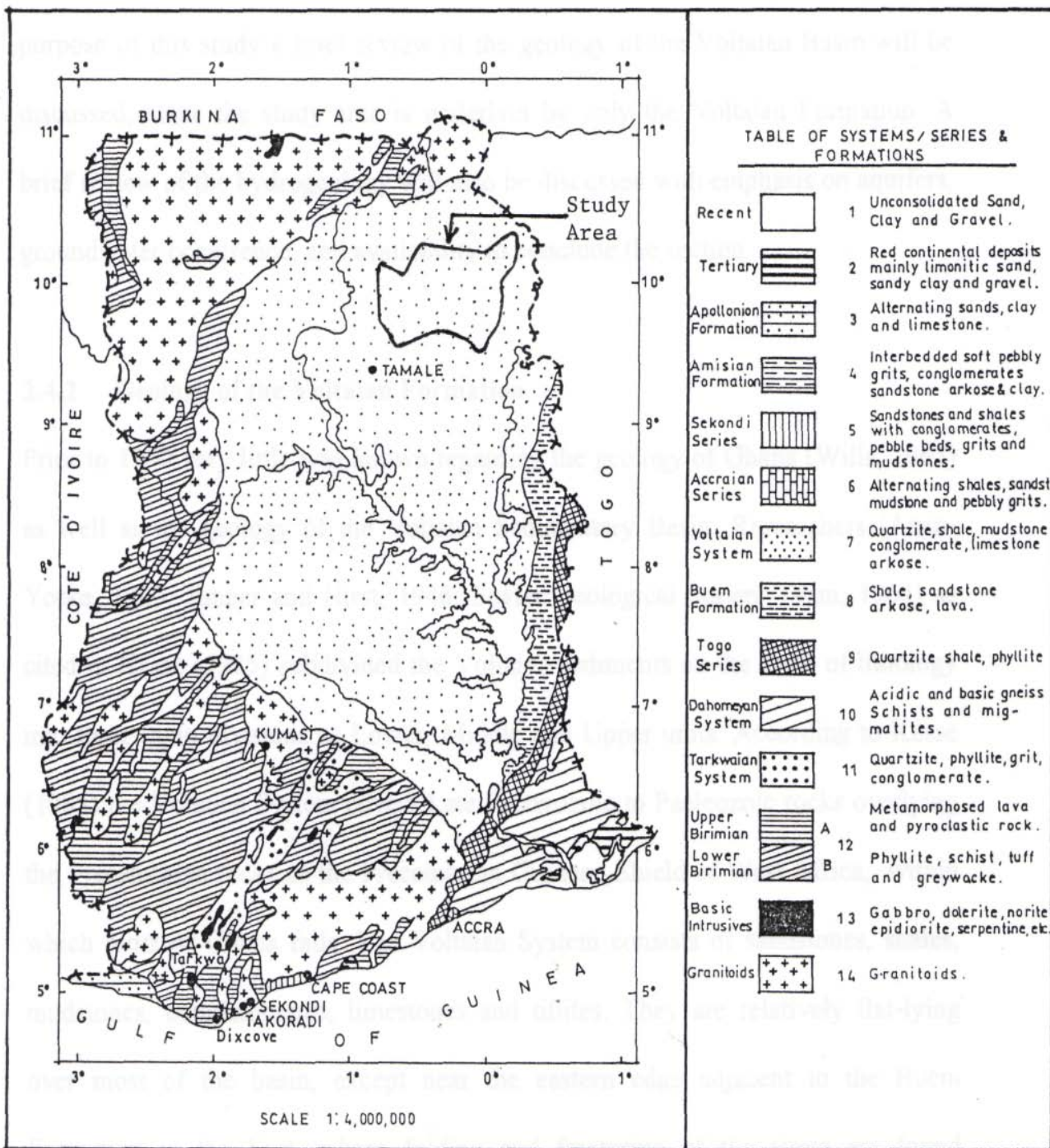


Fig 3.2b. Geological map of Ghana (After Kesse, 1985).

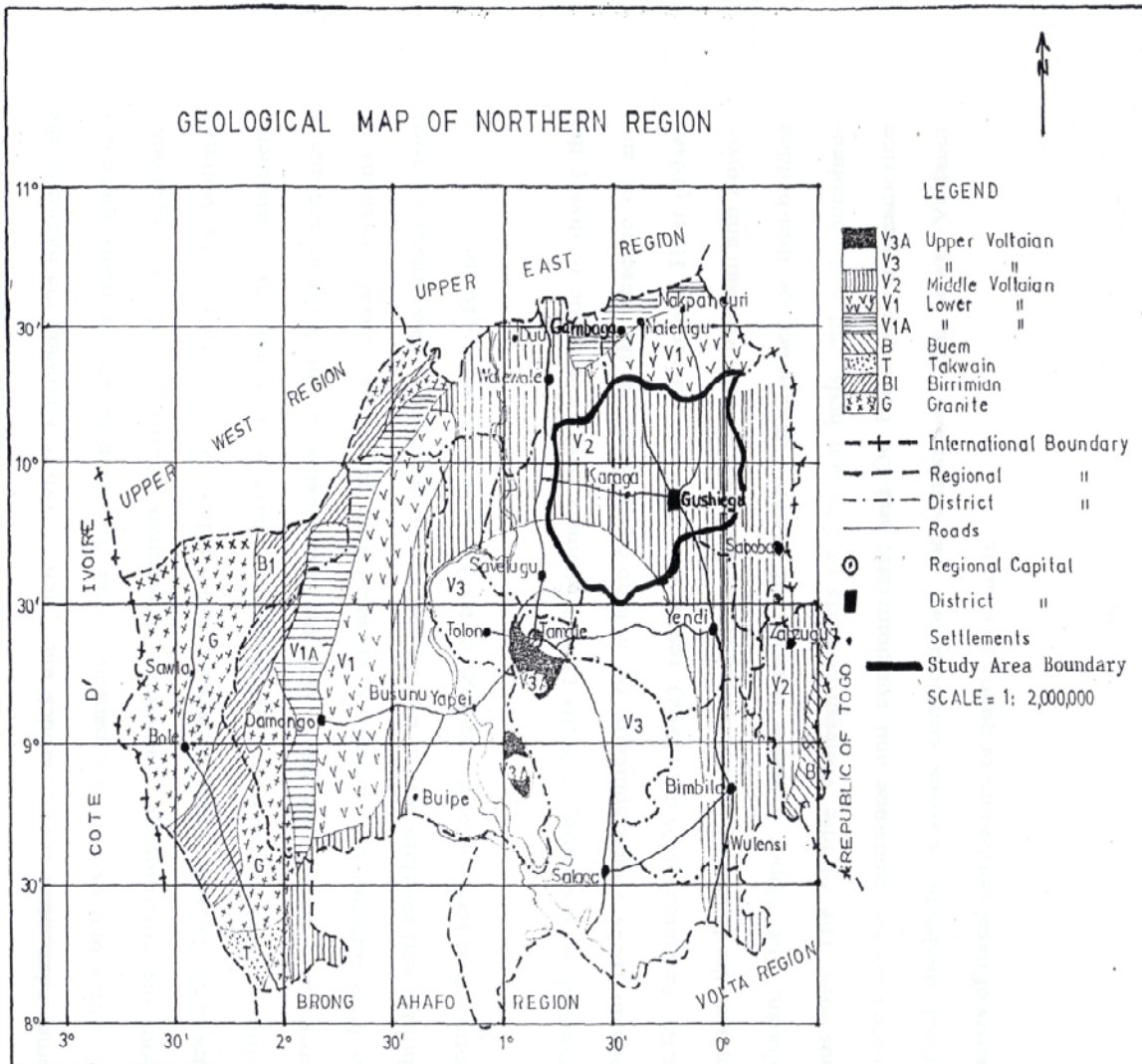


Fig 3.2c. Geological map of the Northern Region of Ghana (After Kesse, 1985).

3.3. SOCIO-ECONOMIC CONDITION

Studies conducted by Asante et al (2002) show a high probability of out migration in communities with scarce, low-quality drinking water sources. They also provide some analysis of water-related diseases and relate migration to water access in the Volta Basin. Economic activities are virtually non-existent

since the people depend on subsistence agriculture to sustain a living. With the increasing irregularity of rainfall patterns, huge annual crop losses occur which discourage a good many from engaging in this enterprise. Accordingly, over 59% of the rural population lives in extreme poverty (Ghana Statistical Service, 2000b). Poverty alleviation, especially in this area has been one of the major challenges in Ghana (Engel, et al 2003). The road map to this, however, begins with a sustainable water supply system. Groundwater resources constitute the most viable solution to the rural water supply problems and strenuous efforts are being made to assess our fortunes in terms of these resources in Ghana. This is particularly significant in the face of interests of government in utilizing this resource for irrigation to boost the Agric sector and alleviate poverty in the rural areas, especially among the Volta Basin dwellers. The increasing popularity of groundwater resource as the solution to the water delivery system stems from the fact that the resource has certain features that make it attractive as a source of potable water supply (Quist et al., 1988).

CHAPTER FOUR

4.0 THE ELECTROMAGNETIC (EM) METHOD, PRINCIPLES AND FIELD PROCEDURES

The Electromagnetic (EM) method is based on the measurements of EM fields associated with alternating currents induced in the surface by a primary field. The primary inducing field is produced by passing an alternating current through a coil or along a long wire placed over the ground. The primary field spreads out in space both above and below the ground and induces currents in subsurface conductors, according to the laws of EM induction. These currents create secondary EM fields, which distort the primary field. In general, the resultant field, which may be picked by a suitable receiving coil, will differ from the primary field in intensity, phase, and direction and reveal the presence of the conductors. A major advantage of these methods over the electrical resistivity methods is that they do not require conductive ground connections (Sharma, 1986). However, in the presence of a conducting body the magnetic component of the EM field penetrating the ground induces alternating currents, or eddy currents, to flow in the conductor (Fig 4.1).

4.1. ELEMENTARY ELECTROMAGNETIC THEORY

An electromagnetic field may be described by four field vectors: E, H, B, and D. Maxwell's equations in a form which relate these electric and magnetic field vectors are:

$$\nabla \times \mathbf{E} = -\partial \mathbf{B} / \partial t \quad \dots \quad (1)$$

$$\nabla \times \mathbf{H} = \mathbf{J} + \partial \mathbf{D} / \partial t \quad \dots \quad (2)$$

$$\nabla \cdot \mathbf{B} = 0 \quad \dots \quad (3)$$

$$\nabla \cdot \mathbf{D} = \rho \quad \dots\dots\dots (4)$$

Where \mathbf{E} is the electric field intensity (Vm^{-1})

\mathbf{B} is the magnetic flux density (Wbm^{-2} or Tesla)

\mathbf{H} is the magnetic field density (Am^{-1})

\mathbf{J} is the current density (Am^{-2})

\mathbf{D} is the electric displacement (Cm^{-2}) and

\mathbf{Q} is the electric charge density (Cm^{-3}).

The physical meaning or significance of these equations are summarized as follows: Equation (1) is the mathematical statement of Faraday’s law of electromagnetic induction; which states that electric field exists in a region of a time-varying magnetic field, such that the induced e.m.f is proportional to the negative rate of change of magnetic flux. Equation (2) contains the statement of Ampere’s law: every current flow produces a magnetic field around itself, which is proportional to the total current (conduction plus displacement current). Equation (3) simply states that isolated magnetic poles (magnetic single poles) do not exist. Equation (4) is the mathematical statement of Coulomb’s law: the lines of electric field start from and end on electric charges.

4.2 Fundamental Physical Quantities and Field Equations

In homogenous isotropic media the physical quantities relating the electric and magnetic field vectors are:

$$\mathbf{D} = \epsilon \mathbf{E}; \mathbf{B} = \mu \mathbf{H}; \mathbf{J} = \sigma \mathbf{E} \quad \dots\dots\dots (5)$$

where ϵ is the dielectric permittivity (Fm^{-1}), μ is the magnetic permeability (H/m), and σ is the electric conductivity (mhm^{-1}) of the medium.

According to Grant and West (1965), by using these relationships we can reduce or simplify Maxwell’s

equations in terms of only two vectors, \mathbf{E} and \mathbf{H} . Further, by assuming for \mathbf{E} and \mathbf{H} a time dependence of the form $\mathbf{E}(\mathbf{t}) = \mathbf{E}_0 e^{i\omega t}$, it can be proved that equations (1) and (2) take the following form (See Appendix A).

$$\nabla^2 \mathbf{E} = i\omega\mu\sigma\mathbf{E} - \epsilon\mu\omega^2\mathbf{E} \dots\dots\dots (6)$$

$$\nabla^2 \mathbf{H} = i\omega\mu\sigma\mathbf{H} - \epsilon\mu\omega^2\mathbf{H} \dots\dots\dots (7)$$

Where $\omega (=2\pi f)$ is the angular frequency of the field. These are basic equations for propagation of electric and magnetic field vectors in an isotropic homogenous medium with physical properties ϵ, μ , and σ . In air and poorly conducting rocks, $\sigma = 0$, $\epsilon = \epsilon_0 = 8.85 \times 10^{-12} \text{ Fm}^{-1}$ and $\mu = \mu_0 = 4\pi \times 10^{-7} \text{ Hm}^{-1}$.

With these small values, both the real and imaginary parts become so small that the right-hand side of equations (6) and (7) are practically zero. Therefore, for non-conducting media or rocks the field equations become

$$\nabla^2 \mathbf{E} = 0, \quad \nabla^2 \mathbf{H} = 0 \dots\dots\dots (8)$$

However, in media of moderate to high conductivity such as saline water, massive sulphide and graphite we have $\sigma \approx 1-10^3 \text{ mhm}^{-1}$, $\epsilon \approx 10\epsilon_0$ and $\mu \approx \mu_0$. With these values the first terms on the right-hand side of equations (6) and (7) become quite significant, but the second terms are still negligible. Therefore, in media or rocks of appreciable or finite conductivity, the equations are simplified to

$$\nabla^2 \mathbf{E} = i\omega\mu\sigma\mathbf{E}, \quad \nabla^2 \mathbf{H} = i\omega\mu\sigma\mathbf{H} \dots\dots\dots (9)$$

The relative magnitude of the term $\omega\mu\sigma$ is of great physical significance, both with regard to the attenuation of electromagnetic fields and the generation of induced fields (Sharma, 1986).

4.2.1 Electromagnetic Field Attenuation

According to Sherrif (1991), attenuation is the reduction in amplitude or energy caused by the physical characteristics of the transmitting media or system, including geometric effects such as the decrease in amplitude of a wave with increasing distance from the source. This means that, as stated by Telford *et al.* (1994), the electromagnetic wave is attenuated in travelling through some media but not in free space. The attenuation is due to the interaction of the electromagnetic waves with matter as they are propagated through it. In effect, there is a decrease in amplitude or energy of the waves.

The amplitude of a plane wave is reduced by the factor $e^{-\alpha z}$ in travelling a distance of Z meters, where the attenuation factor is α (Sheriff, 1991). It can be shown (Appendix B) from the solution of Equation (9) that the attenuation factor is given by

$$\alpha = \sqrt{\omega\mu\sigma/2} \dots\dots\dots (10)$$

The physical meaning, as given by Telford *et al.*(1994) is that when α is small, the magnetic field will propagate through the medium without much attenuation and in the process fail to induce any appreciable current flow in it. Consequently, very little secondary magnetic field will be generated. Consequently, when α is large, the large surface creates a large secondary magnetic field, out of phase with the original, which partially or completely cancels the primary field. Since $\omega=2\pi f$, α is frequency dependent (as well as conductivity σ). Thus the rate of attenuation depends on the frequency and the electrical properties of the rock material through which the electromagnetic wave travels. Therefore, the higher the frequency, the greater the rate of attenuation (Dobrin and Savit, 1988).

4.2.2 Depth of Penetration of Electromagnetic Fields

The depth of penetration, Z_s , can be defined as the depth at which the amplitude of the field A_z , is decreased by the factor e^{-1} compared with its surface amplitude A_0 . (i.e. $A_z=A_0e^{-1}$). The depth of penetration of electromagnetic field depends upon its frequency and the electrical conductivity of the medium through which it is propagating (Kearey and Brooks, 1984). However, since the attenuation factor, α also depends on frequency and electrical conductivity, the depth of penetration, Z_s will in turn depend on the attenuation factor, α . The depth at which the amplitude is reduced to $1/e$ (i.e. of 37%) of its surface value is known as the skin depth, Z_s (Sharma, 1986; 1997). The depth of penetration is given by $Z_s = 1/\alpha$.

Thus from equation (10), Z_s is given by

$$Z_s = 1/\sqrt{(\omega\mu\sigma/2)} \dots\dots\dots (11)$$

Since $\omega=2\pi f$ and $\mu = \mu_0 = 4\pi \times 10^{-7} \text{Hm}^{-1}$, substituting in (11) we obtain

$$Z_s = 503.8/\sqrt{\sigma f} = 503.8(\sigma f)^{-1/2} \dots\dots\dots (12)$$

when Z_s is in metres (m), σ in siemen per metre (Sm^{-1}) and f in Hertz (Hz)

The depth of penetration thus increases as both the frequency of the electromagnetic field and the conductivity of the ground decreases. Therefore, the frequency dependence of the depth of penetration places constraints on the electromagnetic method. This is because very low frequencies are difficult to generate and measure (Kearey and Brooks, 1984). Moreover, electromagnetic methods are limited by depth of the induced current penetration. Therefore, electromagnetic methods are not used for oil exploration because of the depth penetration limitation (Robinson and Coruh, 1988).

4.3. PRINCIPLE OF THE GEOPHYSICAL ELECTROMAGNETIC METHOD

The underlying basic principle of the geophysical EM method is the principle of electromagnetic induction. EM methods are based on the measurement of EM fields associated with alternating current induced in the subsurface by a primary field (Sharma,1986).

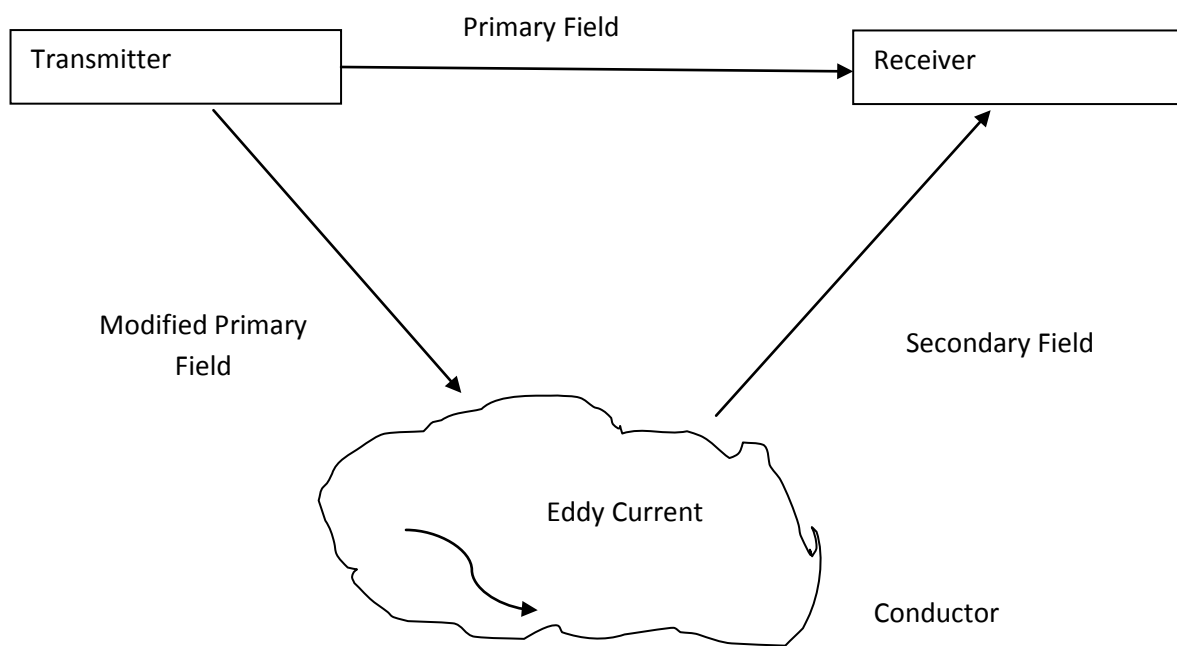


Fig 4.1. General Principle of EM surveying (Keary and Brooks, 1987).

An alternating current is passed through the transmitter coil of many turns of wire, which generates the primary or inducing field. The primary field spreads out in space, both above and below the ground or surface and induces alternating or eddy currents, to flow in the subsurface conductor, in accordance with the laws of EM induction. The eddy currents generate secondary EM field, which travel to the receiver as shown in Fig 4.1 The receiver coil then responds to the resultant field due to the primary and secondary

fields. The resultant field response differs from the response from the primary field alone in amplitude (intensity), phase, and direction. These differences between the transmitted and received EM fields reveal the presence of the conductor and provide information on its geometry and electrical properties (Kearey and Brooks, 1984; Sharma, 1997).

4.3.1 Theory of the Geophysical Electromagnetic Method

A time-varying magnetic field arising from alternating current in the transmitter coil, T_x induces very small currents in the earth (assumed uniform). These induced currents generate a secondary magnetic field, H_s which is sensed, together with the primary field, H_p by the receiver coil, R_x located at a short distance, S from the transmitter coil as in Fig 4.2 (McNeil, 1980).

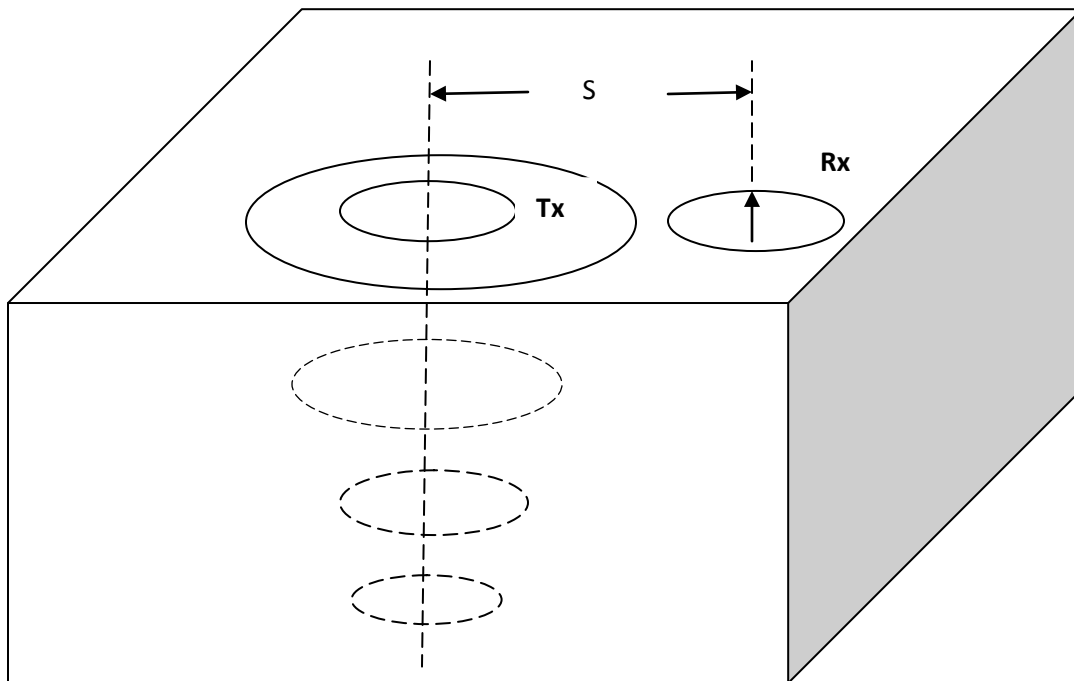


Fig 4.2 Induced current flow in homogenous half space (Modified after McNeil, 1980).

In general the secondary magnetic field, H_s , is a complicated function of the intercoil spacing s , the operating frequency f , and the ground conductivity σ . However under certain constraints (Appendix C), the secondary magnetic field H_s is a very simple function of these variables. The constraints (condition of low induction numbers) are incorporated in the design of the GEONICS EM 34-3 equipment so that the secondary magnetic field is given by

$$H_s/H_p = i\omega\mu_0\sigma s^2/4 \dots\dots\dots (13)$$

Where H_s = Secondary magnetic field at the receiver coil,

H_p = Primary magnetic field at the receiver coil,

$$i = \sqrt{-1}$$

$$\omega = 2\pi f$$

f = frequency (Hz)

μ_0 = permeability of free space,

σ = ground conductivity (mohm^{-1})

s = intercoil spacing (m)

The ratio of the secondary to the primary magnetic field is now linearly proportional to the terrain conductivity, σ . This is a fact, which makes it possible to construct linear terrain conductivity meter to give a direct reading by simply measuring the ratio.

Given H_s/H_p , the apparent conductivity, σ_a indicated by the instrument is defined as

$$\sigma_a = (4/\omega\mu_0s^2) \times (H_s/H_p) \dots\dots\dots (14)$$

where σ_a is in mho (siemen) per metre or millimho per metre.

Substituting $\omega=2\pi f$ in equation (2.25) we obtain

$$\sigma_a = (4/ 2\pi f \mu_0 s^2) \times (H_s/H_p) \dots\dots\dots(15)$$

$$\text{Therefore , } \sigma_a = (2/ \pi f \mu_0 s^2) \times (H_s/H_p) \dots\dots\dots(16)$$

This gives the apparent conductivity, σ_a in terms of the frequency, f and intercoil spacing, s .

Substituting k for $(4/ 2\pi f \mu_0 s^2)$

$$\text{We have } \sigma_a = k \times (H_s/H_p) \dots\dots\dots(17)$$

Where $k=(4/ 2\pi f \mu_0 s^2) = \text{constant}$

4.3.2 Field Parameters Measured

The Geonics EM 34-3 instrument, is designed to directly measure linear conductivity under certain constraints defined as ‘operation under low induction number’ by simply measuring the ratio of secondary and primary magnetic fields. Given the ration H_s/H_p , the apparent conductivity, σ_a , indicated by the instrument, at a given frequency f and intercoil spacing, S , is defined as;

$$\sigma_a = (2/ \pi f \mu_0 s^2) \times (H_s/H_p)$$

It should be noted that the linear relationship between the ratio H_s/H_p and σ_a holds only for low to moderate conductivities. The breakdown point for the EM 34-3 is 200 mS/m when the coils are oriented in the vertical dipole mode and about 1000 mS/m when the orientation is in the horizontal dipole mode (Sharma, 1997). However, the range of conductivities encountered during this project was far below the breakdown point of the instrument.

4.4. CONDUCTIVITY IN ROCKS

Basically the electrical conductivity (σ) of a substance is a measure of the ease or difficulty with which an electrical current can be made to flow through it. With an exception – metallic minerals, graphites and some clay – most soil materials are poor conductors and any significant current flow in these soils is mainly due to the included water and its ionic content. It is expressed mathematically as (McNeil et al., 1995):

$$\sigma = G L / A \text{ mhos/m.}$$

Where $G = I/V$ mhos, $A =$ area, $V =$ voltage, $I =$ current and $G =$ conductance.

4. 4. 1. Factors affecting terrain conductivity

Most soil and rock minerals are electrical insulators of very high resistivity. However, on rare occasions conductive minerals such as magnetite, specular hematite, carbon, graphite, pyrite and pyrrhotite occur in sufficient quantities in rocks to greatly increase their overall conductivity. This note assumes that minerals are absent (McNeill, 1980).

The effective resistivity of the rock can be expressed in terms of the resistivity and volume of the pore water present according to an empirical formula due to Archie (1942).

$$\rho_e = a\Phi^{-m}S^{-n}\rho_w \dots\dots\dots(18)$$

where ρ_e is the effective resistivity of the rock, Φ is the fractional pore volume (porosity), S is the fraction of the pores containing water, ρ_w is the resistivity of water in pores, $n=2$, and a, m are empirical constants: $0.5 \leq a \leq 2.5, 1.3 \leq m \leq 2.5$. But ρ_w can vary considerably according to the quantities and conductivities of dissolved salts as chlorides, sulphates, and other minerals present. Electrical

conductivity is, therefore, determined (McNeil, 1980) for both rocks and soils by

Porosity: shape and size of pores, number, size and shape of interconnecting passages

The extent to which pores are filled by water that is, the moisture content

The concentration of dissolved electrolytes in the contained moisture

Temperature and phase state of the pore water

Amount and composition of colloids (McNeill, 1980).

4.5 INSTRUMENTATION AND FIELD PROCEDURE

The EM 34-3 instrument designed by Geonics Limited, Canada was used during this project to locate groundwater potential zones for siting boreholes, by measuring the ground conductivity. This instrument employs electromagnetic (inductive) techniques. A special feature is that, the operating frequency and coil separation are chosen such that a direct readout of ground conductivity in millimhos per meter can be obtained at selected depths.

4.5.1 Instrument Hardware

The EM 34-3 equipment consists of a battery operated transmitter and receiver unit, a transmitter and receiver coil or loop of about 800 mm in diameter. It uses three frequency/coil spacing pairs. The coil spacings are 10, 20, and 40 m, using frequencies of 6400, 1600, and 400 Hz respectively. The operational range of the instrument is 1-1000 mS/m (Sharma, 1997).

4.5.2 Operation of Geonics EM 34-3 Instrument

The instrument is simple to operate. The coils are placed at a known distance apart and coplanar, either

both horizontal on the ground or both vertical. The transmitter is turned on and the distance between the transmitter and receiver is adjusted. The apparent terrain conductivity is then read from the receiver directly. When both coils are placed horizontally on the ground, the transmitter generates an electric field with a vertical dipole, thus this is called the vertical dipole mode. Similarly, when the coils are vertical the equipment is in the horizontal dipole mode. The vertical dipole mode has a greater penetration depth than the horizontal dipole mode. Where the vertical dipole conductivity exceeds the horizontal dipole reading, the main contribution to the ground conductivity is coming from deeper than 39 % of the spacing between the coils. This fact allows the instrument to be used quantitatively to interpret the variation of ground conductivity with depth (Payne, 1990). Table 5-1 shows the exploration of ground conductivity with depths for the Geonics EM 34-3 instrument, at various intercoil spacing.

Table 4.1 Exploration depths for Geonics EM 34-3 at various intercoil spacing (McNeil et al., 1995).

Intercoil Spacing (meters)	Exploration Depths (meters)	
	Horizontal Dipoles	Vertical Dipoles
10	7.5	15
20	15	30
30	30	60

4.6 FIELD PROCEDURES

4.6.1 TERRAIN EVALUATION

Terrain evaluation is an inherent part of every groundwater exploration programme. It precedes all geophysical investigations and its main objective is to locate the best site for carrying out geophysical surveys, by identifying surface features, which are characteristic indicators of the presence of subsurface water bearing formations.

It involves a very careful observation of the surface physiographic and geologic features in the survey area such as vegetation, outcrops, stream patterns, springs, the location of any previous boreholes or wells, exposed fractures and the direction of runoffs or the slope of the terrain. Much information is also sought from members of the community, on environmentally prohibitive locations such as rubbish dumps, cemeteries and toilets.

After collating all this information, suitable locations are then demarcated for geophysical surveys.

4.6.2 ELECTROMAGNETIC TRAVERSING METHOD

The objective of an electromagnetic traverse is to locate areas where the pattern of ground conductivity, matches a hydrogeological and geophysical model for a high yielding aquifer.

The transmitter and receiver units are contained in small shoulder bags and handled together with their individual separate coils. The principal coil spacing must be determined. Where the depth to static water is less than 15 meters, a 20 meter coil spacing should be used, but where greater than 15 meters, the coil spacing should be 40 meters (Beeson and Jones, 1988). Hence, the former was used because the depth to static water level was less than 15 meters for most of the areas under study. The transmitter and receiver

are connected by a cable, whose length is that of the required coil spacing.

The traverse is carried out with the receiver ahead of the transmitter, in the direction of the traverse. The transmitter operator stops at the measurement station and the receiver operator moves the receiver coil backward or forward until his meter indicates correct inter-coil spacing. He then marks this position and reads the terrain conductivity from a second meter also on the receiver. The conductivity read is an apparent value because the sub-surface is non-homogenous.

During traversing, attention is paid to areas which have adequate conductance at depth; this is normally indicated by values of the vertical dipole being greater than those of the horizontal dipole (Beeson and Jones, 1988). When such an anomalous feature is located, the centre point is marked and recorded on field sheets. It is interesting to note that when used in the vertical dipole mode (horizontal coil system) the device is responsive to the presence of relatively low-conductivity steeply dipping structures such as water bearing fracture zones, whereas in the horizontal dipole mode (vertical coil system) the device is quite insensitive to such structures and give fairly accurate measurements of ground conductivity in close proximity to them (Sharma, 1997).

When the survey is completed, the various anomaly patterns are analysed and the most promising sites selected for drilling. It should be mentioned that, World Vision International (WVI) has been engaged in groundwater exploration in this area for sometime and the knowledge acquired through experience is that the results from electromagnetic profiling, normally give good indications of potential borehole sites. This is why Vertical Electrical Sounding (VES), was not carried out before drilling. However, it is recommended that an integrated approach (the use of several geophysical techniques in the same area to investigate a sub-surface feature) should be adopted in future exploration work by WVI in the study area. This is because every geophysical method has its own limitations in the type of information it provides; a

combination of two or more methods generally yields extra information which may help to reduce the ambiguity inherent in the interpretation of some types of geophysical data (Sharma, 1986). This would help minimize the unpleasant situation of drilling dry holes, thereby increasing their rate of success.

CHAPTER FIVE

5.0 ANALYSIS AND INTERPRETATION OF THE FIELD RESULTS

5.1 QUALITATIVE INTERPRETATION OF THE FIELD RESULTS

Although many of the geophysical methods require complex methodology and relatively advanced mathematical treatment in interpretation, much information may be derived from a simple assessment of the survey data (Keary and Brooks, 1984).

In all survey methods it is the local variation in a measured parameter, relative to some normal background value, that is of primary interest. Such variation is attributed to a localized sub-surface zone of distinctive physical property and possible geological importance. A local variation of this is known as a geophysical anomaly (Keary and Brooks, 1984).

In general, interpretations of geophysical anomalies are inherently ambiguous because any given anomaly could be attributed to an infinite number of possible sources (Parasnis, 1986). Hence, an important task in interpretation is to decrease this ambiguity by using all available external constraints on the nature and form of the anomalous body. Such constraints include geological information derived from surface outcrops, boreholes, mines and from other complementary geophysical techniques (Keary and Brooks, 1984).

In this chapter, the terrain conductivity data measured along traverses in all the communities in the study area has been presented. The graphical plots show the variation of the terrain conductivity along the profiles, using the 20 meter intercoil spacing in both the horizontal and vertical dipole modes. The approximate depths of investigation for the two dipole modes are given as;

Horizontal dipole mode: 15 meters

Vertical dipole mode: 30 meters

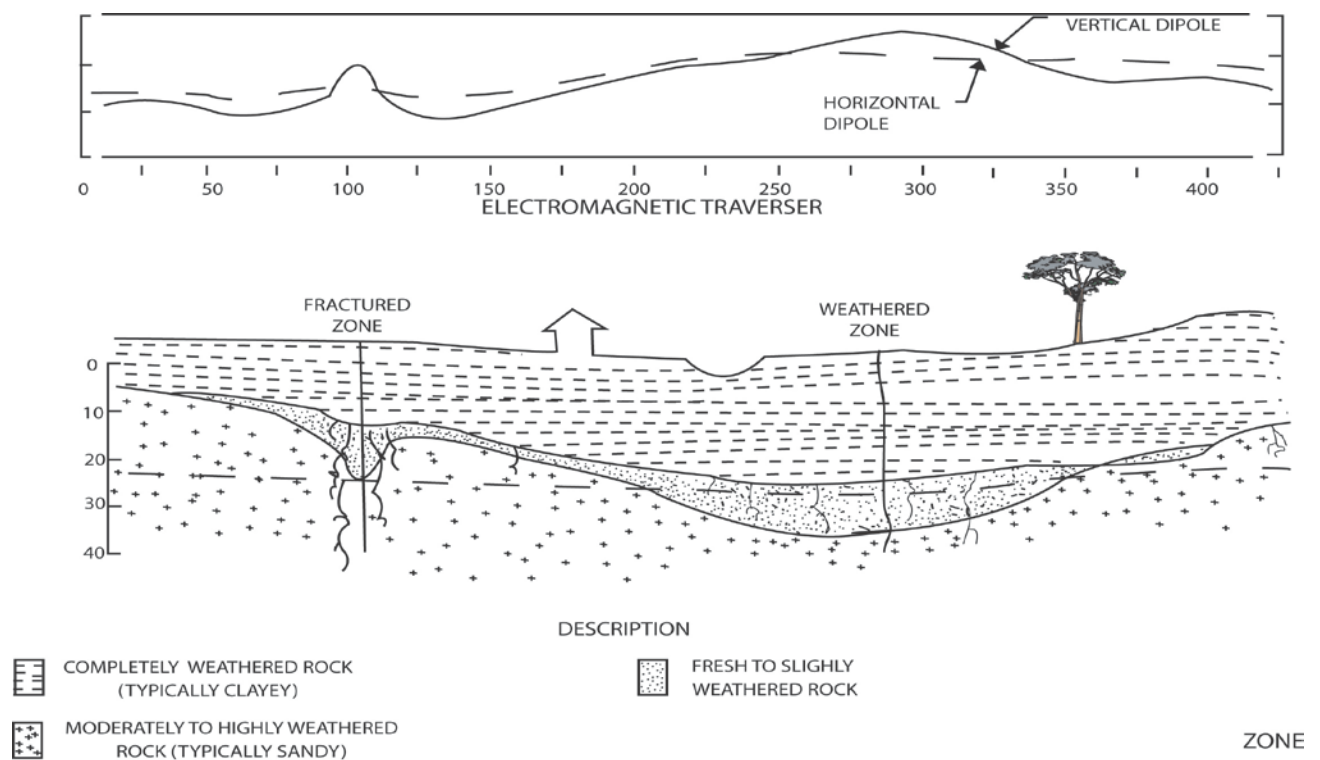
5.2 GEOPHYSICAL CRITERIA FOR THE SELECTION OF DRILLING POINTS

Interpretations were carried out qualitatively on the basis that fractured and deeply weathered subsurface zones, which have a high potential for groundwater accumulation, produce on the plotted traverses, sharp positive peaks of a deeper electromagnetic response crossing over the peak of a shallower response. An anomaly of this kind is referred to as a cross-over and it's indicated by values of the vertical dipole mode being greater than those of the horizontal dipole mode (VRWSS, Vol III). An example of such a geophysical model with the conductivity response in the vertical dipole and horizontal dipole modes is shown in Fig. 6.1. Such anomalies give evidence of the presence of weathered or fractured subsurface zones, with possible groundwater potential. Sometimes high conductivity zones which show a coincidence in the values of the vertical and horizontal dipole modes, usually referred to as a 'neck', can also be suitable sites to locate boreholes.

The response of the conductivity meter to fracture zones and weathered zones are characterized by high electrical conductivities in both the vertical and horizontal dipole modes relative to background levels, and a higher conductivity for the vertical dipole than for the horizontal dipole as shown in Fig 6.1 (modified after Palacky et al.,).

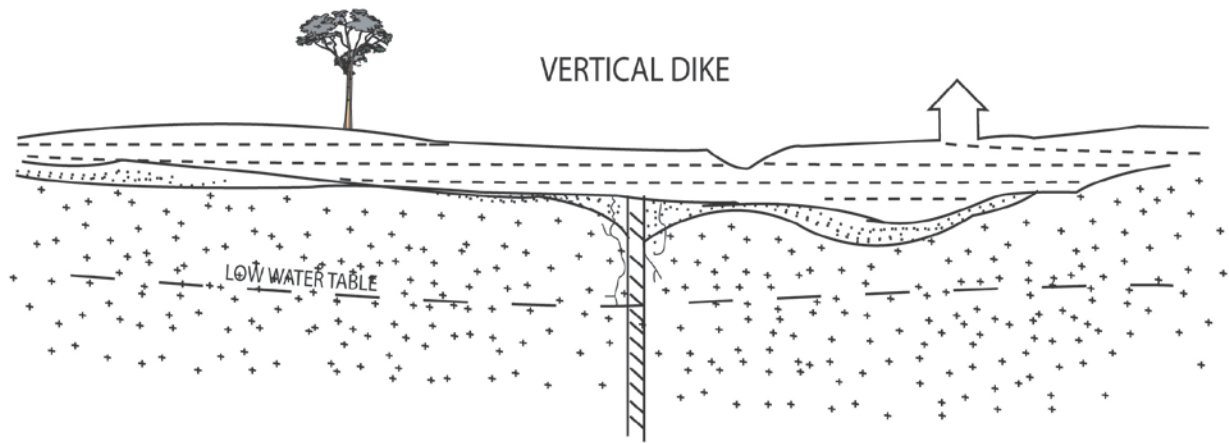
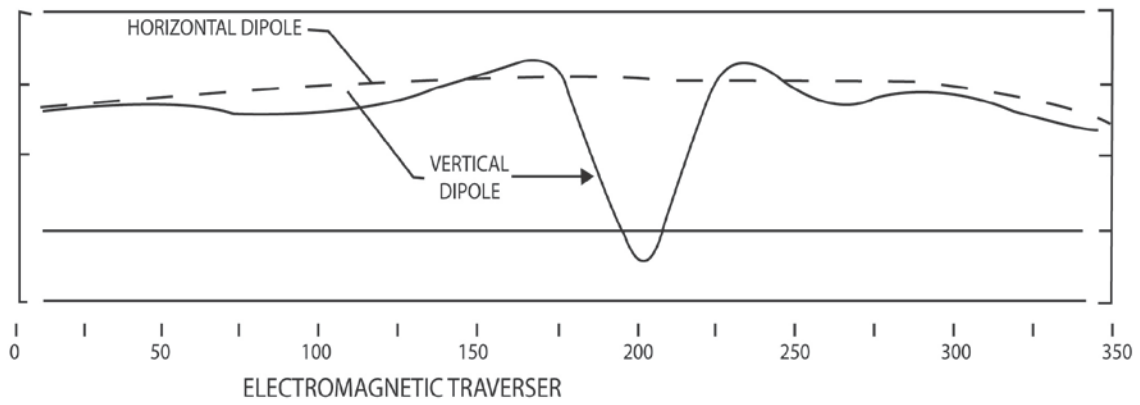
The EM conductivity meter responds to highly conductive vertical dikes or a highly conductive material that has been masked in a manner which is significantly different from its response to other subsurface features. The curve is characterized by very low or negative readings over the dike and relatively high readings from the material as shown in Fig 6. 2 (modified after McNeil, 1980).

In addition to these criteria, knowledge of the target range of the terrain conductivity values for groundwater in the study area is also helpful. Within the areas dominated by shales, groundwater usually occurs when the terrain conductivity lies between 28-65 mS/m, while in the sandstone areas the target range of the terrain conductivity values for groundwater is 12-24 mS/m. These ranges of values are all considered in the selection of potential drilling points.



Geophysical model: Frature and weathered zones Modifiec after Palacky et al., 1981

Fig 5.1 Geophysical Model: fractured zone and weathered zone (Modified after Palacky et al., 1981).



DESCRIPTION

- | | |
|---|--|
|  Completely weathered rock |  Fresh to slightly weathered rock |
|  Moderately to highly weathered rock (dry) |  Highly conductive dike |

Geophysical model : Vertical dike (Modified after McNeill, 1980b)

Fig. 5.2. Geophysical model: Vertical dike (Modified after McNeill, 1980b).

5.3. INTERPRETATION OF FIELD RESULTS

5.3.1 Nakpoligu in the Gushiegu-Karaga District

Profile 1

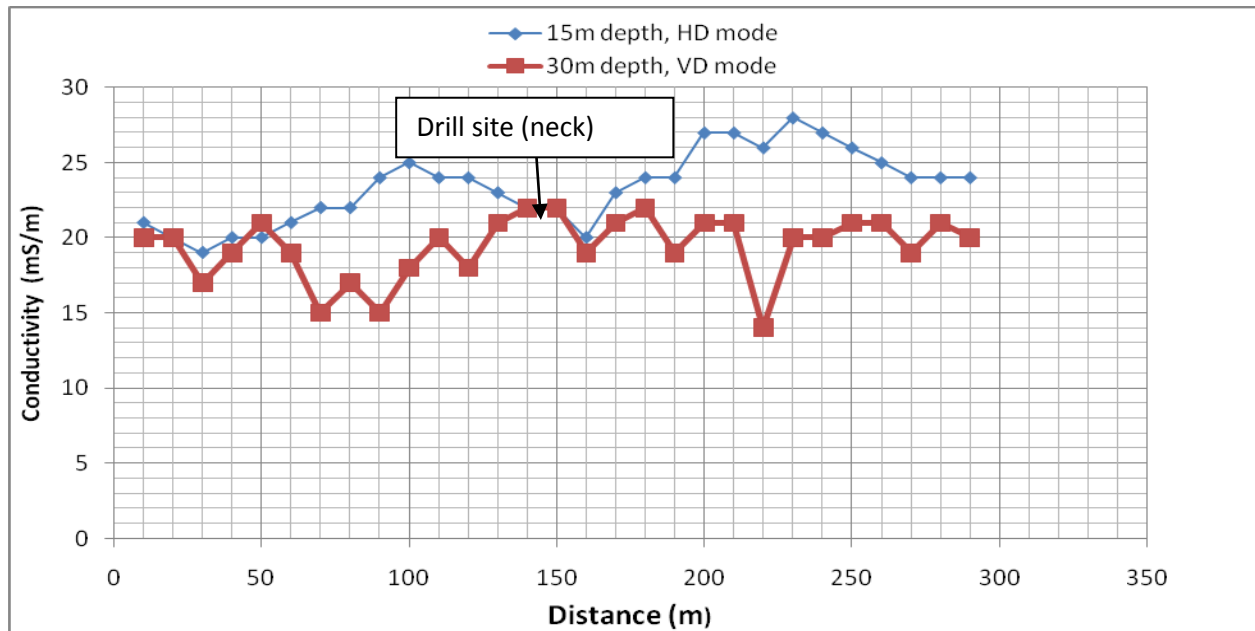


Fig 5.3. Terrain Conductivity measurements along profile 1 using a 20 m coil at Nakpoligu.

The results for the HD mode indicate that there is a decrease in terrain conductivity along the traverse up to the 30 m point with a value of 19 mS/m. It begins to increase gradually up to a value of 25 mS/m at the 100 m point. It then falls again until we obtain a “neck” between the 140 m point and the 150 m point. For the VD mode which shows an erratic graph, there is a decrease in the terrain conductivity up to the 30 m point with the value of 17 mS/m, after which there is a rise up to a value of 21 mS/m at the 50 m point. It then falls again and then gradually again until we obtain a “neck” between the 140 m and 150 m point with the value of 22 mS/m depicting a complex subsurface geology. This point was chosen as a potential drilling site because of the anomaly of a “neck” which is an indication of adequate conductance

at depth, which could also be due to fracturing or weathered zones and may constitute an effective exploitable source of ground water. The subsurface rocks are likely to be siltstone.

Profile 2

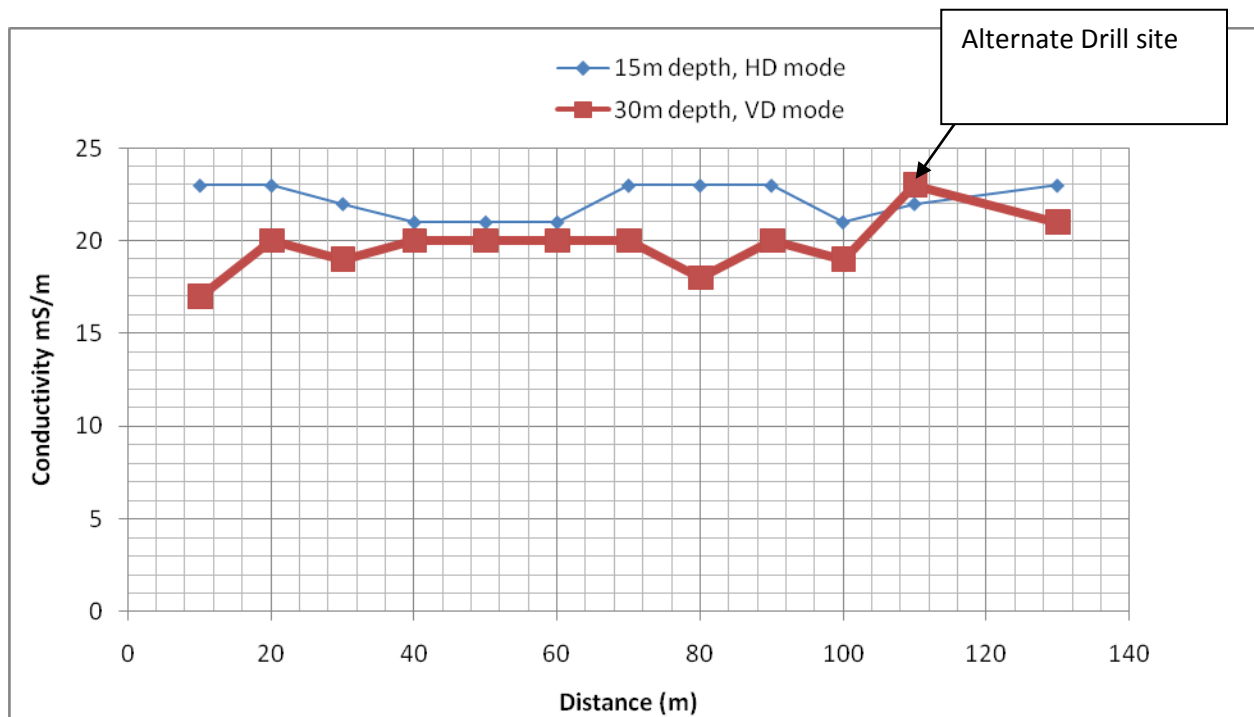


Fig 5.4. Terrain Conductivity measurements along profile 2 using the 20 m coil at Nakpoligu.

The results for the HD mode indicate an erratic behaviour which is seen in the decrease in terrain conductivity along the traverse from 23 mS/m up to the 60 m point with a value of 21 mS/m. It begins to increase back to the value of 23 mS/m again at the 90 m point. It is then followed by a decline in conductivity down to 21 mS/m at the 100 m point. Finally, there is an increase again back to the value of 23 mS/m at the 30 m point. For the VD mode, there is an increase in terrain conductivity up to the 40 m point with a value of 20 mS/m. This remains constant for a while up to the 70 m point. After this, there is

a decline again, followed by an increase in the terrain conductivity up to the 90 m point with the value of 20 mS/m. This is followed by a decrease in terrain conductivity again and then finally an increase in the terrain conductivity up to the 24 mS/m. At this point the anomaly observed was a “cross over” between the VD mode and the HD mode at the 110 m point with a terrain conductivity value of 23 mS/m; meaning that the VD value, which has a deeper penetration depth compared to the HD mode, is greater than the HD value at this point. This effect here could be as a result of a number of reasons but the most probable is a fractured or weathered zone, which has possible groundwater potential, hence, its selection as an alternate drilling site. This point however was not drilled as at the time of writing this report.

5.3.2 Yibeyili in the Gushiegu-Karaga District

Profile 1

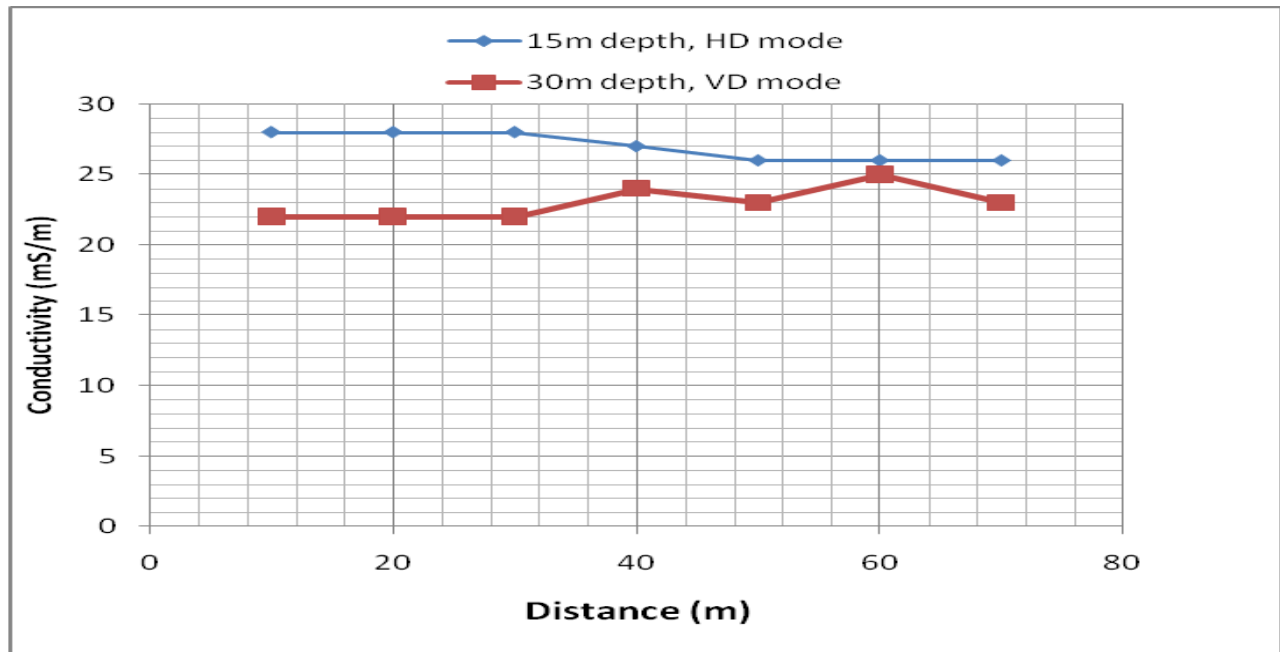


Fig 5.5. Terrain Conductivity measurements along profile 1 using the 20 m coil at Yibeyili.

The results of the HD mode from the beginning of the graph indicate a laterally homogenous subsurface with conductivities of 23 mS/m and 21 mS/m. This begins with an initial terrain conductivity with the value of 23 mS/m along the traverse until the 30 m point where there is a decline in the terrain conductivity down till the 50 m point with a value of 26 mS/m. This remains constant till the end of the traverse. For the VD mode, the results show a similar behaviour from the beginning of the traverse till the 30 m point with a terrain conductivity value of 24 mS/m, followed by a rise and fall until it arrives at the 60 m point with a value of 25 mS/m. This is finally followed with a fall at the end of the traverse. From the results obtained during this traverse in particular it was becoming increasingly obvious that the traverse was providing no interesting prospects for groundwater considering the nature of the behaviour

of the graph, hence the team decided to consider a second profile.

Profile 2

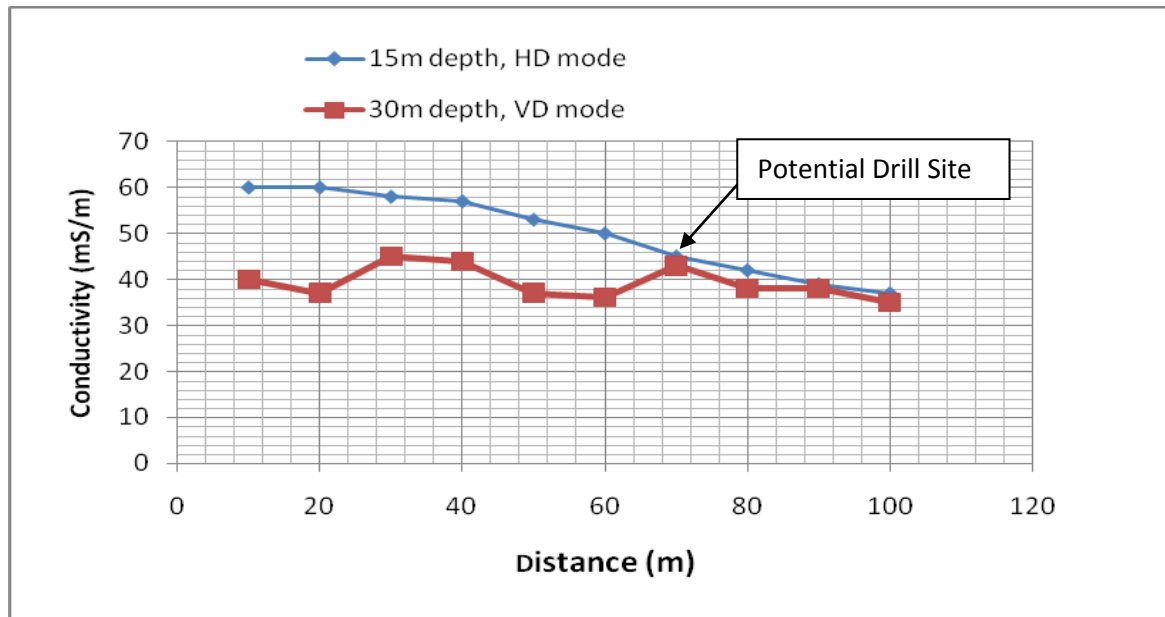


Fig 5.6. Terrain Conductivity measurements along profile 2 using the 20 m coil at Yibeyili.

The HD mode traverse depicts a constant decrease in terrain conductivity from a very high value of 60 mS/m down to the least value of 40 mS/m. But the erratic nature of the VD mode profile suggests a complex subsurface geology with an anomaly of a “neck” occurring at the 70 m point with a terrain conductivity value of 42 mS/m; where the “neck” refers to the point where the VD value at a point equals the HD value at that same point. This anomaly suggests an indication of adequate conductance at depth, which could also be due to fractured or weathered zone and may constitute an effective exploitable source of ground water. The subsurface rocks are likely to be siltstones.

5.3.3 Pishigu in the Gushiegu-Karaga District

Profile 1

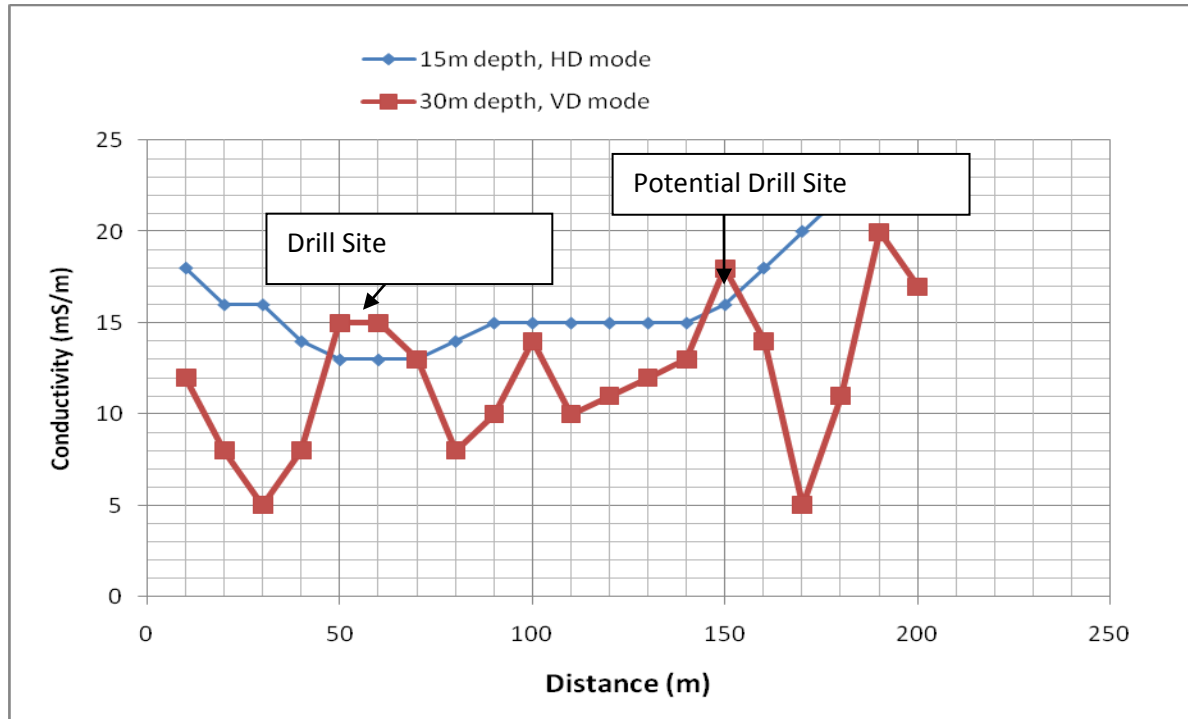


Fig 5.7. Terrain Conductivity measurements along profile 1 using the 20 m coil at Pishigu

The conductivities measured at the 15 m depth decrease from the first observation point which has a value of 18 mS/m to 13 mS/m at the 50 m point; it then rises to the value of 15 mS/m at the 90 m point. It then remains fairly constant for a while until it reaches the 140 m point. After this point there is a sharp rise from the 15 mS/m to 22 mS/m at the 180 m point. It then remains constant until the end of the profile. The conductivities of the 30 m depth show an erratic nature suggesting a complex subsurface geology. The anomaly observed here was at the 55 m point where there is a “cross over” between the HD mode and the VD mode. Hence, the choice of that point as a drilling site. A similar anomaly is observed at the 150 m point where there is another “cross over”, hence its selection as a potential

drilling site. The “cross over” could be attributed to a number of reasons but the most probable is a fractured or weathered zone, which has possible groundwater potential, hence the reason for their selection. Since the “cross over” points are mainly within the range of 10 to 20 mS/m, it can be speculated that the area was mainly made up of sandstones.

Profile 2

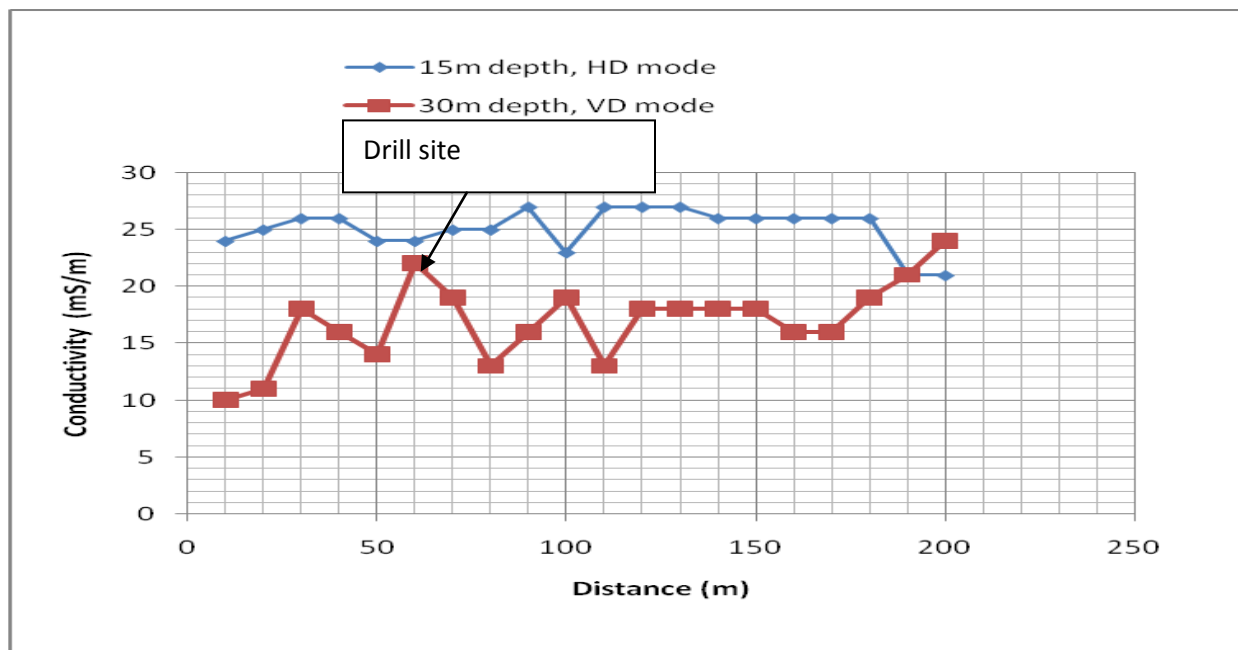


Fig 5.8. Terrain Conductivity measurements along profile 2 using the 20 m coil at Pishigu

The results for the HD mode indicate an increase in terrain conductivity along the traverse from the 10 m point at the value of 24 mS/m to a value of 26 mS/m at the 40 m point. It then decreases back to the 24 mS/m again at the 50 and 60 m point. This is followed by an increase in terrain conductivity up to the value of 27 mS/m at the 90 m point. After which there is a decrease in conductivity again down to a value of 23 mS/m and then an increase back to the value of 26 mS/m at the 110 m point. From this point to the 180 m point, the terrain conductivity remains constant. Finally there is a decrease in conductivity to a

value of 21 mS/m. For the VD mode, we observe an erratic behaviour in terrain conductivity beginning with an increase in conductivity from the value of 10 mS/m at the 10 m point to the 18 mS/m at the 30 m point. This is followed by a decline in conductivity down to the value of 14 mS/m at the 50 m point, after which there is a sharp rise in terrain conductivity up to the value of 22 mS/m at the 60 m point, then a decline again down to a value of 13 mS/m at the 80 m point. This erratic behaviour continues for a while until it assumes a constant value of 18 mS/m between the 120 and 150 m point. Finally, there is a decline again followed by a rise till the end. The anomaly observed was at the 60 m point where we note a sharp rise in terrain conductivity from the value of 14 mS/m up to the value of 22 mS/m. This anomalous behaviour gave room for some speculation for possible groundwater potential. This effect here could be as a result of a number of reasons but the most probable is a fractured or weathered zone, which have possible groundwater potential. Hence, its selection as an alternate drilling site. This point however was not drilled as at the time of writing this report.

5.3.4 Tindang in the Gushiegu-Karaga District

Profile 1

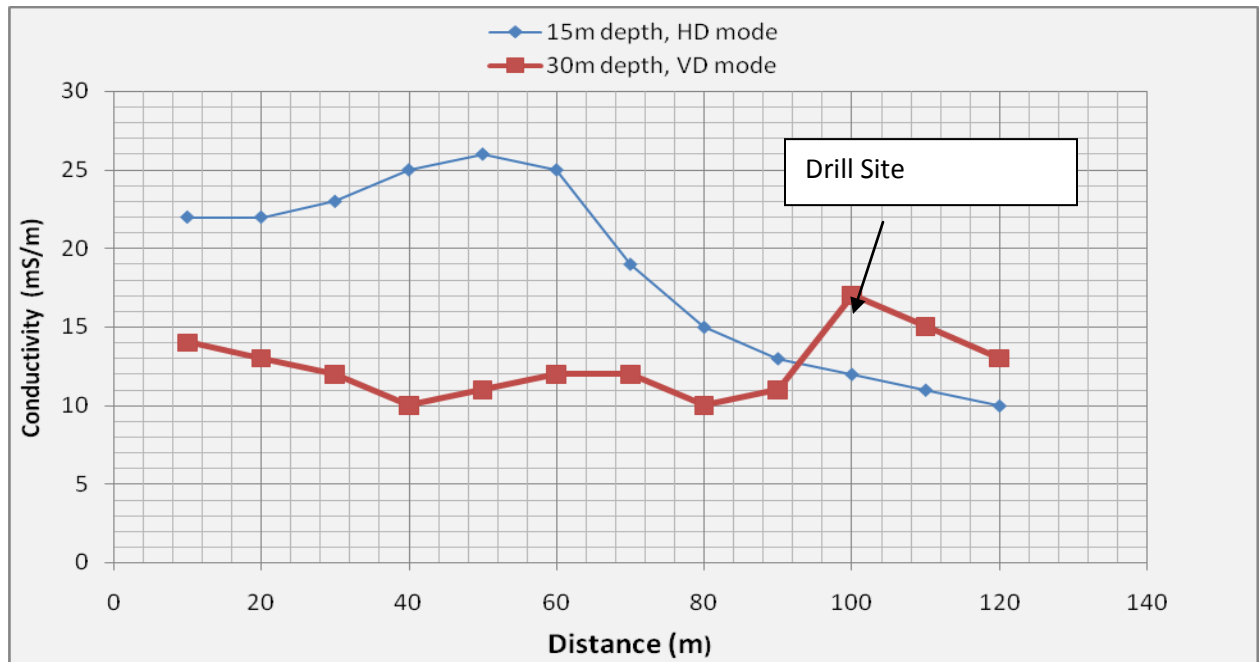


Fig 5.9a. Terrain Conductivity measurements along profile 1 using the 20 m coil at Tindang.

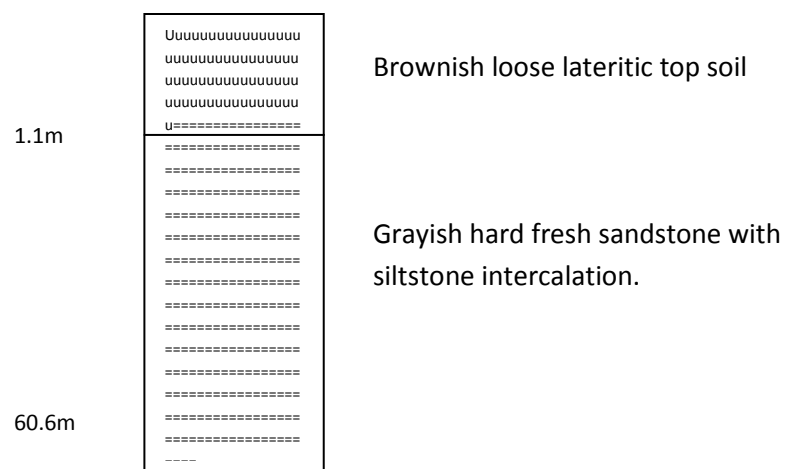


Fig 5.9b. Lithologic Log of point 30 m on profile 1 at Tindang.

The HD mode traverse depicts a constant increase in terrain conductivity from an initial value of 22 mS/m at the 10 m point up to a peak of 26 mS/m, from which it falls constantly till it gets to the minimum point of 10 mS/m. But the erratic nature of the VD mode profile suggests a complex subsurface geology with an anomaly of a cross-over occurring at the 100 m point with a terrain conductivity value of 17 mS/m. This means that the VD value, which has a deeper penetration depth compared to the HD mode, is greater than the HD value at this point. This effect here could be as a result of a number of reasons but the most probable is a fractured or weathered zone, which has possible groundwater potential. Hence, its selection as a possible drilling site. From the range of values of the VD mode, it can be speculated the area is mainly made up of sandstones.

The geological log on fig 6.9b indicates a two-layer earth model of this site after it was drilled. The top layer consists of brownish loose lateritic top soil of thickness 1.1 m, whilst the second layer is made up of grayish hard fresh sandstone with siltstone intercalations. The drilling was abandoned in this layer after no aquifer zone was intercepted at 60.6 m. The geophysical results agree very well with the geological log, because the results show that the subsurface could be sandstone and the log proves that, though there is an intercalation with siltstone.

Profile 2

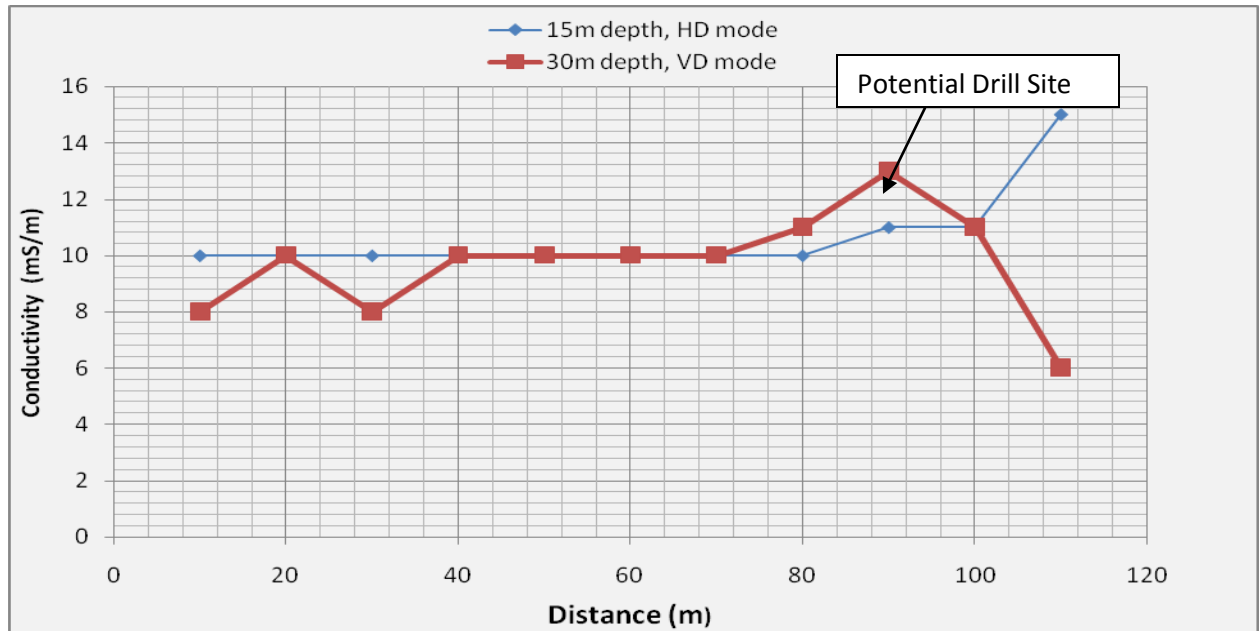


Fig 5.10. Terrain Conductivity measurements along profile 2 using the 20 m coil at Tindang

The results of the HD mode from the beginning of the graph indicate a laterally homogenous subsurface with a constant conductivity of 10 mS/m between the 10 m and the 80 m point. This is followed by a rise in conductivity up to a value of 15 mS/m. For the VD mode, there is an initial rise in terrain conductivity from the value of 8 mS/m at 10 m point up to a value of 10 mS/m at the 20 m point. This is followed by a fall in conductivity back to the initial value of 8 mS/m at the 30 m point. After this there is another rise in terrain conductivity back to the 10 mS/m again. This remains constant from the 40 m to the 70 m point. This is followed with a steady rise in conductivity to a value of 13 mS/m at the 90 m point. Finally, there is a decline in terrain conductivity right till the end of the traverse. The anomaly observed here was at the 20 m point where there is a “neck” between the HD mode and the VD mode. Hence, the choice of that point as a drilling site. A similar anomaly is observed at the 90 m point where there is another “cross over”, hence its selection as a potential drilling site. The “cross over” could be attributed to a number of

reasons but the most probable is a fractured or weathered zone, which has possible groundwater potential, hence the reason for their selection. Since the ‘cross over’ points are mainly within the range of 10 to 20 mS/m, it can be speculated that the area was mainly made up of sandstone.

5.3.5 Zulogu in the Gushiegu-Karaga District

Profile 1

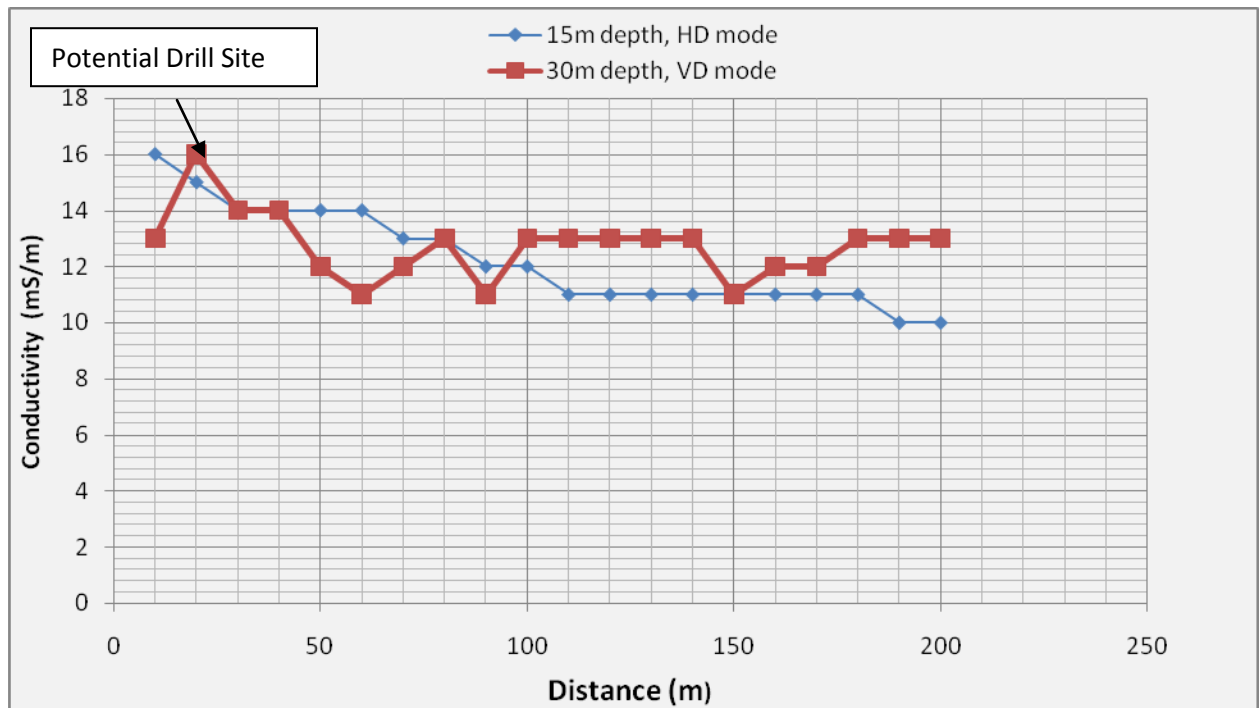


Fig 5.11. Terrain Conductivity measurements along profile 1 using the 20 m coil at Zulogu

The subsurface sampled by the HD mode profile depicts a step by step drop in terrain conductivity up to the 110 m point with a value of 11 mS/m where it remains constant for a long distance of 60 m and then falls again after that point as shown by the nature of the curve. The conductivity variation for the VD

mode is rather erratic, depicting a complex geology underground. The anomalies around the 20 and between the 100 and 140 m points could be due to a number of reasons, but most likely dike-like structures or a highly conductive material that has been masked by having negative responses. The 20 m point that has a conductivity of 16 mS/m and is also a “cross over” point was selected for drilling. Sandstones could possibly be the subsurface rocks here. This point however was not drilled as at the time of writing this report.

Profile 2

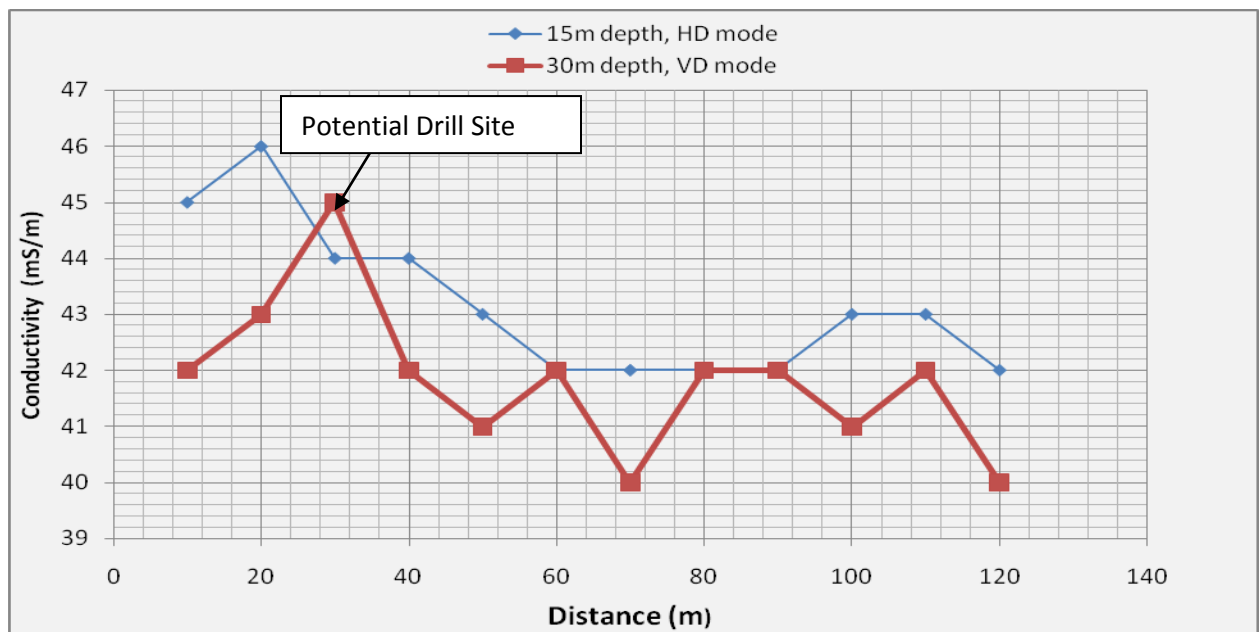


Fig 5.12. Terrain Conductivity measurements along profile 2 using the 20 m coil at Zulogu

The subsurface sampled by the HD mode of the second profile depicts an initial rise in terrain conductivity at the 20 m point with a high value of 46 mS/m. This is followed by a similar step by step drop in terrain conductivity up to a value of 41 mS/m at the 100 m point where it then rises and falls

shortly at the 110 m point with a value of 41 mS/m as shown by the nature of the curve. The conductivity variation for the VD mode is rather erratic, depicting a complex geology underground. The main anomaly which occurs at the 30 m point with a value of 45 mS/m could be due to a number of reasons, but most likely dike-like structures or a highly conductive material that has been masked by having negative responses. This point that has a conductivity of 16 mS/m and is also a ‘‘cross over’’ point was selected for drilling. This point however was not drilled as at the time of writing this report.

5.3.6 Gorgu in the Gushiegu-Karaga

Profile 1

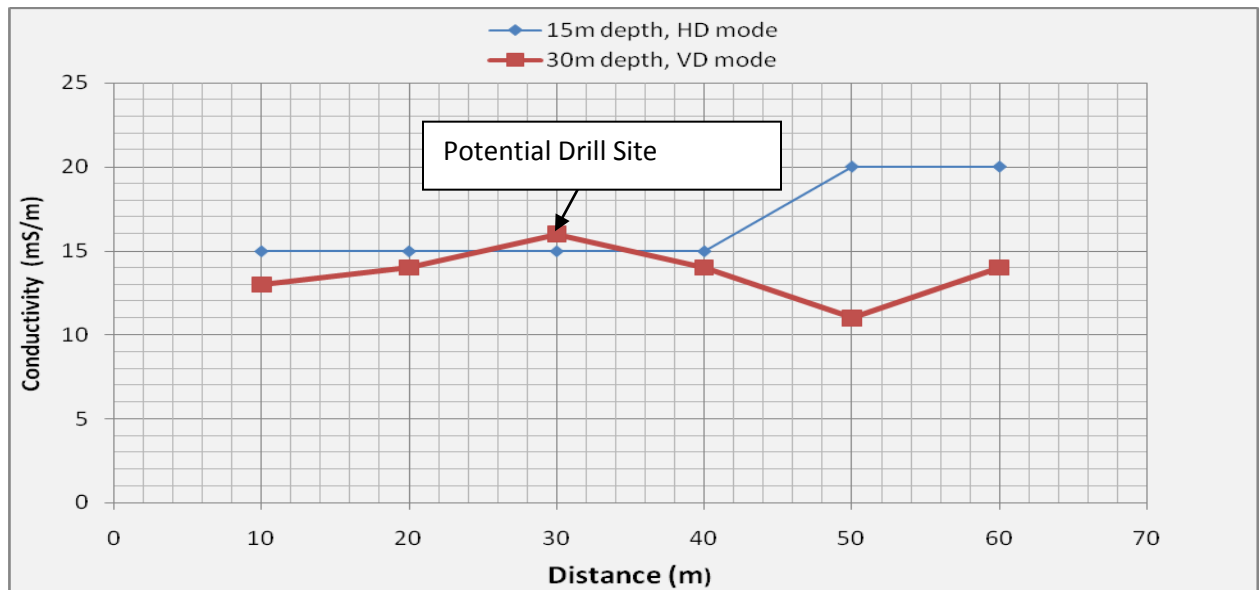


Fig 5.13a. Terrain Conductivity measurements along profile 1 using the 20 m coil at Gorgu

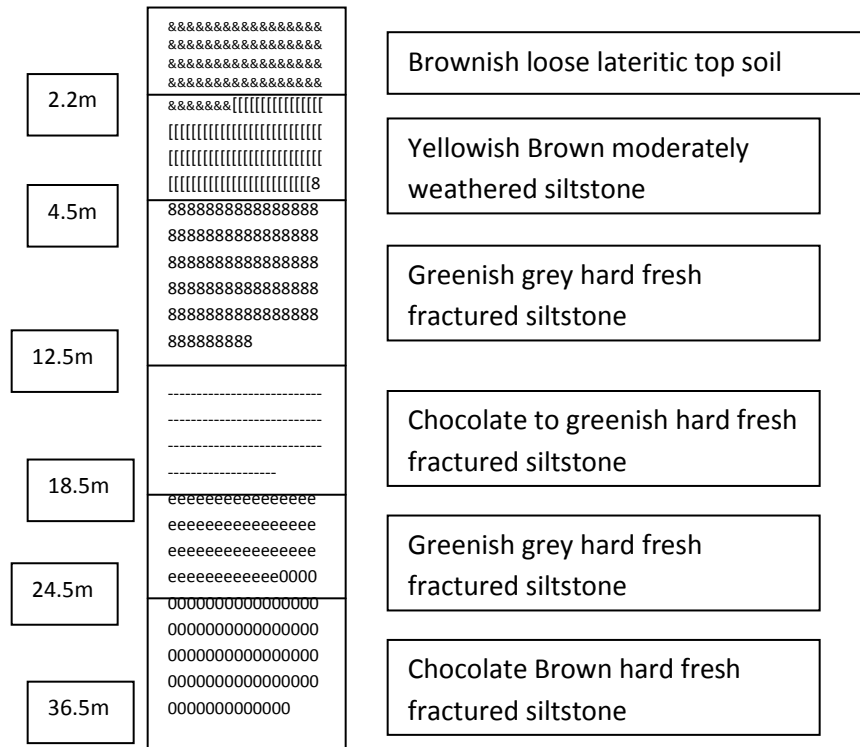


Fig 5.13b. Lithologic log of point 30 m on the profile 1 at Gorgu

The conductivities measured at the 15 m depth depict a constant homogenous subsurface between the 10 and the 40 m point with a value of 15 mS/m, after which there is a sharp rise from the value of 15 mS/m to 20 mS/m at the 50 m point and remains until the end of the profile. The conductivities of the 30 m depth show an increase in terrain conductivity from the initial value of 13 mS/m at the 10 m point up to the value of 16 mS/m at the 30 m point. The anomaly observed here as shown from the curve can be seen at the 30 m point with the value of 16 mS/m where there is a “cross over” between the HD mode and the VD mode, hence, the choice of that point as a drilling site. The “cross over” could be attributed to a number of reasons but the most probable is a fractured or weathered zone, which has possible groundwater potential, hence the reason for its selection.

The geological log on fig 6.13b indicates a six-layer earth model of the site after it was drilled. The top layer consists of brownish loose lateritic top soil of thickness 2.2 m, whilst the second layer is made up of

yellowish brown moderately weathered Siltstone with sandstone intercalated. The third, fourth, fifth and sixth layers were made up of greenish grey hard fresh fractured siltstone, chocolate to greenish hard fresh fractured siltstone, greenish grey hard fresh fractured siltstone and chocolate brown hard fresh fractured siltstone respectively. The aquifer zone was intercepted at a depth of 36.5 m with a yield of 73 litres/min. The geophysical results agree very well with the geological log, because the results show that the subsurface could be sandstone and the log proves that, though there is an intercalation with siltstone.

Profile 2

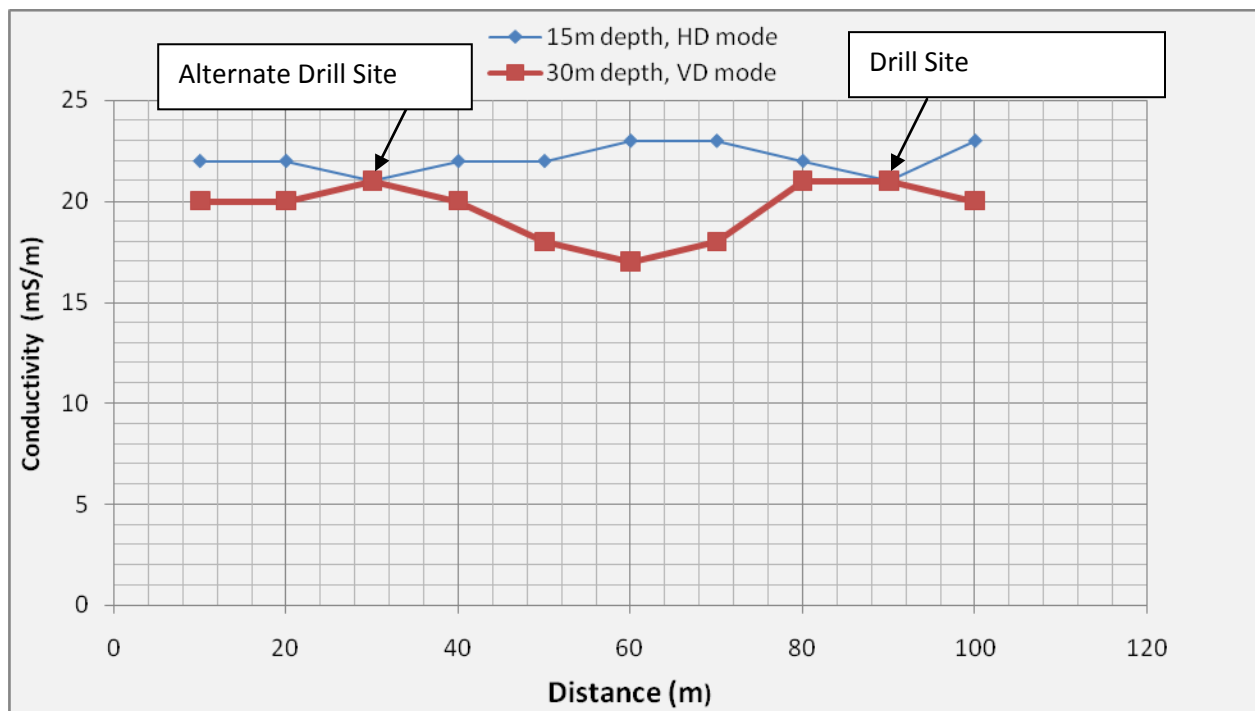


Fig 5.14a. Terrain Conductivity measurements along profile 2 using the 20 m coil at Gorgu

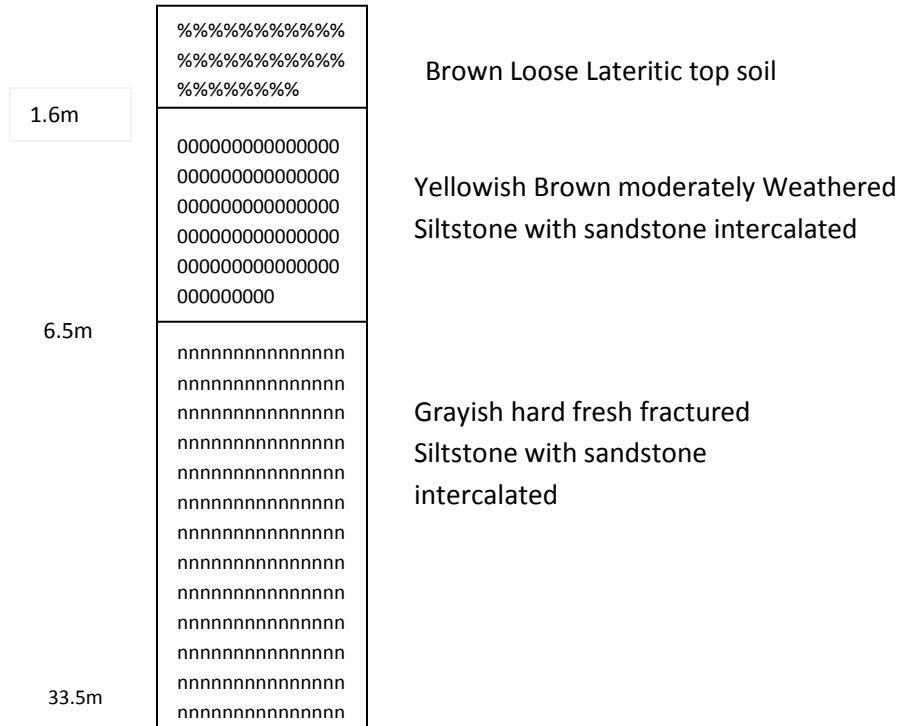


Fig 5.14b. Lithologic log of Point 90 m on the profile 2 at Gorgu.

The HD mode profile depicts a homogenous subsurface geology as shown by a constant value of terrain conductivity (22 mS/m) from the start of the traverse up to the 50 m point, except for the slight fall in conductivity at the 30 m point. The conductivity then rises to 23 mS/m at the 60 and 70 m points, after which it falls to the 21 mS/m at the 90 m point. Finally, the terrain conductivity rises again to the 23 mS/m at the 100 m point. The VD mode shows a homogenous subsurface geology between the 10 and 40 m point and also between the 80 and 100 m point with terrain conductivities of 20 and 21 mS/m respectively. Between the 40 and 80 m point there is a fall in terrain conductivity down to the value of 17 mS/m at the 60 m point. This shows a complex geology as portrayed by the curve. The anomalous zones however are noticed at the 30 and 90 m points where there is a “neck” with a value of 21 mS/m. Hence, the 90 m point was selected for drilling.

The geological log on fig 6.13b indicates a six-layer earth model of the 90 m point when it was drilled.

The top layer consists of brownish loose lateritic top soil of thickness 1.6 m, whilst the second layer is made up of yellowish brown moderately weathered sandstone. Below this is the grayish hard fresh sandstone intercalated with siltstone. The aquifer zone was intercepted at a depth of 33.5 m with a yield of 21litres/ min.

5.3.7 Nanduli in the Gushiegu-Karaga District

Profile 1

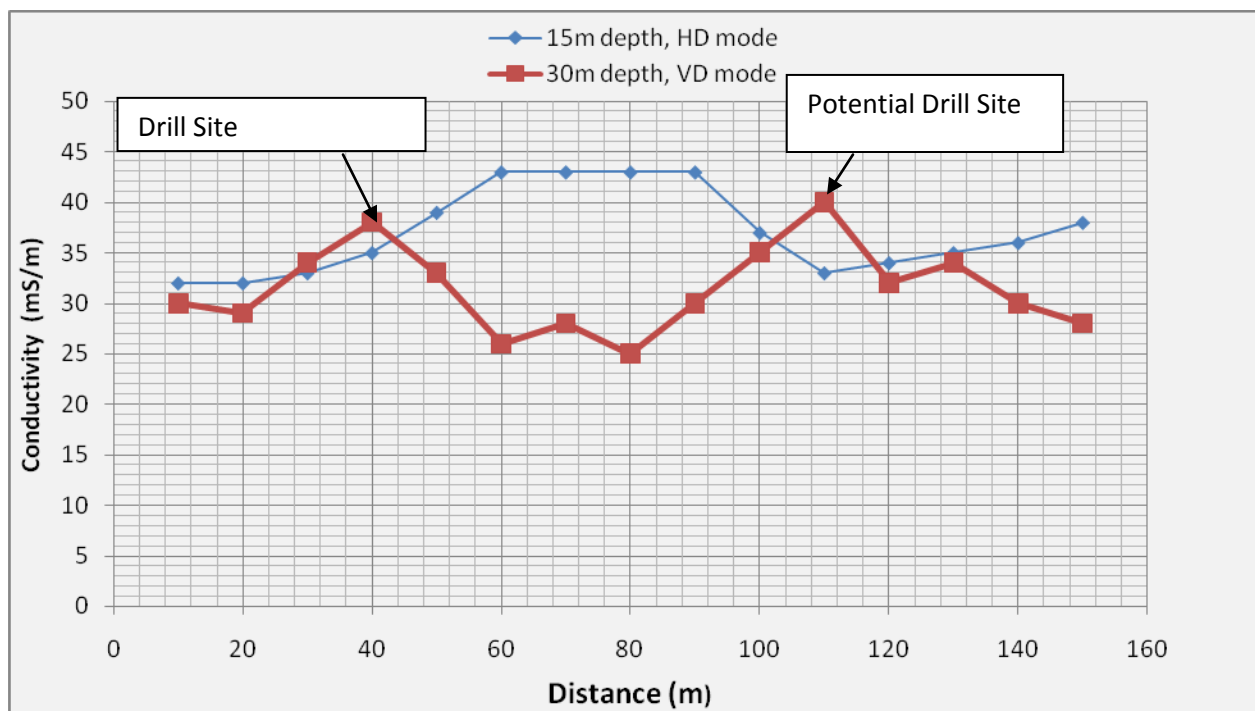


Fig 5.15a. Terrain Conductivity measurements along profile 1 using the 20 m coil at Nanduli

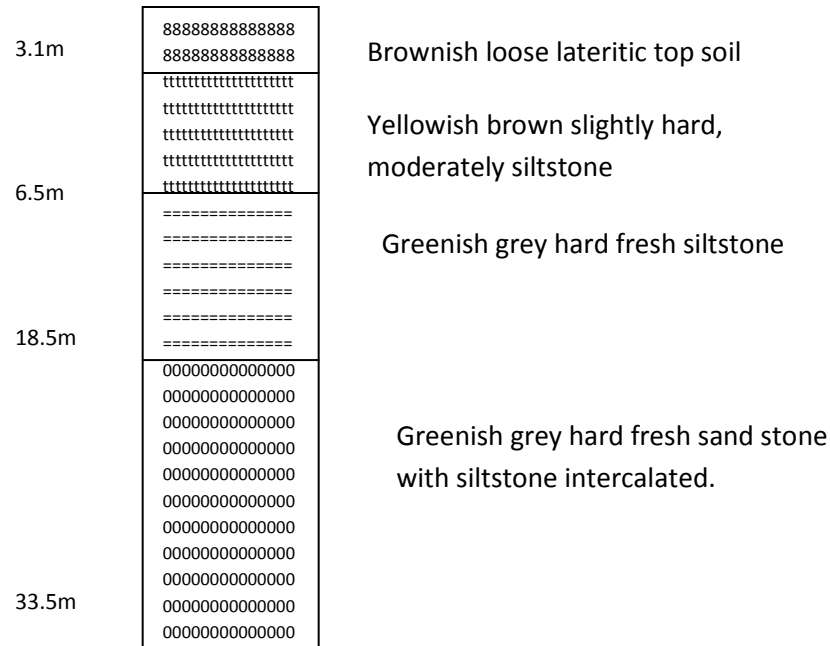


Fig 5.15b. Lithologic Log of Point 110 m of profile 1 at Nanduli

The results for the HD mode indicate a constant increase in terrain conductivity along the traverse from the 10 m point at a value of 24 mS/m to a value of 43 mS/m at the 60 m point and then remains constant from that point up to the 90 m point. It is then followed by a decrease in terrain conductivity down to the value of 33 mS/m at the 110 m point. After this there is an increase in conductivity again up to a value of 38 mS/m at the 150 m point which happens to be the end of the traverse. For the VD mode, we observe an erratic behaviour in terrain conductivity beginning with an initial decrease in conductivity from the value of 30 mS/m at the 10 m point to the 29 mS/m at the 20 m point. This is followed by a fall in conductivity down to the value of 38 mS/m at the 40 m point, after which there is a fall in terrain conductivity down to the value of 26 mS/m at the 60 m point, then a slight increase again up to a value of 28 mS/m at the 70 m point. This is followed by a fall in conductivity down to the value of 25 mS/m at the 80 m point, and then a sharp rise to the value of 40 mS/m at the 110 m point. This rise and fall behaviour

continues to the end of the traverse with a value of 28 mS/m at the 150 m point. The anomalies observed here were at the 40 and 110 m points where there are “cross-overs”. This anomalous behaviour gave room for some speculation for possible groundwater potential. This effect here could be as a result of a number of reasons but the most probable is a fractured or weathered zone, which has possible groundwater potential. Hence, their selection as the potential drilling sites.

The geological log on fig 6.13b indicates a four-layer earth model when the 40 m point was drilled. The top layer consists of brownish loose lateritic top soil of thickness 1.6 m, whilst the second layer is made up of yellowish brown moderately weathered sandstone. Below this is the greenish grey hard fresh sandstone intercalated with siltstone. The aquifer zone was intercepted at a depth of 33.5 m with a yield of 30Litres/ min.

5.3.8 Nakpale in the Zabzugu-Tatale District

Profile 1

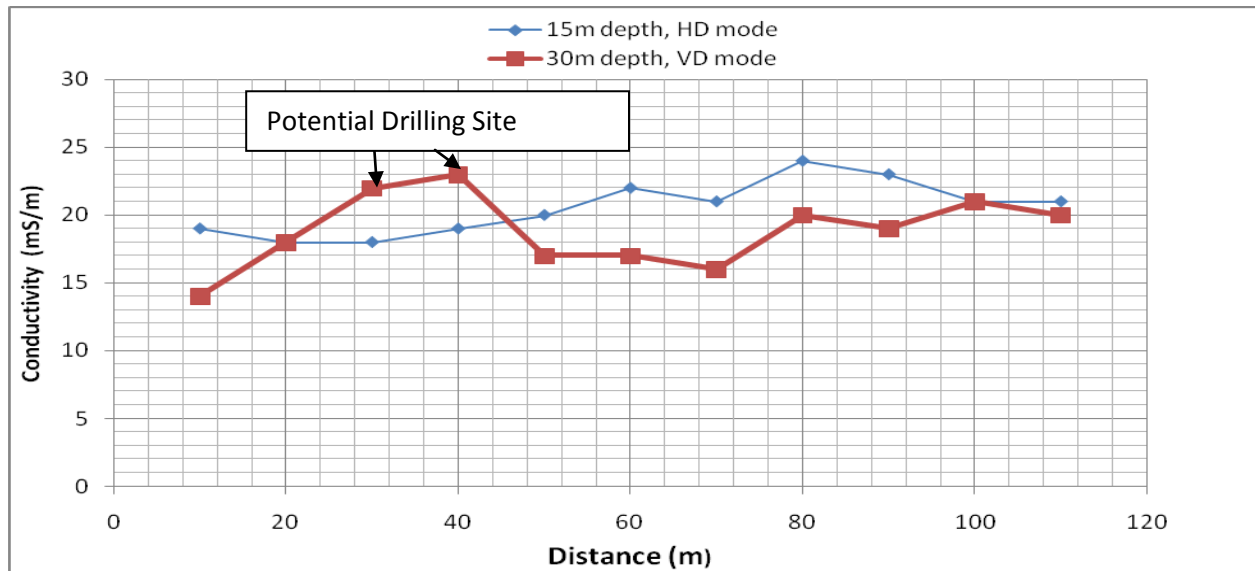


Fig 5.16. Terrain Conductivity measurements along profile 1 using a 20 m coil at Nakpale.

The results for the HD mode indicate a decrease in terrain conductivity along the traverse up to the 30 m point with a value of 18 mS/m. It begins to increase gradually up to a value of 22 mS/m at the 60 m point. It then falls to a value of 21 mS/m at the 70 m point, after which there is a rise to a peak value of 24 mS/m at the 80 m point. Finally, there is a fall in terrain conductivity down to a value of 21 mS/m between the 100 and 200 m points. For the VD mode which shows an erratic graph, there is an increase in the terrain conductivity up to the 30 m point with the value 18 mS/m and then up to a value of 19 mS/m at the 40 m point. This is followed by a sharp fall in conductivity down to a value of 16 mS/m at the 70 m point, after which there is an increase in conductivity up to a value of 20 mS/m at the 90 m point. Finally, there is a rise and then a fall down to the end of the traverse. An anomalous zone is observed between the 30 and 40 m point. These points indicate “cross-overs” which could be as a result

of a number of reasons but the most probable is a fractured or weathered zone, which has possible groundwater potential. Hence, their selection as potential drilling sites. These points however were not drilled as at the time of writing this report.

Profile 2

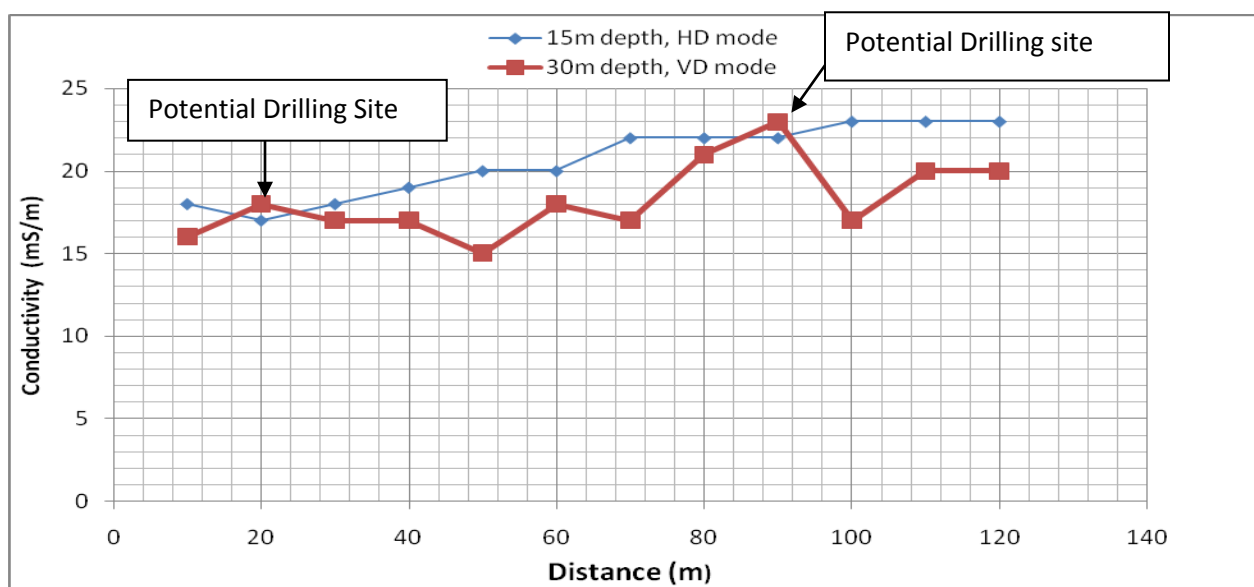


Fig 5.17. Terrain Conductivity measurements along profile 2 using the 20 m coil at Nakpale.

The results for the HD mode indicate a rise in terrain conductivity from the initial value of 18 mS/m at the 10 m point to a value of 22 mS/m at the 70 m point. The terrain conductivity at this point remains the same up to the 90 m point where it rises again to a value of 23 mS/m and then remains constant till the end of the profile. The VD mode shows an erratic behaviour with yielding anomalies at the 20 and 90 m point. The anomalies observed here as shown on the curve are “cross-overs” which obviously present us with some interesting consideration. At these points the value of terrain conductivity observed in the VD

mode, which has a deeper penetration depth compared to the HD mode exceeds the HD value. This effect here could be as a result of a number of reasons but the most probable is a fractured or weathered zone, which has possible groundwater potential. Hence, their selection as potential drilling sites. These points however were not drilled as at the time of writing this report.

Profile 3

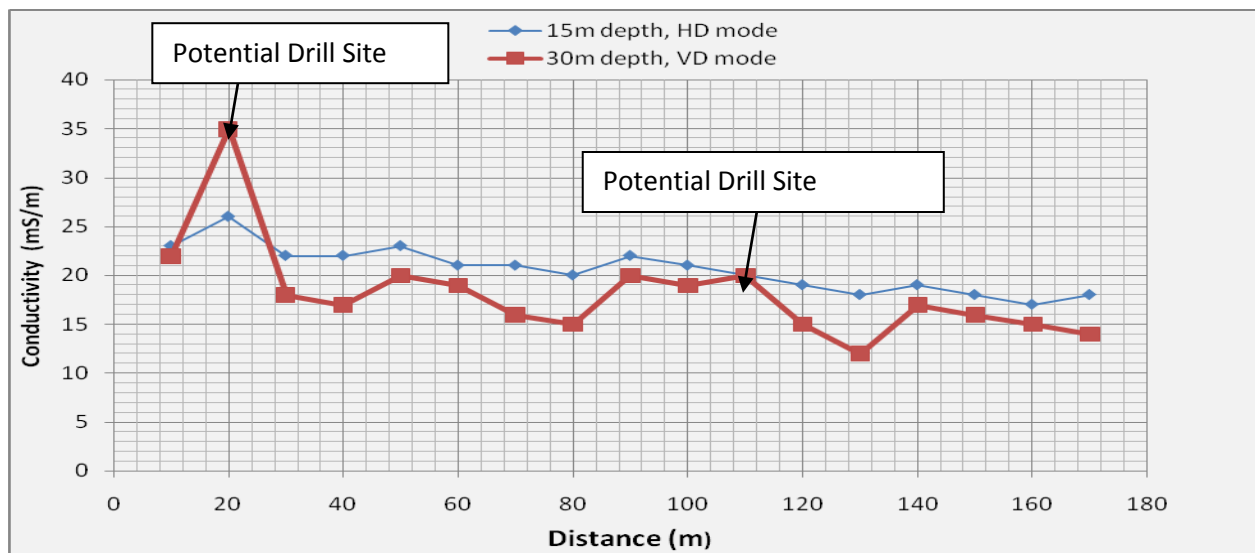


Fig 5.18. Terrain Conductivity measurements along profile 3 using the 20 m coil at Nakpale.

The HD mode traverse depicts an initial rise in terrain conductivity from an initial value of 23 mS/m to a value of 26 mS/m at the 20 m point. This is followed by a step by step decline in conductivity down to the end of the profile with a value of 18 mS/m at the 170 m point. The erratic nature of the VD mode profile suggest a complex subsurface geology with an anomaly of a “cross over” at the 20 m point with a high terrain conductivity of 35 mS/m. We also notice a “neck” occurring at the 110 m point with a terrain conductivity value of 20 mS/m. Hence, these points where selected as potential drilling sites. These points although selected, where however not drilled at the time of writing this report.

5.3.9 Bencharignadom in the Zabzugu-Tatale District

Profile 1

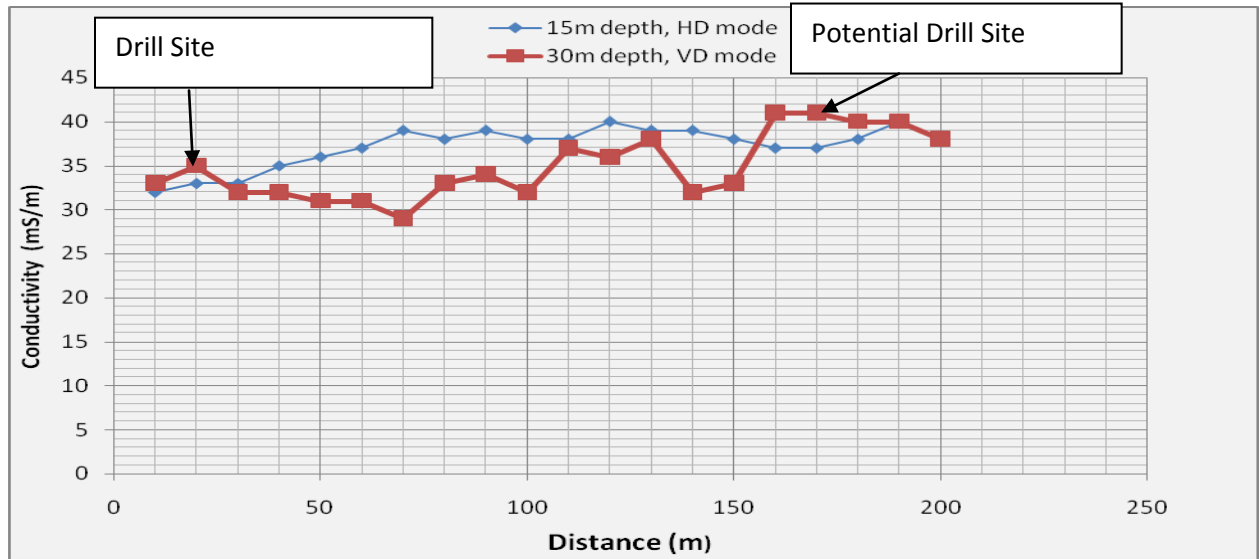


Fig 5.19a. Terrain Conductivity measurements along profile 1 using the 20 m coil at Bencharignado

they were selected as potential drilling sites.

The geological log on Fig 6.13b indicates a six-layer earth model of the 20 m point when it was drilled. The top layer consists of light reddish brown gray brownish soft sandy lateritic top soil of thickness 1.8 m, whilst the second layer is made up of pinkish yellowish brown slightly hard moderately weathered quartzites. The third, fourth, fifth and sixth layers were made up of yellowish brown slightly hard moderately weathered quartzites, light grey hard fresh fractured quartzite, light grey hard fresh fractured quartzite with siltstone intercalations, and dark grey hard fresh fractured quartzites respectively. The aquifer zone was intercepted at a depth of 36.65 m with a yield of 29 litres/min.

Profile 2

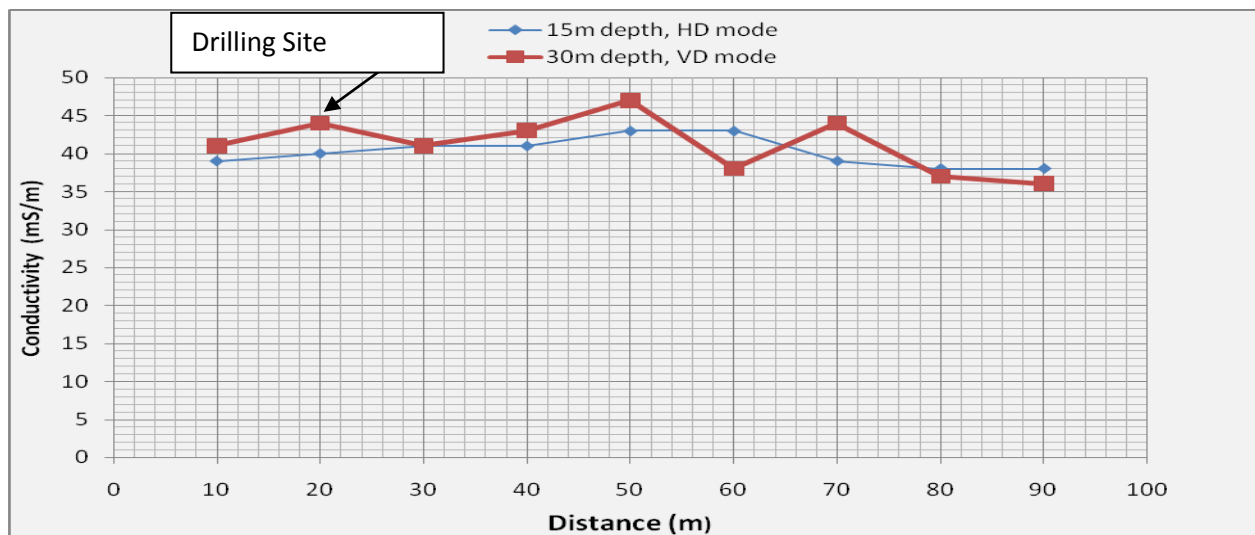


Fig 5.20. Terrain Conductivity measurements along profile 2 using the 20 m coil at Bencharignadom

The conductivities measured at the 15 m depth shows a steady rise in terrain conductivity from the first observation point which has a value of 39 mS/m to 41 mS/m at the 50 m point; it then remains constant

for a while until it reaches the 60 m point. After this point there is a decline till it reaches a value of 38 mS/m at the 80 m point where it remains constant till the end of the profile. The conductivities of the 30 m depth show a more erratic nature suggesting a complex subsurface geology. The anomalies observed here were at the 20, 50 and 70 m points where we notice “cross overs” between the HD mode and the VD mode. The “cross overs”, could be attributed to a number of reasons but the most probable interpretation is attributed to fractured or weathered zone, which have possible groundwater potential, hence the reason for their selection. The choice of the 20 m point over all the others was due to the fact that the transect of that lineament along that point extends through the community other than the other points. When this point was drilled, the yield was 29 litres/min at a depth of 36.6 m.

5.3.10 Jatodor in the Zabzugu-Tatale District

Profile 1

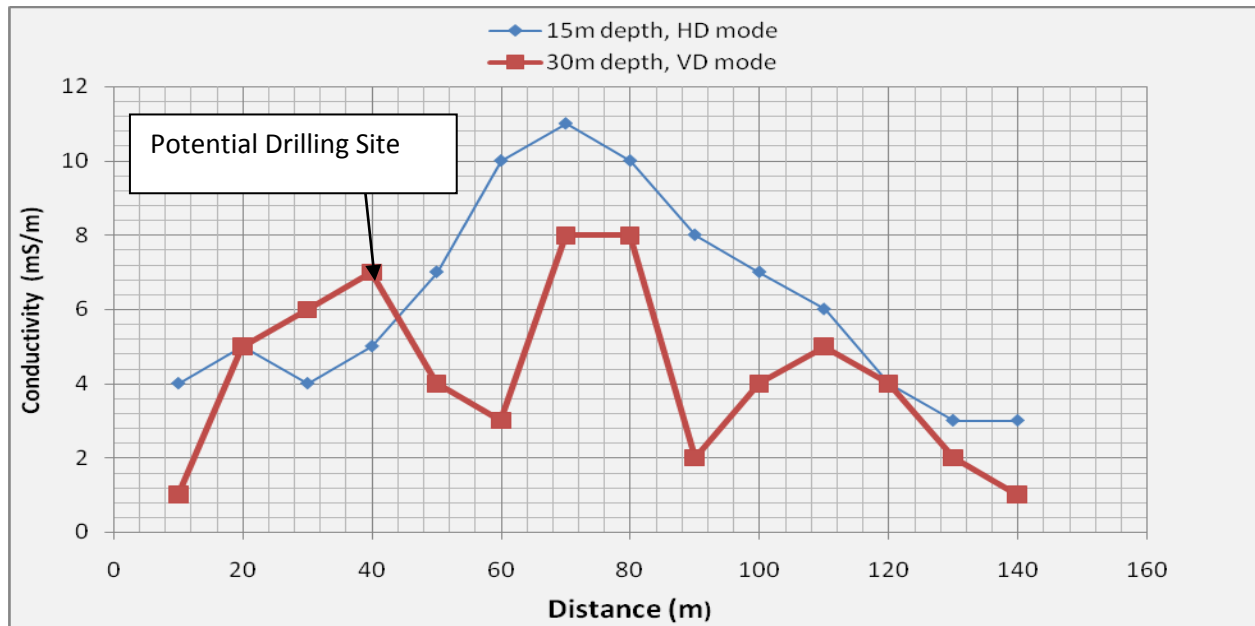


Fig 5.21. Terrain Conductivity measurements along profile 1 using the 20 m coil at Jatodor

The results for the HD mode indicate a steep rise in terrain conductivity along the traverse from the 10 m point at a value of 4 mS/m to a peak value of 11 mS/m at the 70 m point. It then begins to decrease down to the lowest value of 3 mS/m. This sharp rise in terrain conductivity could be attributed to the presence of a high conductive substance. The sharp rise in conductivity shows there could be some conductive material at shallow depth. For the VD mode, we observe an erratic behaviour in terrain conductivity beginning with an increase in conductivity from the value of 1 mS/m at the 10 m point to 7 mS/m at the 40 m point. This is followed by a decline in conductivity down to the value of 3 mS/m at the 60 m point. After which there is a sharp rise in terrain conductivity up to the value of 8 mS/m at the 60 m point, then a decline again down to a value of 2 mS/m at the 80 m point. Finally, there is a rise followed by a fall in

conductivity till the end of the profile. For the VD mode, there are three anomalous zones; around the 60 and 80 m point with the value of 3 and 2 mS/m respectively. This may be due to dike-like structures with negative responses, but the one between the 30 and 40 m points with a value of 6 mS/m suggests a weathering and possibly fracturing. The 40 m point was selected for drilling because it was a “cross over”, hence has a higher ground water potential than the other anomalous zones. This point however was not drilled as at the time of writing this report.

Profile 2

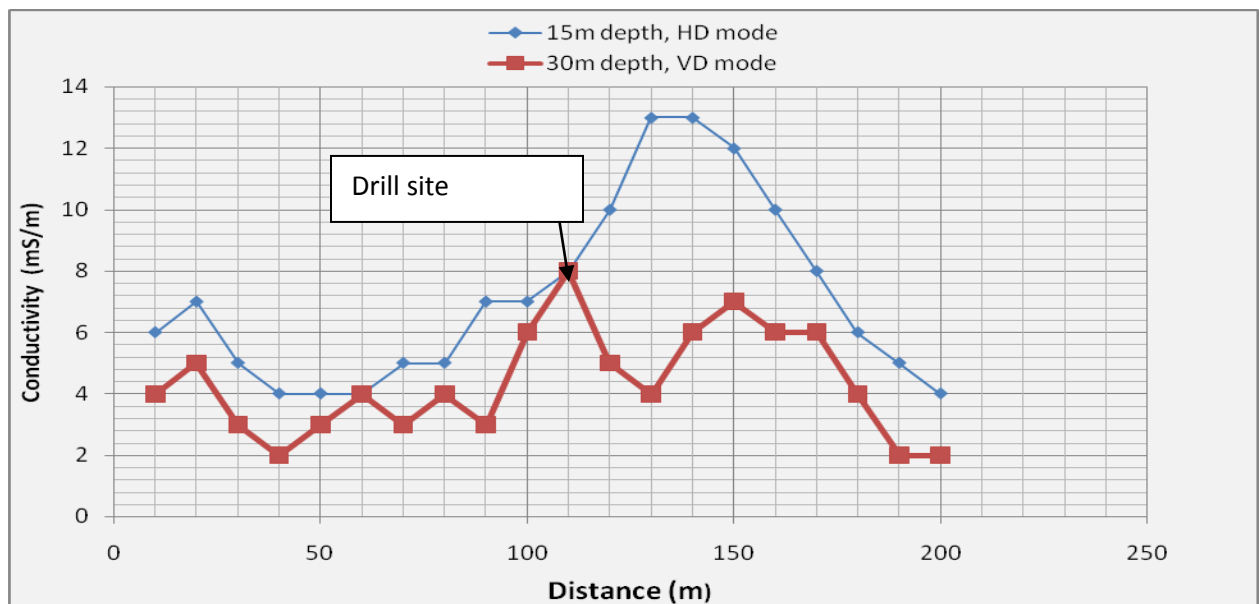


Fig 5.22. Terrain Conductivity measurements along profile 2 using the 20 m coil at Jatodor

The HD mode traverse as shown on the graph assumes an initial increase in terrain conductivity from an initial value of 6 mS/m at the 10 m point up to a value of 7 mS/m and then declines down to a trough value of 4 mS/m. After this it assumes a steady rise in conductivity to a peak value of 13 mS/m at the 50

and 60 m point. This is followed by a fall in conductivity down to the initial trough value of 4 mS/m. But the erratic nature of the VD mode profile suggests a complex subsurface geology with an anomaly of a neck occurring at the 110 m point with a terrain conductivity value of 8 mS/m. The neck refers to the point where the VD value at a point is equal to the HD value at that same point. This means that the VD value, which has a deeper penetration depth compared to the HD mode, is equal to the HD value at this point. This effect here could be as a result of a number of reasons but the most probable is a fractured or weathered zone, which has possible groundwater potential. Hence, its selection as a possible drilling site. When this site was drilled, the yield was 117 liters/min, at 51.8 m depth.

Profile 3

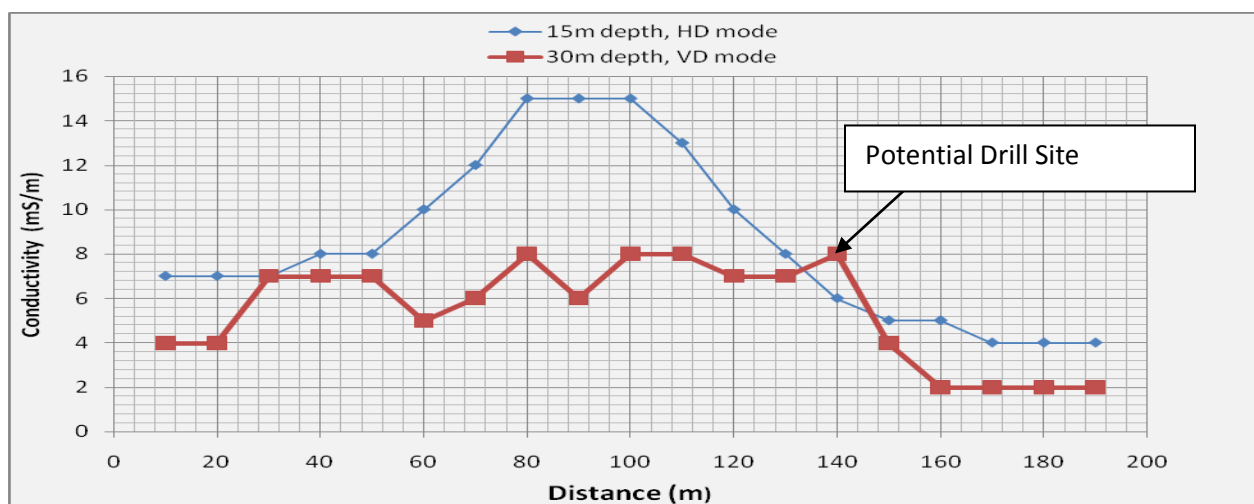


Fig 5.23. Terrain Conductivity measurements along profile 3 using the 20 m coil at Jatodor

The results of the HD mode from the beginning of the graph indicate a laterally homogenous subsurface geology with a constant conductivity of 7 mS/m between the 10 and the 30 m points. This is followed by a rise in conductivity up to a peak value of 15 mS/m between the 80 and 100 m points. Finally, there is a decline in conductivity from this point down to a value of 4 mS/m at the 190 m point which happens to

be the end of the profile. The results of the VD mode show an erratic behaviour which depicts a complex subsurface geology. This erratic nature continues right until the end of the profile. The anomaly observed here is that of a cross-over, which occurred at the 140 m point. The “cross overs” could be attributed to a number of reasons but the most probable is a fractured or weathered zone, which have possible groundwater potential, hence the reason for its selection as a possible drilling site.

Profile 4

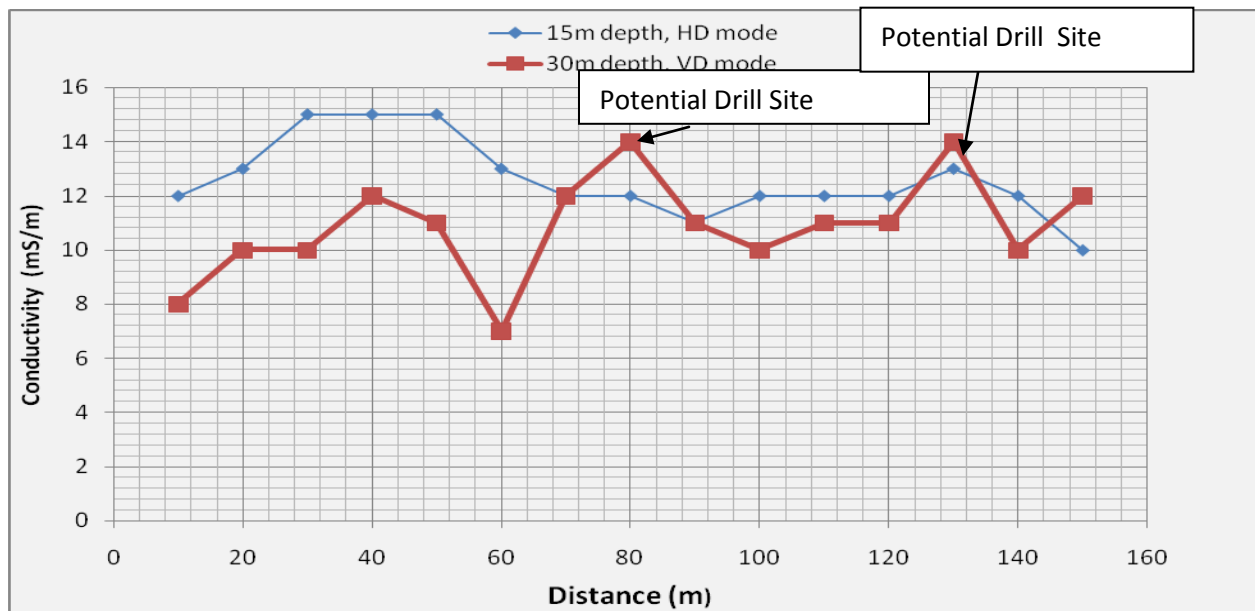


Fig 5.24. Terrain Conductivity measurements along profile 4 using the 20 m coil at Jatodor

The subsurface sampled by the HD mode profile depicts an initial rise in terrain conductivity from an initial value of 12 mS/m at the 10 m point to 15 mS/m between the 30 and 50 m points respectively. This is followed by a steady drop in terrain conductivity down to a value of 11 mS/m at the 90 m point, after which, there is an increase in conductivity up to a value of 12 mS/m at the 100 m point, where it remains constant up to the 12 mS/m at the 120 m point. Finally, there is a rise followed by a fall till the end of the profile. The conductivity variation for the VD mode is rather erratic, depicting a complex geology

underground. The anomalies observed are at the 80 and 130 m points where there are “cross-overs” which could be as a result of weathered and fractured zones, which have possible groundwater potential.

5.3.11 Benatabe East in the Zabzugu-Tatale District

Profile 1

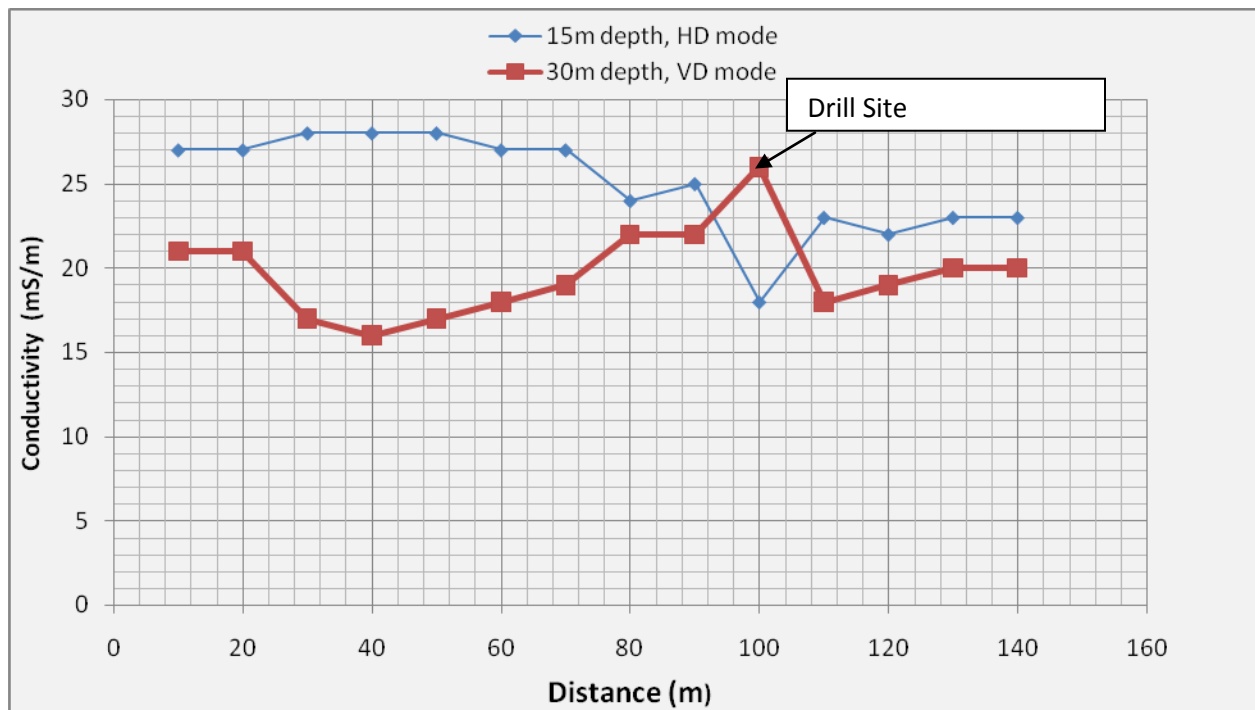


Fig 5.25a. Terrain Conductivity measurements along profile 1 using the 20 m coil at Benatabe East.

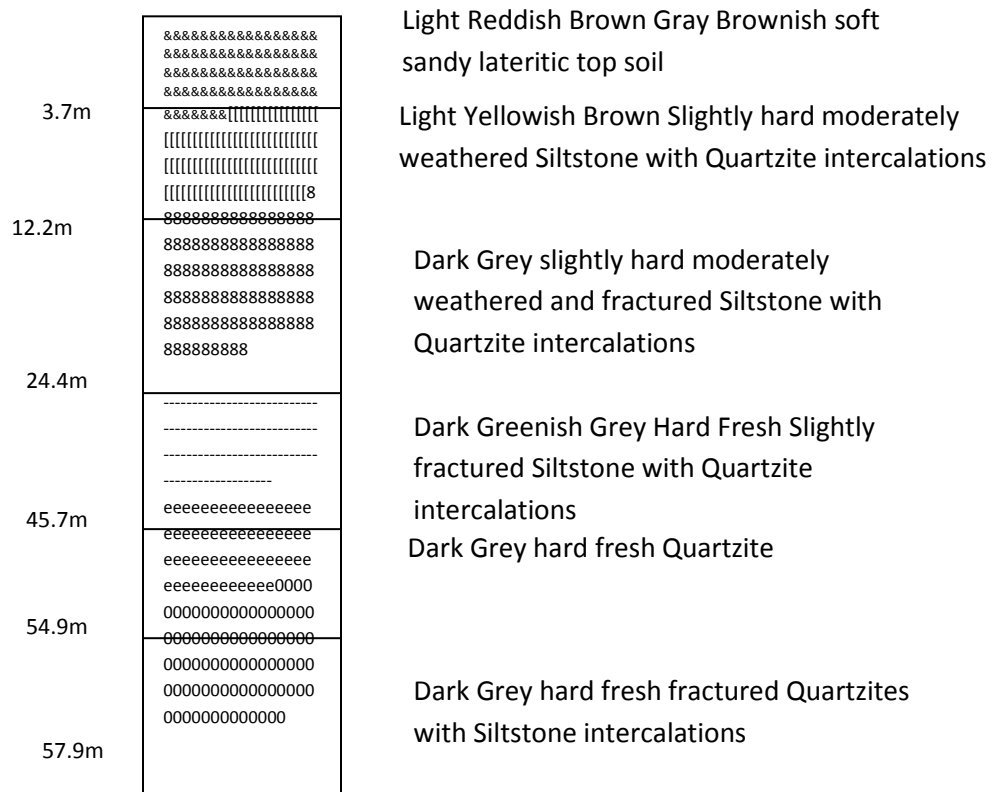


Fig 5.25b. Lithologic Log of the 100 m point at profile 1 at Benatabe East.

The subsurface sampled by the HD mode depicts a constant homogenous subsurface at the 20 m point with a value of 28 mS/m between the 30 and 50 m points. This is followed by a gradual decline in conductivity down to a value of 18 mS/m at the 100 m point. Finally, there is an increase in terrain conductivity which continues to the end of the profile as shown by the curve. The conductivity variation for the VD mode is marked by a decline from the beginning to a trough value of 16 mS/m at the 40 m point. This is followed by an increase in terrain conductivity to a peak value of 26 mS/m at the 100 m point where we observe a cross-over between the HD mode and the VD mode. Finally, there is a decline in terrain conductivity down to a value of 18 mS/m at the 110 m point, followed by an increase up to the

value of 20 mS/m at the 140 m point which happens to be the end of the profile. The anomaly observed at the trough value of 16 mS/m at the 40 m point could be due to a number of reasons, but most likely, dike-like structures or a highly conductive material that has been masked by having negative responses. Hence, the more probable option was the anomaly of the cross-over observed at the 100 m point. This point was therefore selected as a potential drilling site.

The geological log on fig 6.25b indicate a six-layer earth model of the 100 m point when it was drilled. The top layer consists of light reddish brown gray brownish soft sandy lateritic top soil of thickness 3.7 m, whilst the second layer is made up of light yellowish brown slightly hard moderately weathered siltstone with quartzites intercalations. The third, fourth, fifth and sixth layers were made up of dark grey slightly hard moderately fractured and weathered quartzites, dark greenish grey hard fresh slightly fractured siltstones with quartzite intercalations, Dark Grey hard fresh quartzites and dark grey hard fresh fractured quartzites respectively. The aquifer zone was intercepted at a depth of 57.9 m with a yield of 12 litres/min.

Profile 2

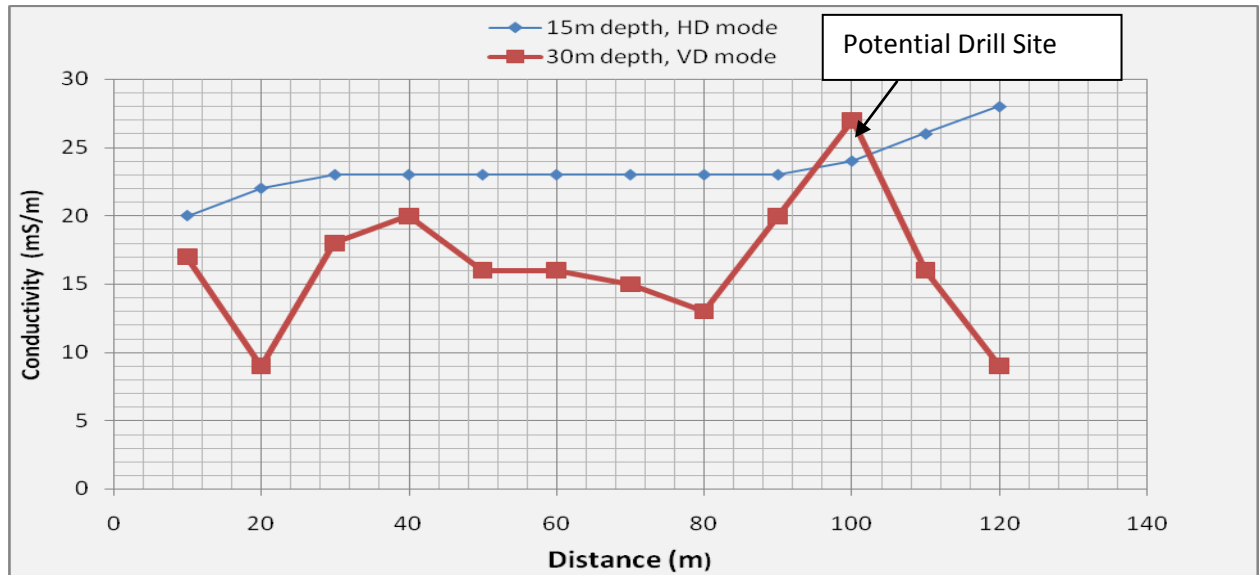


Fig 5.26. Terrain Conductivity measurements along profile 2 using the 20 m coil at Benatabe East.

The HD mode profile depicts a homogenous subsurface geology as shown by a constant value of terrain conductivity of 23 mS/m between the 30 and the 90 m points after which there is a steady increase in conductivity to a value of 28 mS/m at the 120 m point which marks the end of the profile. The VD mode profile shows an erratic behaviour which depicts a very complex subsurface geology. This erratic nature continues to the end of the profile. The anomaly observed here was at the 100 m point where there is a notable “cross-over” between the HD mode and the VD mode, hence its selection as a potential drill point.

5.3.12 Gor Kukani in the Zabzugu-Tatale District

Profile 1

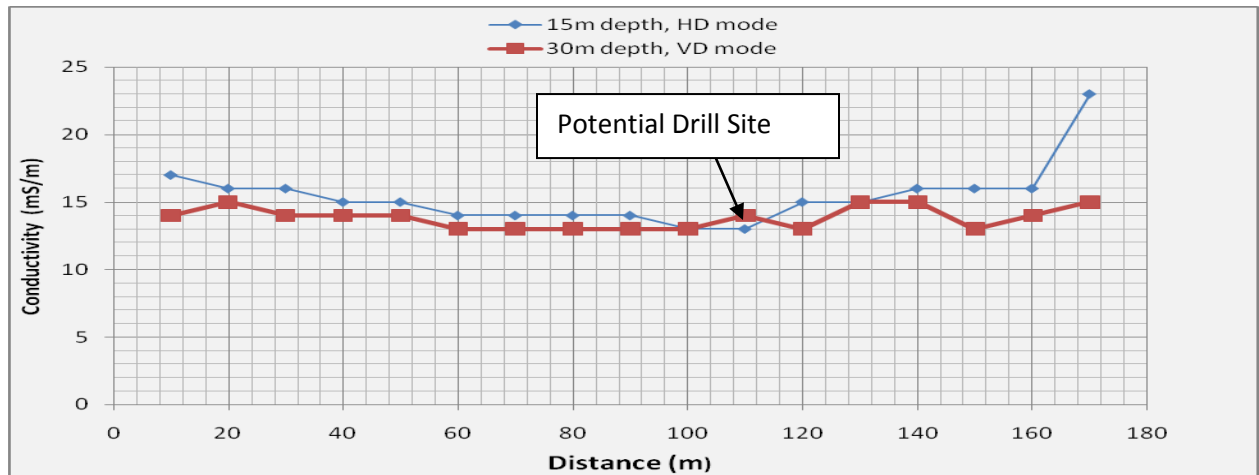


Fig 5.27. Terrain Conductivity measurements along profile 1 using the 20 m coil at Gor Kukani.

The conductivities measured at the 15 m depth depicts a constant homogenous subsurface between the 60 and the 90 m point with a value of 14 mS/m, after which there is a gradual increase till the end of the profile. The conductivities of the 30 m depth also show a constant homogenous subsurface between the 60 and the 100 m point with a value of 14 mS/m. This is followed by an erratic behaviour which continues till the end of the profile. There was no major anomaly observed here except the cross-over observed as shown from the curve at the 110 m point with the value of 14 mS/m where there is a slight “cross over” between the HD mode and the VD mode hence, the choice of that point as a drilling site. The “cross over” could be attributed to a number of reasons but the most probable is a fractured or weathered zone, which has possible groundwater potential, hence the reason for its selection. Since the “cross over” points are mainly within the range of 10 to 20 mS/m, it can be speculated that the area was mainly made up of sandstone. However, when this point was drilled, it was a dry hole.

Profile 2

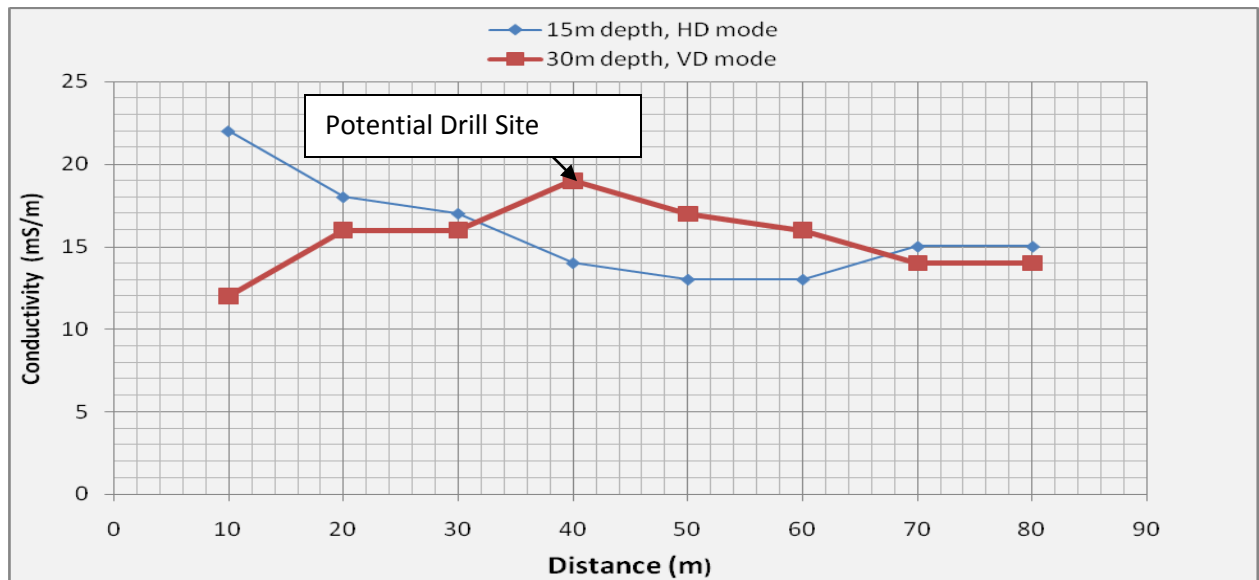


Fig 5.28 Terrain Conductivity measurements along profile 2 using the 20 m coil at Gor Kukani.

The results for the HD mode indicate a steady decrease increase in terrain conductivity along the traverse from the 10 m point at a value of 22 mS/m to a value of 14 mS/m at the 50 m point. This remains constant up to 60 m point and then rises again to a value of 15mS/m till the end of the profile as shown by the curve. For the VD mode, we observe a rise in terrain conductivity beginning with an initial value of 12 mS/m at the 10 m point to 19 mS/m at the 40 m point. This is followed by a fall in conductivity down to the value of 14 mS/m at the 80 m point which is the end of the profile. An anomalous zone was however realized between the 40 and 60 m points where we notice a “cross over”. These anomalous zones gave room for some speculation for possible groundwater potential. This effect here could be as a result of a number of reasons but the most probable is a fractured or weathered zone, which has possible groundwater potential. Hence, its selection as the potential drilling sites.

5.3.13 Batigmodo in the Zabzugu-Tatale District

Profile 1

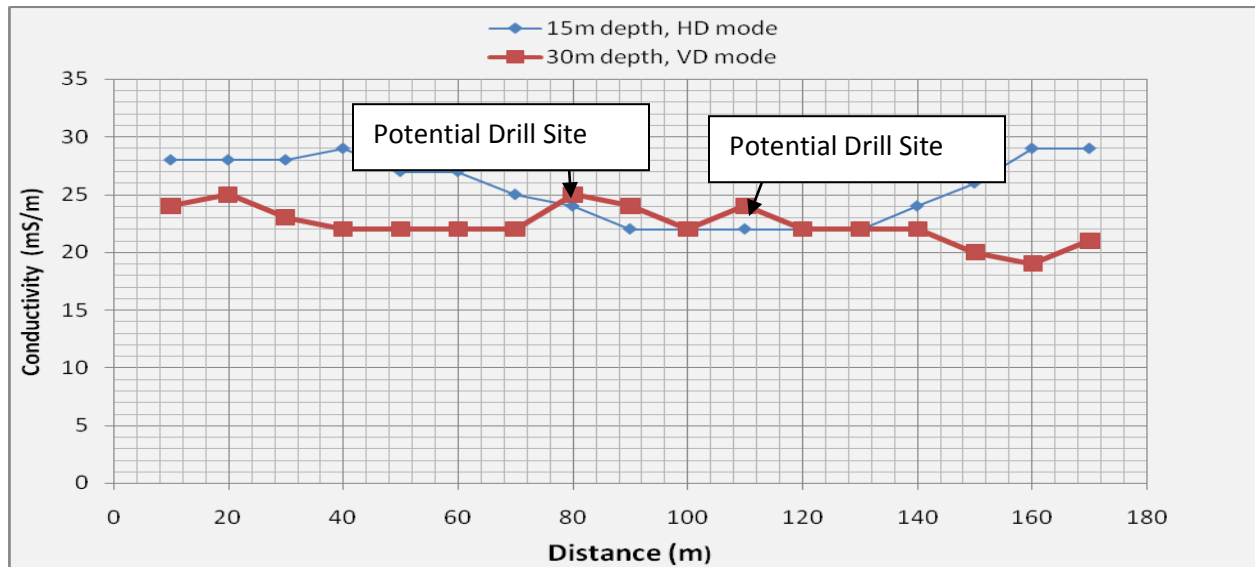


Fig 5.29 Terrain Conductivity measurements along profile 1 using the 20 m coil at Batigmodo

The conductivities measured at the 15 m depth depict a constant homogenous subsurface between the 10 and the 30 m points with values ranging between 28 mS/m and 29mS/m, after which there is a decline from the value of 29 mS/m to 22 mS/m at the 90 m point. After this, the curve depicts another constant homogenous subsurface between the 90 and the 130 m points with a value of 22 mS/m. Finally, there is an increase in terrain conductivity to a value of 29 mS/m at the end of the profile. The conductivities of the 30 m depth also depicts a constant homogenous subsurface between the 40 and 70 m points with a value of 22 mS/m. This is followed by erratic behaviour where we notice a rise and fall feature till the end of the profile. The anomalies observed here as shown from the curve can be seen at the 80 and 110 m point where we have “cross overs”. The “cross overs” could be attributed to a number of reasons but the most probable is a fractured or weathered zone, which has possible groundwater potential, hence the

reason for their selection.

Profile 2

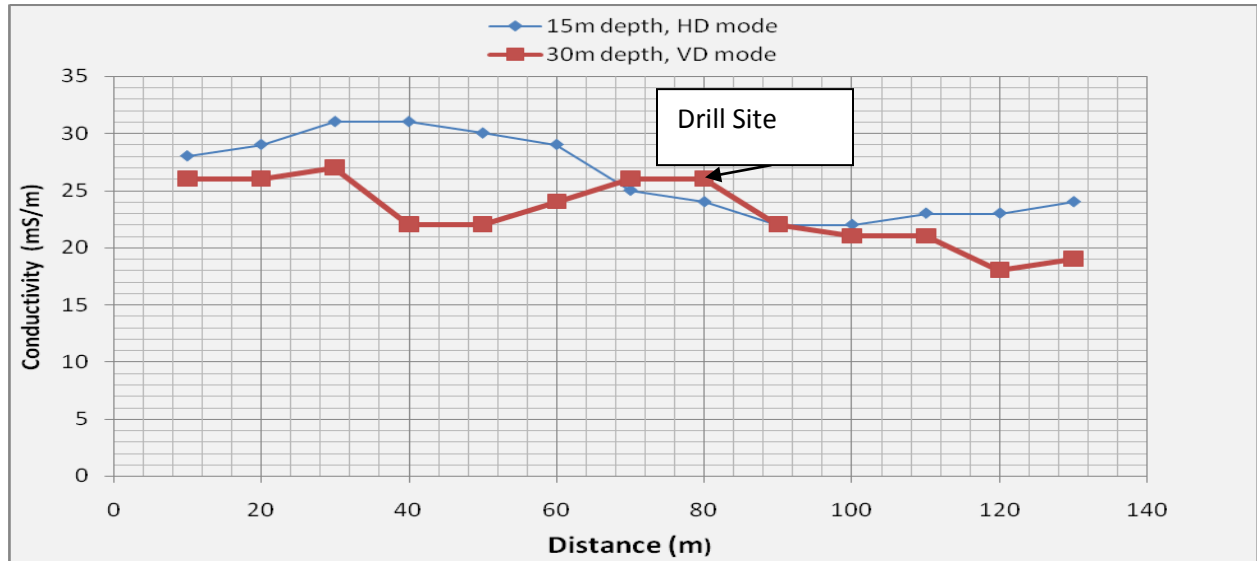


Fig 5.30. Terrain Conductivity measurements along profile 2 using the 20 m coil at Batigmado

The results for the HD mode indicate an increase in terrain conductivity along the traverse up to a value of 31 mS/m at the 30 m point. The conductivity then begins to decrease gradually up to the 100 m point with a value of 22 mS/m and then rises up to a value of 24 mS/m at the end of the profile. The VD mode shows an erratic graph, which could mean the presence of a very complex subsurface geology. An anomalous zone is observed between the 70 and 80 m points. These points indicate “cross-overs” which could be as a result of a number of reasons but the most probable is a fractured or weathered zone, which has possible groundwater potential. Hence, its selection as a potential drilling site. When the 80 m point was drilled, the yield was 34 litres/min at a depth of 30.5m.

Profile 3

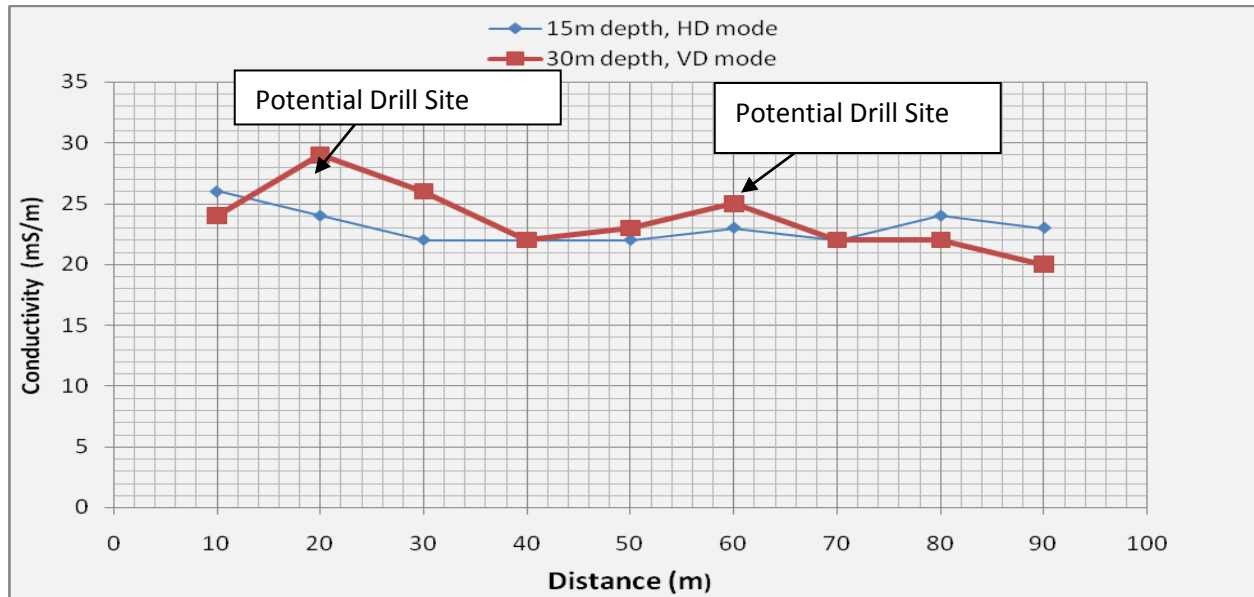


Fig 5.31. Terrain Conductivity measurements along profile 3 using the 20 m coil at Batigmodo

The results for the HD mode indicate a decline in terrain conductivity from the initial value of 26 mS/m at the 10 m point to a value of 22 mS/m at the 70 m point. The HD mode depicts a homogenous subsurface geology. The VD mode shows an erratic behaviour, showing a complex subsurface geology. The anomalies observed here as shown on the curve are “cross-overs” which obviously presents us with some interesting consideration. These anomalies can be noticed at the 20 and 60 m points with values of 29 and 25 mS/m. At these points the value of terrain conductivity observed in the VD mode, which has a deeper penetration depth compared to the HD mode exceeds the HD value. This effect here could be as a result of a number of reasons but the most probable is a fractured or weathered zone, which has possible groundwater potential. Hence, their selection as potential drilling sites.

5.3.14 Bikpanjib in the Zabzugu-Tatale District

Profile 1

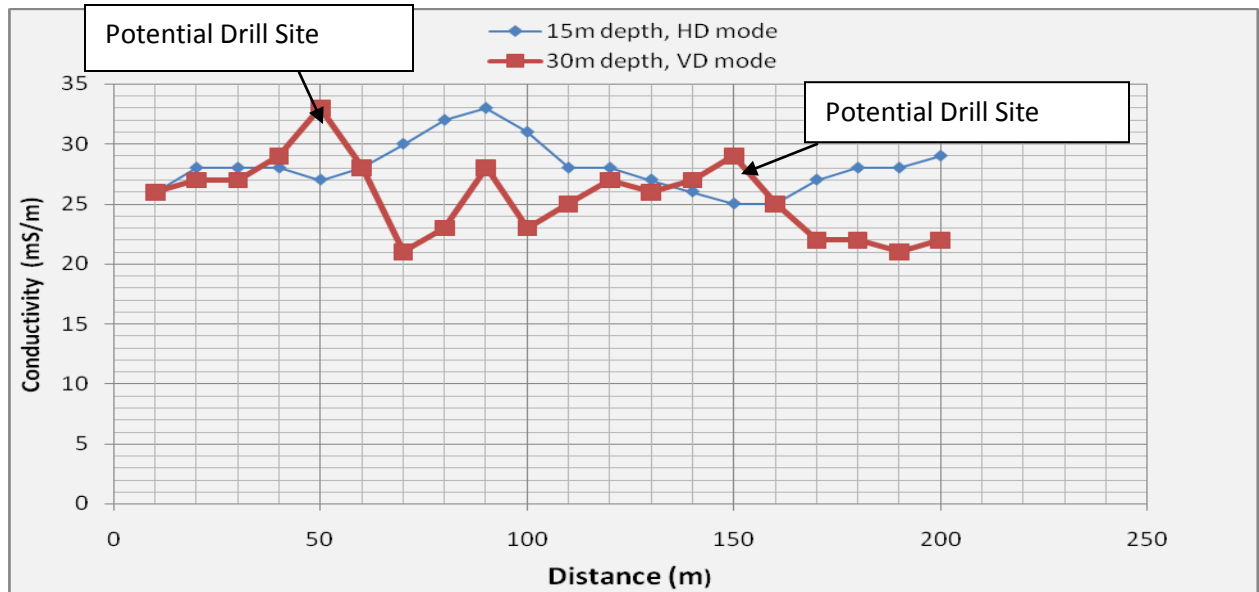


Fig 5.32. Terrain Conductivity measurements along profile 1 using the 20 m coil at Bikpanjib

The conductivities measured at the 15 m depth shows a steady rise in terrain conductivity from the first observation point which has a value of 28 mS/m to 33 mS/m at the 90 m point. After this point there is a steady decrease in conductivity down to a value of 26 mS/m at the 150 m point. This is followed by a rise in terrain conductivity till the end of the profile as shown by the curve. The conductivities of the 30 m depth show a more erratic nature suggesting a complex subsurface geology. The anomalies observed here were at the 50 and 150 m point with values of 27 mS/m and 25 mS/m respectively where we notice “cross overs” between the HD mode and the VD mode. The “cross overs”, could be attributed to a number of reasons but the most probable interpretation is attributed to fractured or weathered zone, which have possible groundwater potential, hence the reason for their selection.

Profile 2

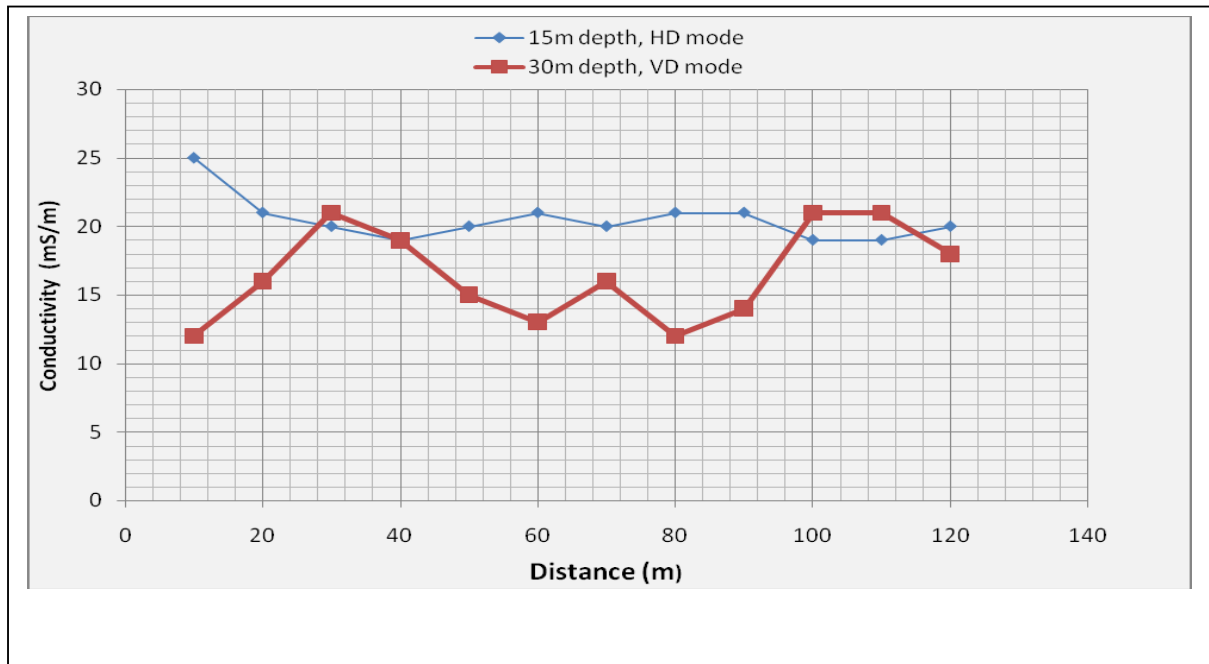


Fig 5.33. Terrain Conductivity measurements along profile 2 using the 20 m coil at Bikpanjib

The results for the HD mode indicate a decrease in terrain conductivity along the traverse down to a value of 31 mS/m at the 30 m point. The curve begins to depict a constant homogenous subsurface geology between the 40 and 90 m point at the end of the profile. The VD mode shows an erratic graph, which could mean the presence of a very complex subsurface geology. The anomalous zones at the 30 m and also between the 100 and 110 m points. These points indicate “cross overs” which could be as a result of a number of reasons but the most probable is a fractured or weathered zone, which have possible groundwater potential. Hence, they were pegged as potential drilling sites.

Profile 3

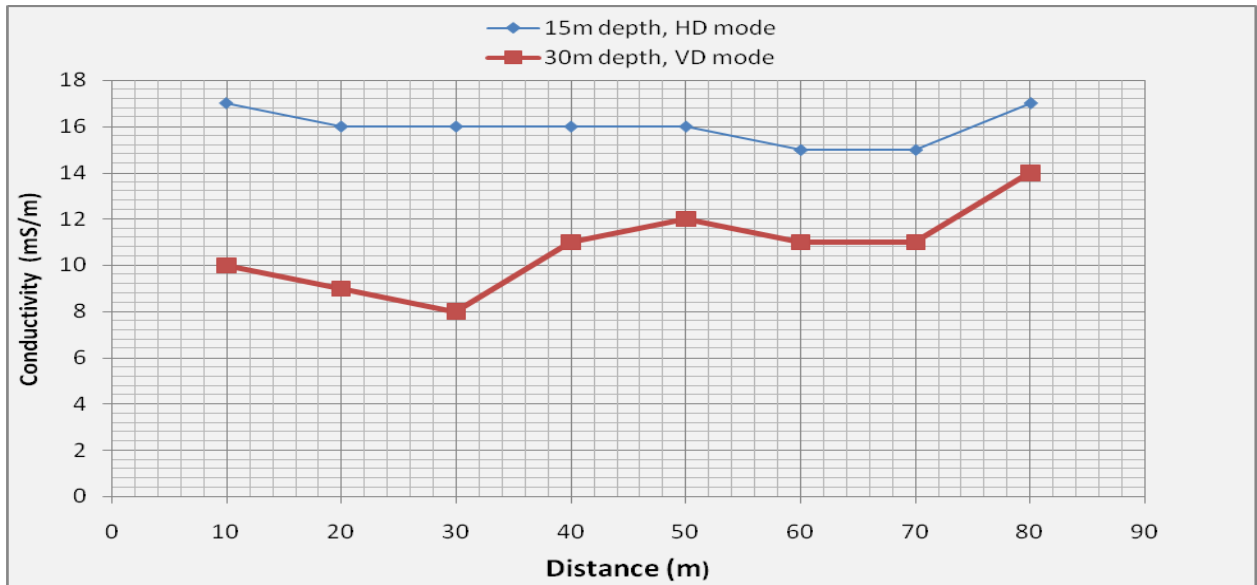


Fig 5.34. Terrain Conductivity measurements along profile 3 using the 20 m coil at Bikpanjib

The HD mode profile depicts a constant homogenous subsurface from the 20 m point to the 50 m point with a terrain conductivity value of 16 mS/m. This is followed by a fall in terrain conductivity and then a rise at the end of the profile. The VD mode profile shows an erratic behaviour which depicts a complex subsurface geology but as shown from the curve there is a complete absence of anomalous zones within the subsurface and as such no point was selected for drilling. Sandstones are likely to be the surface rocks.

Profile 4

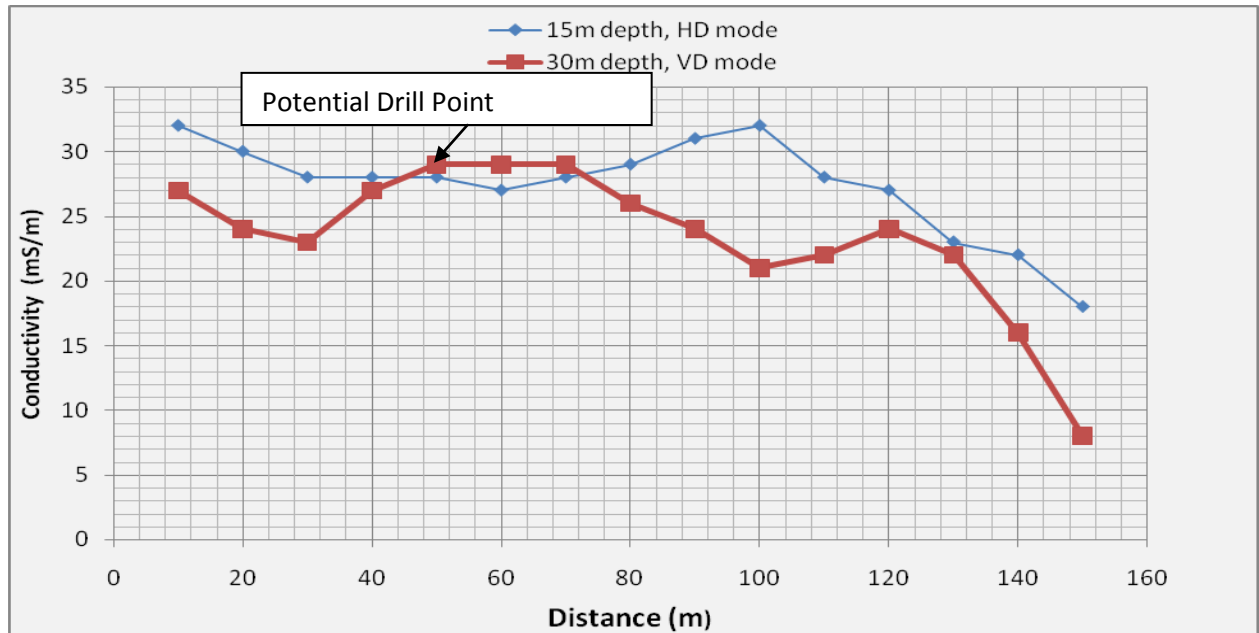


Fig 5.35. Terrain Conductivity measurements along profile 4 using the 20 m coil at Bikpanjib

The results for the HD mode indicate a decrease in terrain conductivity along the traverse down to a value of 28 mS/m at the 30 m points. This is followed by a homogenous subsurface geology between the 30 and 50 m points. After this, there is an increase in terrain conductivity up to a value of 32 mS/m at the 100 m point. Finally there is a decline in conductivity down to the end of the profile. The VD mode shows an erratic graph, which could mean the presence of a very complex subsurface geology. An anomalous zone is observed between the 50 and 70 m point. These points indicate “cross-overs” which could be as a result of a number of reasons but the most probable is a fractured or weathered zone, which has possible groundwater potential. Hence, the selection of this area as a potential drilling site.

Table 5.1 Summary of log results for both districts

Community	borehole no.	borehole depth/m	aquifer depth/m	bedrock depth/m	screen pipes/m	borehole status	potential yield (l/min)	Geology
Nakpoligu	NAK-01	42.0	41.0	4.0	38-45	Successful	21.0	Sandstone
Yibeyile	YIB-01	60.0		8.0		Dry		Sandstone
Gorgu	GOG-01	43.0	36.5	4.0	30-44	Successful	73	Siltstone
	GOG-02	40.0	33.5	6.0	31-45	Successful	21	Siltstone
Becharignadom	BEC-01	43.0	40.0	3.0	40-43	Successful	29.0	Quartzite
Gor Kukani	GOR-01	55.0		14		Dry		Quartzite
Jatodor	JAT-01	61.0	50.0	15.0	48-60	Successful	117.0	Quartzite
Benatabe East	BEN-01	58.0	57.9	18.0	17-23	Successful	10.0	Quartzite
TOTAL		402	258.9	72.0			271	
AVERAGE		50.3	32.4	9.0			33.9	
MAX.		61.0	57.9	18.0			117.0	
MIN.		40.0	33.5	3.0			10.0	

Table 5:2 Summary of test drilling and Success rate in both districts

District	Rock Type	BH Drilled	Successful BH	Success Rate (%)
Gushiegu-Karaga	Sandstone	4	3	75
Zabzugu-Tatale	Quartzite	4	3	75
TOTAL		8	6	75

CHAPTER SIX

6.0 CONCLUSIONS AND RECOMMENDATIONS

6.1 Conclusions

This project was accomplished using the 20 m intercoil spacing of the Geonics EM 34 conductivity meter both in the vertical and horizontal dipole modes to carry out the profiling to determine the anomalies related to the zones of weathering, fracturing and dike-like structures, which could be conductive faults or shear zones, and hence are possible groundwater potential zones.

The potential rocks forming the aquifer in the Gushiegu-Karaga district are mostly fracture and weathered siltstone and sometimes with sandstone intercalations. The potential rocks forming the Zabzugu-Tatale district are mostly the highly fractured quartzite with siltstone intercalations.

Groundwater in the study area of the Gushiegu-Karaga district could be intercepted on the average between the depth of 30-60 m. The yields of some of the boreholes in the area are: Nakpoligu-73 litres/min, Gorgu-21 litres/min and Nanduli- 30 litres/min.

On the other hand, the groundwater in the study area of the Zabzugu-Tatale district was intercepted on the average between the depths of 30-70 m. The yields of the boreholes in the area are: Jatodor -117 litres/min, Benatabe East -12 litres/min, Bikpanjib -29 litres/min, Nakpale -10 litres/min and Batigmado - 34 litres/min.

From the lithologic log of three boreholes in the study area of the Gushiegu-Karaga district, it was found that all had the same top soil of brown loose laterite with the subsurface underlain with hard fresh fractured siltstone with at times, sandstone intercalations. On the other hand, when the lithologic logs of

three boreholes in the study area of the Zabzugu-Tatale district were considered, it was found that they all had a top soil of brown sandy laterite with the subsurface underlain with grey hard fresh quartzites with at times, siltstone intercalations.

The drilling of the boreholes was based on the geophysical investigations and it was to study the hydraulic characteristics of the recharge area and to provide water for the communities. The drilling results which shows a success rate of 75% which is greater than the previous rate of 60% obtained by Menye et al (Prospecting for Groundwater using the Electromagnetic Method in the middle Voltaian Sedimentary Basin of the Northern Region of Ghana-A case study of Gushiegu-Karaga District, December 2005) Hence, it can be concluded that the geophysical investigations has proven to be very successful.

6.2 Recommendations

Due to the high cost of drilling, wet wells with insufficient water should not be quickly abandoned. They should be hydro-fractured to open up the small fractures to link other fractures for more water to flow into such wells to improve successful drilling results and potable water supply.

Also, due to the ambiguity or uncertainty associated with geophysical data analysis, it is recommended that the integrated approach, i.e. the combination of two or more geophysical techniques such the Vertical Electrical Sounding and other EM methods should be considered in the future to ensure a more accurate selection of potential drilling sites.

In the future, it is recommended that geophysical results from the study area should be modeled and correlated with the drilling results. This can help geologists and geophysicists working in the area to see whether their predictions are reliable or not.

REFERENCES

- Aning Acheampong Akwasi, 2000, Groundwater Prospecting in Northern Sekyere West District Using the Electromagnetic Method, 7-22
- Asseez, L. O., 1972, Rural water supply in the Basement Complex of Western State, Nigeria. *Hydro. Sci. Bull.*, 17 (1), 97-110.
- Beeson, S., and Jones, C. R. C., 1988, The combined EMT / VES Geophysical Method for siting boreholes. *Groundwater*, Vol. 26, No. 1, pp 54-63.
- Bischoff, J., 1983, Development of geophysical instrument for tropical regions, in Lourenco, J. S., and Rijo, L., Eds., Proc., Internat. Symp. Appl. Geophys. In Tropical Regions, 1982: Belem, Brazil, 276 - 302.
- Blyth, F. G. H. and Freitas, M. PL, 1974, A Geology for Engineers. 7th Ed, ELBA /Edward's Arnold. 213-226
- Challenges in Africa Hydrology and Water Resources, 1984, Proceedings of the Harare Symposium). *IAHS Publ. no. 144*.
- Dickson Adomako, 1996, The Use of EM-34 Electromagnetic Terrain Conductivity and Geoelectrical Method in Hydrogeological Investigation, 29-30
- Diagana, B., 1996, Improving Water Supply Systems in Rural West and Central Africa. <http://www.idrc.ca/books/focus/804/chap.11.html>.
- Enslin, J. F., 1943, Basins of decomposition in igneous rocks: their importance as underground water reserves and their location by the electrical resistivity method. *Trans. Geol. Soc. S. Afr.* 46, 1-12.
- Faniran, A. and Omorinbola, E. O., 1980, Evaluating the shallow groundwater reserves in Basement

- Complex areas: a case study of southwestern Niger *J. Mining. Geol* 17(1), 65-79.
- Ghana's Water Resources, Management Challenges Studies, Ministry of Works Housing, 1998.
- Halcrow Consultancy Report, 1995, Consultancy services for the Restructuring of the Water Sector, Final Report by Halcrow and Partners for Republic of Ghana, Ministry of Works and Housing.
- Isaac Nkrumah, 2000, The Exploration of Groundwater in the Western Part of Tolu Kumbungu District Using Electromagnetic (EM) and Resistivity Methods, 18-36
- J. R. T., Cratchley, C. R. and Preston, A. M., 1980, The location of aquifers in crystalline rocks and alluvium in Northern Nigeria using combined EM and resistivity techniques. *Quarter. J. En gin. Geol. London.* 21, 159-175
- International Reference Centre for Community Water Supply and Sanitation. 1981, Technical paper 18. *WHO Collaborating Centre.*
- John, T., 1998, A civil action in EOS, Transactions, A. G. U., March 1999, Vol. 80, No. 13. p. 143.
- Keary, P. and Brooks, M., 1987, An Introduction Geophysical Exploration, *Blackwell Scientific Publication.* 1-9, 171-245
- Kofi Ampong, 2000, Groundwater Prospecting in Southern Sekyere West District using the Electromagnetic Method, 36-37, 93
- G. O., 1985, The Mineral and Rock Resources of Ghana. *A. A. Balkema, Rotterdam.*
- Kwamena, B. D. and Benneh, G., 1980, A Geography of Ghana. *Longmans Group Ltd., London.*

- Laszlo, R. D., 1983, Groundwater in Civil Engineering. *Elsevier Scientific Publ. Co. New York.*
- McNeill, J. D., 1980, Electrical Conductivity Soils and Rocks. *Geonics Limited. Technical Note TN-5.*
- McNeill, J. D. 1980, Electromagnetic Terrain Conductivity of Measurements at Low Induction Numbers. *Geonics Ltd. Technical Note TN-6.*
- McNeill, J. D. and Snelgrove, F. B., 1995, Electromagnetic Geophysical Methods Applied to Groundwater Exploration and Evaluation. *Geonics Limited.*
- Mensah, K., 1999, Water Law Water Right and Water Supply (Africa), GHANA - study country report.
- Micheal, A. M. and Khepar, S. D., 1999, Water well and Pump Engineering. *McGraw-Hill Publ. Co. Ltd. New Delhi.*
- Montgomery, C. W., 1993, Fundamentals Geology. *2nd Ed. Wm. C. Brown Publ. pp. 214-225 Dubuque.*
- Okrah Collins, 2007, Geological Investigation for Groundwater in the Middle Precambrian Basement of Upper Denkyira, *174*
- Omorinbola, E. O., 1980, Verification of some geohydrological implications of deep Weathering in the Base Complex of Nigeria... *Hydro. 56 (2) 347-368.*
- Omorinbola, E. O., 1983a, Deep weathering of interfluves in the Basement Complex of Southwestern Nigeria: its geomorphologic and geohydrological implications. *Trans. Inst. Brit. Geogr (New Series) S (3), 342-360*
- Palacky, G.J., Ritsema L L. and De Jong S. J., 1981, Electromagnetic prospecting for Groundwater in Precambrian terrain in the Republic of Upper Volta. *Geophysical*

Prospecting, Vol. 29, pp. 932-955.

Plummer, C. C. and McGear, D., 1991, *Physical Geology. 5th Ed. Wm. C. Brown Publ. pp. 233-*

252. Dubuque

Rakodi, C, 1996, *The Opinion of Health and Water Service Users in Ghana. The Role of Government in Adjusting Economics, Paper 10, Development Administration Group Policy, School of Public Policy, University of Birmingham.*

Ruddock, E. C., 1967, *Residual soils of the Kumasi district in Ghana. Geotech. 17, 359- 377.*

Santosh, K. G., 1996, *Water Supply Engineering. Khanna Publishers Delhi. .*

Sharma, P. V., 1986, *Geophysical methods in Geology. 2nd Ed. Elsevier Science Pub I. Co. Inc. 301.*

Sikes, H. L., 1934, *The underground Water Resources of Kenya Colony. Crown Agents for the Colonies, Westminster, London. ;*

Telford, W. M., Gerdart L. P., and Sheriff, R. E., 1990, *Applied Geophysics. 2nd Ed. Cambridge University Press.*

Tod, J., 1987, *Bore Site in Kano Slate. Wardrop Engineering Inc. Report to Kano State Agricultural and Rural Development Authority (unpublished).*

Verma, O. P., 1972, *Electromagnetic model experiments simulating conditions encountered in geophysical prospecting: Ph. D. thesis, Univ. of Roorkee, India.*

Verma, O. P., 1983, *Some laboratory electromagnetic studies over resistive bodies in a conductive environment: Revista Brasileira de Gcofisica, 1, 61-66.*

Wilson, E. M., 1993, *Engineering Hydrology. Macmillan, London.*

APPENDIX A

(Telford, 1990)

APPENDIX A

ELEMENTARY ELECTROMAGNETIC (EM) THEORY

The propagation and attenuation of electromagnetic (EM) waves can be understood by using Maxwell's Equations in a form relating the electric and magnetic field vectors:

$$\nabla \times \mathbf{E} = -\frac{\partial \mathbf{B}}{\partial t} \quad \dots\dots\dots \text{A1}$$

$$\nabla \times \mathbf{H} = \mathbf{J} + \frac{\partial \mathbf{D}}{\partial t} \quad \dots\dots\dots \text{A2}$$

where \mathbf{E} is the electric field intensity (Vm^{-1}), \mathbf{B} is the magnetic flux density (T), \mathbf{H} is the magnetic field intensity (Am^{-1}), \mathbf{J} is the electric current density (Am^{-2}), and \mathbf{D} is the electric displacement (Cm^{-2}). Equation A1 expresses Faraday's law: an electric field exists in the region of a time-varying magnetic field, such that the induced emf is proportional to the negative rate of change of magnetic flux. Equation A2 expresses Ampere's law: a magnetic field is generated in space by current flow and the field is proportional to the total current (sum of conduction and the displacement currents) in the region.

Using the vector identity $\nabla \cdot \nabla \times \mathbf{A} = 0$, Equation A1 can be rewritten as

$$\nabla \cdot \nabla \times \mathbf{E} = -\nabla \cdot \frac{\partial \mathbf{B}}{\partial t} = -\frac{\partial}{\partial t} (\nabla \cdot \mathbf{B}) = 0$$

$$\therefore \nabla \cdot \mathbf{B} = 0 \quad \dots\dots\dots \text{A3}$$

Similarly, Equation A2 can be rewritten as

$$\nabla \cdot \nabla \times \mathbf{H} = \nabla \cdot \left(\mathbf{J} + \frac{\partial \mathbf{D}}{\partial t} \right) = \nabla \cdot \mathbf{J} + \nabla \cdot \frac{\partial \mathbf{D}}{\partial t} = 0$$

$$\Rightarrow \nabla \cdot \nabla \times \mathbf{H} = \nabla \cdot \mathbf{J} + \frac{\partial}{\partial t} (\nabla \cdot \mathbf{D}) = 0$$

$$\therefore \nabla \cdot \mathbf{J} = -\frac{\partial}{\partial t} (\nabla \cdot \mathbf{D}) \quad \dots\dots\dots \text{A4}$$

But the divergence of current density is equivalent to the rate of accumulation of charge density i.e. $\nabla \cdot \mathbf{J} = -\frac{\partial q}{\partial t}$. Substituting this in Equation A4, we have

$$\nabla \cdot \mathbf{J} = -\frac{\partial q}{\partial t} = -\frac{\partial}{\partial t} (\nabla \cdot \mathbf{D}).$$

$$\therefore \nabla \cdot \mathbf{D} = q \quad \dots\dots\dots \text{A5}$$

In homogeneous isotropic media, we can express the physical quantities relating the electric and magnetic field vectors as

$$\mathbf{B} = \mu \mathbf{H}; \quad \mathbf{D} = \epsilon \mathbf{E}; \quad \mathbf{J} = \sigma \mathbf{E} \quad \dots\dots\dots \text{A6}$$

where μ , ϵ and σ are respectively magnetic permeability, dielectric permittivity and electric conductivity.

In regions of finite conductivity, charge does not accumulate to any extent during current flow, hence $q = 0$ so that

$$\nabla \cdot \mathbf{J} = 0 \text{ and } \nabla \cdot \mathbf{D} = \epsilon \nabla \cdot \mathbf{E} = 0 \quad \dots\dots\dots \text{A7}$$

Using Equation A6, we can rewrite Equations A1 and A2 respectively as

$$\nabla \times \mathbf{E} = -\mu \frac{\partial \mathbf{H}}{\partial t} \quad \dots\dots\dots \text{A8}$$

$$\nabla \times \mathbf{H} = \sigma \mathbf{E} + \varepsilon \frac{\partial \mathbf{E}}{\partial t} \quad \dots\dots\dots \text{A9}$$

Using the vector identity $\nabla \times (\nabla \times \mathbf{A}) = \nabla(\nabla \cdot \mathbf{A}) - \nabla^2 \mathbf{A}$ and taking the curl of

Equation A8, we have $\nabla \times (\nabla \times \mathbf{E}) = \nabla(\nabla \cdot \mathbf{E}) - \nabla^2 \mathbf{E}$

$$\Rightarrow \nabla \times \left(-\mu \frac{\partial \mathbf{H}}{\partial t} \right) = \nabla(\nabla \cdot \mathbf{E}) - \nabla^2 \mathbf{E}$$

$$\Rightarrow -\nabla^2 \mathbf{E} = \nabla(\nabla \cdot \mathbf{E}) - \nabla \times \left(\mu \frac{\partial \mathbf{H}}{\partial t} \right)$$

But from Equation A7 $\nabla \cdot \mathbf{E} = 0$, $\Rightarrow \nabla^2 \mathbf{E} = \mu \frac{\partial}{\partial t} (\nabla \times \mathbf{H})$. Also, from

$$\text{Equation A9, } \nabla \times \mathbf{H} = \sigma \mathbf{E} + \varepsilon \frac{\partial \mathbf{E}}{\partial t} \quad \Rightarrow \nabla^2 \mathbf{E} = \mu \frac{\partial}{\partial t} \left(\sigma \mathbf{E} + \varepsilon \frac{\partial \mathbf{E}}{\partial t} \right)$$

$$\therefore \nabla^2 \mathbf{E} = \mu \sigma \frac{\partial \mathbf{E}}{\partial t} + \mu \varepsilon \frac{\partial^2 \mathbf{E}}{\partial t^2} \quad \dots\dots\dots \text{A10}$$

Similarly, taking the curl of Equation A9 and using the vector identity we have

$\nabla \times (\nabla \times \mathbf{H}) = \nabla(\nabla \cdot \mathbf{H}) - \nabla^2 \mathbf{H}$. But it follows from Equations A3 and A6 that

$$\nabla \cdot \mathbf{H} = \frac{1}{\mu} \nabla \cdot \mathbf{B} = 0 \quad \Rightarrow \nabla^2 \mathbf{H} = -\nabla \times (\nabla \times \mathbf{H}). \text{ Substituting for } \nabla \times \mathbf{H}$$

$$\text{from A9, we have } \nabla^2 \mathbf{H} = -\nabla \times \left(\sigma \mathbf{E} + \varepsilon \frac{\partial \mathbf{E}}{\partial t} \right)$$

$$\Rightarrow \nabla^2 \mathbf{H} = -\sigma(\nabla \times \mathbf{E}) - \varepsilon \frac{\partial}{\partial t}(\nabla \times \mathbf{E})$$

Also, substituting for $\nabla \times \mathbf{E}$ from Equation A1, we have

$$\nabla^2 \mathbf{H} = \sigma \frac{\partial \mathbf{B}}{\partial t} + \varepsilon \frac{\partial^2 \mathbf{B}}{\partial t^2}. \text{ But } \mathbf{B} = \mu \mathbf{H}$$

$$\therefore \nabla^2 \mathbf{H} = \mu \sigma \frac{\partial \mathbf{H}}{\partial t} + \mu \varepsilon \frac{\partial^2 \mathbf{H}}{\partial t^2} \dots\dots\dots \text{A11}$$

Assuming sinusoidal time variations for \mathbf{E} and \mathbf{H} of the forms $\mathbf{E}(t) = \mathbf{E}_0 e^{i\omega t}$

and $\mathbf{H}(t) = \mathbf{H}_0 e^{i\omega t}$, we have the following expressions:

$$\frac{\partial \mathbf{E}}{\partial t} = i\omega \mathbf{E}_0 e^{i\omega t} = i\omega \mathbf{E}$$

$$\Rightarrow \frac{\partial^2 \mathbf{E}}{\partial t^2} = i^2 \omega^2 \mathbf{E}_0 e^{i\omega t} = i^2 \omega^2 \mathbf{E} = -\omega^2 \mathbf{E}$$

$$\frac{\partial \mathbf{H}}{\partial t} = i\omega \mathbf{H}_0 e^{i\omega t} = i\omega \mathbf{H}$$

$$\Rightarrow \frac{\partial^2 \mathbf{H}}{\partial t^2} = i^2 \omega^2 \mathbf{H}_0 e^{i\omega t} = i^2 \omega^2 \mathbf{H} = -\omega^2 \mathbf{H}, \text{ where } i^2 = -1 \text{ from}$$

Complex Numbers. Substituting these four expressions above in A10 and A11, we have

$$\nabla^2 \mathbf{E} = i\omega \mu \sigma \mathbf{E} - \varepsilon \mu \omega^2 \mathbf{E} \dots\dots\dots \text{A12}$$

$$\nabla^2 \mathbf{H} = i\omega \mu \sigma \mathbf{H} - \varepsilon \mu \omega^2 \mathbf{H} \dots\dots\dots \text{A13}$$

Equations A12 and A13 are the electromagnetic (EM) equations for propagation of electric and magnetic field vectors in an isotropic homogeneous medium having conductivity σ , permeability μ , and dielectric permittivity ϵ .

Comparison of Equations A12 and A13 show that identical relations hold for \mathbf{E} and \mathbf{H} . In air and in poorly conducting rocks (non-conducting media) the real part of the right-hand side of the equations is negligible. Therefore, we have

$$\nabla^2 \mathbf{E} = 0, \quad \nabla^2 \mathbf{H} = 0 \quad \dots\dots\dots \text{A14}$$

However, within a good conductor (conducting medium of finite conductivity) the imaginary parts of the equations are significant. Therefore, we have

$$\nabla^2 \mathbf{E} = i\omega\mu\sigma\mathbf{E}, \quad \nabla^2 \mathbf{H} = i\omega\mu\sigma\mathbf{H} \quad \dots\dots\dots \text{A15}$$

Equation A15 represents diffusion equation, which reduces to Laplace's Equation (A14) in air and in rocks of low conductivity (non-conducting rocks).

APPENDIX B

(Telford, 1990)

APPENDIX B

SOLUTION OF THE DIFFUSION EQUATIONS

The Diffusion Equations for the electric and magnetic field vectors, \mathbf{E} and \mathbf{H} , can be written respectively as:

$$\nabla^2 \mathbf{E} = \mu\sigma \frac{\partial \mathbf{E}}{\partial t} = i\omega\mu\sigma \mathbf{E} \quad \dots\dots\dots \text{B1}$$

$$\nabla^2 \mathbf{H} = \mu\sigma \frac{\partial \mathbf{H}}{\partial t} = i\omega\mu\sigma \mathbf{H} \quad \dots\dots\dots \text{B2}$$

These equations are generally difficult to solve. However, there is one important case in which a solution is readily obtained. That is the case when the wave is plane polarized.

We assume the xy-plane is the plane of polarization, so that the wave is propagating along the z-axis. Also, we assume the solution for Equation B1 of the form $H = H_y(z, t) = H_0 e^{i\omega t + mz}$ B3

Where H is the magnitude of \mathbf{H} . Then we have

$$\begin{aligned} \nabla H &= \frac{\partial H_y}{\partial z} = m H_0 e^{i\omega t + mz} \\ \Rightarrow \nabla^2 H &= \frac{\partial^2 H_y}{\partial z^2} = m^2 H_0 e^{i\omega t + mz} \\ \therefore \nabla^2 H &= m^2 H \quad \dots\dots\dots \text{B4} \end{aligned}$$

$$\text{Also } \frac{\partial H_y}{\partial t} = i\omega H_0 e^{i\omega t + mz}$$

$$\therefore \frac{\partial H_y}{\partial t} = i\omega H \quad \dots\dots\dots \text{B5}$$

Substituting for B4 and B5 in Equation B2 we have $m^2 H = i\omega\mu\sigma H$. Hence,

we can have $m^2 = i\omega\mu\sigma$

$$\Rightarrow m = \pm(1+i)\sqrt{(\omega\mu\sigma/2)}$$

$\therefore m = \pm(1+i)\alpha$, where $\alpha = \sqrt{(\omega\mu\sigma/2)}$ is the attenuation factor.

Since H must be finite when $z = +\infty$, we discard the plus sign and obtain the

$$\text{solution } H_y = H_0 e^{i\omega t - (1+i)\alpha z} = H_0 e^{-\alpha z + i(\omega t - \alpha z)}$$

$$\Rightarrow H_y = H_0 e^{-\alpha z} \left[e^{i(\omega t - \alpha z)} \right] \quad \dots\dots\dots \text{B6}$$

Applying De Moivre's Theorem to Equation B6 we have the expression

$$H_y = H_0 e^{-\alpha z} [\cos(\omega t - \alpha z) + i \sin(\omega t - \alpha z)]$$

Neglecting the imaginary part we can have the required solution as

$$H_y = H_0 e^{-\alpha z} \cos(\omega t - \alpha z) \quad \dots\dots\dots \text{B7}$$

The cosine term represents simple harmonic motion (SHM) with phase shift, αz .

The exponential term is the attenuation of the wave with propagation distance, z .

$$\text{The attenuation term may be written as } \left| H_y / H_0 \right| = e^{-\alpha z} \quad \dots\dots\dots \text{B8}$$

Penetration depth or skin depth, z_s is the distance at which the signal or amplitude of the field is reduced to $1/e$ (i.e. 37%) of its surface value. The skin depth is related to the attenuation factor as $z_s = 1/\alpha = 1/\sqrt{(\omega\mu\sigma/2)}$. Taking $\mu = \mu_0 = 4\pi \times 10^{-7}$ and $\omega = 2\pi f$, we obtain for the skin depth

$$z_s = 1/\sqrt{(2\pi f \times 4\pi \times 10^{-7} \sigma)/2}$$

$$\therefore z_s = 503.8/\sqrt{\sigma f} \text{ m} \dots\dots\dots \text{B9}$$

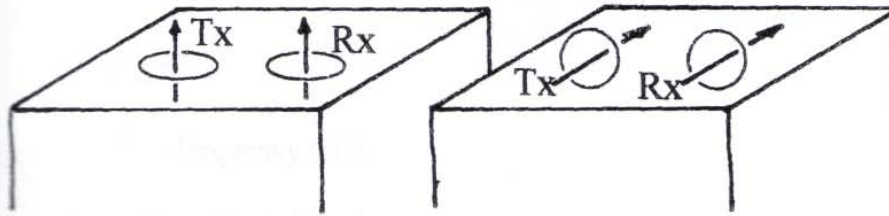
Equation B9 indicates that if the ground conductivity is high (low resistivity) or the frequency of signal is high, or both, the magnetic field will not penetrate the ground to any extent.

APPENDIX C

(McNeil, 1980)

APPENDIX C

THEORY OF OPERATION OF EM34-3 AT LOW INDUCTION NUMBERS



VERTICAL DIPOLE

HORIZONTAL DIPOLE

Fig. C1 Vertical and Horizontal Dipole coil Configurations (After McNeill, 1980)

We consider the two coil configurations as in Figure C1. In each case the measured physical quantity is the ratio of the secondary magnetic field H_s at the receiver to the primary magnetic field H_p in the absence of the homogeneous half-space.

Let the alternating current frequency of the transmitter be f Hz, the terrain conductivity of the homogeneous half-space be σ mSm⁻¹, and the spacing between the two coils be S metres. Then the field ratios for horizontal and vertical dipole configurations are respectively given as:

$$\left(\frac{H_s}{H_p}\right)_H = 2 \left\{ 1 - \frac{3}{(\gamma S)^2} + \frac{1}{(\gamma S)^2} [3 + 3\gamma S + (\gamma S)^2] e^{-\gamma S} \right\} \dots\dots\dots C1$$

$$\left(\frac{H_s}{H_p}\right)_V = \frac{2}{(\gamma s)^2} \left\{ 9 - [9 + 9\gamma s + 4(\gamma s)^2 + (\gamma s)^3] e^{-\gamma s} \right\} \dots\dots\dots C2$$

where $\gamma = \sqrt{i\omega\mu_0\sigma}$

$$\omega = 2\pi f$$

f = frequency (Hz)

μ_0 = permeability of free space

$$i = \sqrt{-1}$$

Equations C1 and C2 are complicated functions of the variable γs , which in turn a complex function of frequency and terrain conductivity. However, $e^{-\gamma s}$ is a monotonically decreasing function for all S.

Let $\gamma s = x$, so that we can rewrite Equations C1 and C2 as

$$\left(\frac{H_s}{H_p}\right)_H = 2 \left\{ 1 - \frac{3}{x^2} + \frac{1}{x^2} [3 + 3x + x^2] e^{-x} \right\} \dots\dots\dots C3$$

$$\left(\frac{H_s}{H_p}\right)_V = \frac{2}{x^2} \left\{ 9 - [9 + 9x + 4x^2 + x^3] e^{-x} \right\} \dots\dots\dots C4$$

Using Maclaurin Series expansion for $e^{-x} = 1 - x + \frac{x^2}{2} - \frac{x^3}{6} + \frac{x^4}{24} + \dots$ we

can again rewrite C3 in a form which can be expanded algebraically as

$$\begin{aligned} \left(\frac{H_s}{H_p}\right)_H &= 2 \left\{ 1 - \frac{3}{x^2} + \frac{1}{x^2} [3 + 3x + x^2] \left[1 - x + \frac{x^2}{2} - \frac{x^3}{6} + \frac{x^4}{24} \dots \right] \right\} \\ &= 2 \left(\frac{1}{2} + \frac{x^2}{8} - \frac{x^3}{24} + \frac{x^4}{24} + \dots \right) \\ \therefore \left(\frac{H_s}{H_p}\right)_H &= 1 + \frac{x^2}{4} - \frac{x^3}{12} + \frac{x^4}{12} + \dots \quad \dots\dots\dots \text{C5} \end{aligned}$$

Similarly

$$\begin{aligned} \left(\frac{H_s}{H_p}\right)_V &= \frac{2}{x^2} \left\{ 9 - [9 + 9x + 4x^2 + x^3] \left[1 - x + \frac{x^2}{2} - \frac{x^3}{6} + \frac{x^4}{24} + \dots \right] \right\} \\ &= \frac{2}{x^2} \left(\frac{x^2}{2} + \frac{x^4}{8} - \frac{5x^5}{24} - \frac{x^7}{24} + \dots \right) \\ \therefore \left(\frac{H_s}{H_p}\right)_V &= 1 + \frac{x^2}{4} - \frac{5x^3}{12} - \frac{x^5}{12} + \dots \quad \dots\dots\dots \text{C6} \end{aligned}$$

At the condition of low induction numbers (i.e. $\gamma s = x \ll 1$) the third order term and higher order terms are very small, hence negligible.

$$\therefore \left(\frac{H_s}{H_p}\right)_H = \left(\frac{H_s}{H_p}\right)_V = 1 + \frac{x^2}{4} = 1 + \frac{(\gamma s)^2}{4} \quad \dots\dots\dots \text{C7}$$

The skin depth is given by $Z_s = \sqrt{\frac{2}{\omega \mu_0 \sigma}}$

the quadrature component of the field which is measured by the equipment.

Hence, the field ratios reduce to the simple expression

$$\left(\frac{H_s}{H_p}\right)_H \cong \left(\frac{H_s}{H_p}\right)_V = \frac{i\omega\mu_0\sigma s^2}{4} \dots\dots\dots C11$$

Therefore, the ratio of the secondary magnetic field to the primary magnetic field is linearly proportional to the apparent terrain conductivity. Thus, measurements taken under the condition of low induction numbers provide an apparent terrain conductivity, σ_a , which the EM34-3 equipment reads, and it is defined by

$$\sigma_a = \frac{4}{\omega\mu_0 s^2} \left(\frac{H_s}{H_p}\right)_{\text{quadrature component}} \dots\dots\dots C12$$

APPENDIX D

SITE NAME: NAKPOLIGU

DISTRICT: GUSHIEGU-KARAGA

TRAVERSE: A

STATION INTERVAL: 10 m

Distance(m)	Apparent Conductivity (mS/m)		Remarks
	15m depth, HD mode	30m depth, VD mode	
10	21	20	
20	20	20	
30	19	17	
40	20	19	
50	20	21	
60	21	19	
70	22	15	
80	22	17	
90	24	15	
100	25	18	
110	24	20	
120	24	18	
130	23	21	
140	22	22	
150	22	22	Alternate Drill Point
160	20	19	
170	23	21	
180	24	22	
190	24	19	
200	27	21	
210	27	21	

SITE NAME: NAKPOLIGU

DISTRICT: GUSHIEGU-KARAGA

TRAVERSE: B

STATION INTERVAL: 10 m

Distance(m)	Apparent Conductivity (mS/m)		Remarks
	15m depth, HD mode	30m depth, VD mode	
10	23	17	
20	23	20	
30	22	19	
40	21	20	
50	21	20	
60	21	20	
70	23	20	
80	23	18	
90	23	20	
100	21	19	
110	22	23	Alternate Drill Point
120	23	21	
130	23	21	

SITE NAME: YIBEYILE

DISTRICT: GUSHIEGU-KARAGA

TRAVERSE: A

STATION INTERVAL: 10 m

Distance(m)	Apparent Conductivity (mS/m)		Remarks
	15m depth, HD mode	30m depth, VD mode	
10	28	22	
20	28	22	
30	28	22	
40	27	24	
50	26	23	
60	26	25	
70	26	23	

SITE NAME: YIBEYILE

DISTRICT: GUSHIEGU-KARAGA

TRAVERSE: B

STATION INTERVAL: 10 m

Distance(m)	Apparent Conductivity (mS/m)		Remarks
	15m depth, HD mode	30m depth, VD mode	
10	60	40	
20	60	37	
30	58	45	
40	57	44	
50	53	37	
60	50	36	
70	45	43	Alternate Drill point
80	42	38	
90	39	38	
100	37	35	

SITE NAME: PISHIGU

DISTRICT: GUSHIEGU-KARAGA

TRAVERSE: A

STATION INTERVAL: 10 m

Distance(m)	Apparent Conductivity (mS/m)		Remarks
	15m depth, HD mode	30m depth, VD mode	
10	18	12	
20	16	8	
30	16	5	
40	14	8	
50	13	15	
60	13	15	Drill Site
70	13	13	
80	14	8	
90	15	10	
100	15	14	
110	15	10	
120	15	11	
130	15	12	
140	15	13	
150	16	18	Potential Drill Site
160	18	14	
170	20	5	
180	22	11	
190	22	20	
200	22	17	

SITE NAME: PISHIGU

DISTRICT: GUSHIEGU-KARAGA

TRAVERSE: B

STATION INTERVAL: 10 m

Distance(m)	Apparent Conductivity (mS/m)		Remarks
	15m depth, HD mode	30m depth, VD mode	
10	24	10	
20	25	11	
30	26	18	
40	26	16	
50	24	14	
60	24	22	Drill Site
70	25	19	
80	25	13	
90	27	16	
100	23	19	
110	27	13	
120	27	18	
130	27	18	
140	26	18	
150	26	18	
160	26	16	
170	26	16	
180	26	19	
190	21	21	
200	21	24	

SITE NAME: TINDANG

DISTRICT: GUSHIEGU-KARAGA

TRAVERSE: A

STATION INTERVAL: 10 m

Distance(m)	Apparent Conductivity (mS/m)		Remarks
	15m depth, HD mode	30m depth, VD mode	
10	22	14	
20	22	13	
30	23	12	
40	25	10	
50	26	11	
60	25	12	
70	19	12	
80	15	10	
90	13	11	
100	12	17	Potential Drill Site
110	11	15	
120	10	13	

SITE NAME: TINDANG

DISTRICT: GUSHIEGU-KARAGA

TRAVERSE: B

STATION INTERVAL: 10 m

Distance(m)	Apparent Conductivity (mS/m)		Remarks
	15m depth, HD mode	30m depth, VD mode	
10	10	8	
20	10	10	
30	10	8	
40	10	10	
50	10	10	
60	10	10	
70	10	10	
80	10	11	
90	11	13	Potential Drill Site
100	11	11	
110	15	6	

SITE NAME: TINDANG

DISTRICT: GUSHIEGU-KARAGA

TRAVERSE: A

STATION INTERVAL: 10 m

Distance(m)	Apparent Conductivity (mS/m)		Remarks
	15m depth, HD mode	30m depth, VD mode	
10	22	14	
20	22	13	
30	23	12	
40	25	10	
50	26	11	
60	25	12	
70	19	12	
80	15	10	
90	13	11	
100	12	17	
110	11	15	
120	10	13	

SITE NAME: TINDANG

DISTRICT: GUSHIEGU-KARAGA

TRAVERSE: B

STATION INTERVAL: 10 m

Distance(m)	Apparent Conductivity (mS/m)		Remarks
	15m depth, HD mode	30m depth, VD mode	
10	10	8	
20	10	10	
30	10	8	
40	10	10	
50	10	10	
60	10	10	
70	10	10	
80	10	11	
90	11	13	
100	11	11	
110	15	6	

SITE NAME: ZULOGU

DISTRICT: GUSHIEGU-KARAGA

TRAVERSE: A

STATION INTERVAL: 10 m

Column1	Apparent Conductivity (mS/m)	Column2	Column3
Distance(m)	15m depth, HD mode	30m depth, VD mode	Remarks
10	16	13	Potential Drill Site
20	15	16	
30	14	14	
40	14	14	
50	14	12	
60	14	11	
70	13	12	
80	13	13	
90	12	11	
100	12	13	
110	11	13	
120	11	13	
130	11	13	
140	11	13	
150	11	11	
160	11	12	
170	11	12	
180	11	13	
190	10	13	
200	10	13	

SITE NAME: ZULOGU

DISTRICT: GUSHIEGU-KARAGA

TRAVERSE: B

STATION INTERVAL: 10 m

Column1	Apparent Conductivity (mS/m)		Column2	Column3
	Distance(m)	15m depth, HD mode		
10	45	42		
20	46	43		
30	44	45	Potential Drill Point	
40	44	42		
50	43	41		
60	42	42		
70	42	40		
80	42	42		
90	42	42		
100	43	41		
110	43	42		
120	42	40		

SITE NAME: GORGU

DISTRICT: GUSHIEGU-KARAGA

TRAVERSE: A

STATION INTERVAL: 10 m

Distance(m)	Apparent Conductivity (mS/m)		Remarks
	15m depth, HD mode	30m depth, VD mode	
10	22	20	
20	22	20	
30	21	21	
40	22	20	
50	22	18	
60	23	17	
70	23	18	
80	22	21	
90	21	21	Potential Drill Point
100	23	20	

SITE NAME: GORGU

DISTRICT: GUSHIEGU-KARAGA

TRAVERSE: B

STATION INTERVAL: 10 m

Distance(m)	Apparent Conductivity (mS/m)		Remarks
	15m depth, HD mode	30m depth, VD mode	
10	15	13	
20	15	14	
30	15	16	Potential Drill point
40	15	14	
50	20	11	
60	20	14	

SITE NAME: NANDULI

DISTRICT: GUSHIEGU-KARAGA

TRAVERSE: A

STATION INTERVAL: 10 m

Distance(m)	Apparent Conductivity (mS/m)		Remarks
	15m depth, HD mode	30m depth, VD mode	
10	32	30	
20	32	29	
30	33	34	
40	35	38	Alternate Drill Point
50	39	33	
60	43	26	
70	43	28	
80	43	25	
90	43	30	
100	37	35	
110	33	40	Drill Point
120	34	32	
130	35	34	
140	36	30	
150	38	28	

SITE NAME: NAKPALE

DISTRICT: ZABZUGU-TATALE

TRAVERSE: A

STATION INTERVAL: 10 m

BEARING: 328°

Distance(m)	Apparent Conductivity (mS/m)		Remarks
	15m depth, HD mode	30m depth, VD mode	
10	19	14	
20	18	18	
30	18	22	Drill Site
40	19	23	
50	20	17	
60	22	17	
70	21	16	
80	24	20	
90	23	19	
100	21	21	
110	21	20	

SITE NAME: NAKPALE

DISTRICT: ZABZUGU-TATALE

TRAVERSE: B

STATION INTERVAL: 10 m

BEARING: 333°

Distance(m)	Apparent Conductivity (mS/m)		Remarks
	15m depth, HD mode	30m depth, VD mode	
10	18	16	
20	17	18	
30	18	17	Potential Drill Site
40	19	17	
50	20	15	
60	20	18	
70	22	17	
80	22	21	
90	22	23	Potential Drill Site
100	23	17	
110	23	20	
120	23	20	

SITE NAME: NAKPALE

DISTRICT: ZABZUGU-TATALE

TRAVERSE: C

STATION INTERVAL: 10 m

BEARING: 075°

	Apparent Conductivity (mS/m)		
Distance(m)	15m depth, HD mode	30m depth, VD mode	Remarks
10	23	22	
20	26	35	
30	22	18	
40	22	17	
50	23	20	
60	21	19	
70	21	16	
80	20	15	
90	22	20	
100	21	19	
110	20	20	Drill Site
120	19	15	
130	18	12	
140	19	17	
150	18	16	
160	17	15	
170	18	14	

SITE NAME: BENCHARIGNADOM

DISTRICT: ZABZUGU-TATALE

TRAVERSE: A

STATION INTERVAL: 10 m

BEARING: 170°

Distance(m)	Apparent Conductivity (mS/m)		Remarks
	15m depth, HD mode	30m depth, VD mode	
10	32	33	
20	33	35	Potential Drill Site
30	33	32	
40	35	32	
50	36	31	
60	37	31	
70	39	29	
80	38	33	
90	39	34	
100	38	32	
110	38	37	
120	40	36	
130	39	38	
140	39	32	
150	38	33	
160	37	41	
170	37	41	Potential Drill Site
180	38	40	
190	40	40	
200	38	38	

SITE NAME: BENCHARIGNADOM

DISTRICT: ZABZUGU-TATALE

TRAVERSE: B

STATION INTERVAL: 10 m

BEARING: 15°

Distance(m)	Apparent Conductivity (mS/m)		Remarks
	15m depth, HD mode	30m depth, VD mode	
10	39	41	
20	40	44	Potential Drill Site
30	41	41	
40	41	43	
50	43	47	
60	43	38	
70	39	44	
80	38	37	
90	38	36	

SITE NAME: JATODOR

DISTRICT: ZABZUGU-TATALE

TRAVERSE: A

STATION INTERVAL: 10 m

BEARING: 278°

Distance(m)	Apparent Conductivity (mS/m)		Remarks
	15m depth, HD mode	30m depth, VD mode	
10	4	1	
20	5	5	
30	4	6	
40	5	7	Potential Drill Site
50	7	4	
60	10	3	
70	11	8	
80	10	8	
90	8	2	
100	7	4	
110	6	5	
120	4	4	
130	3	2	
140	3	1	

SITE NAME: JATODOR

DISTRICT: ZABZUGU-TATALE

TRAVERSE: B

STATION INTERVAL: 10 m

BEARING: 278°

Column1	Apparent Conductivity (mS/m)		
Distance(m)	15m depth, HD mode	30m depth, VD mode	Remarks
10	6	4	
20	7	5	
30	5	3	
40	4	2	
50	4	3	
60	4	4	
70	5	3	
80	5	4	
90	7	3	
100	7	6	
110	8	8	Drill Site
120	10	5	
130	13	4	
140	13	6	
150	12	7	
160	10	6	
170	8	6	
180	6	4	
190	5	2	
200	4	2	

SITE NAME: JATODOR

DISTRICT: ZABZUGU-TATALE

TRAVERSE: C

STATION INTERVAL: 10 m

BEARING: 275°

Column1	Apparent Conductivity (mS/m)	Column2	Column3
Distance(m)	15m depth, HD mode	30m depth, VD mode	Remarks
10	7	4	
20	7	4	
30	7	7	
40	8	7	
50	8	7	
60	10	5	
70	12	6	
80	15	8	
90	15	6	
100	15	8	
110	13	8	
120	10	7	
130	8	7	
140	6	8	Potential Drill Site
150	5	4	
160	5	2	
170	4	2	
180	4	2	
190	4	2	

SITE NAME: JATODOR

DISTRICT: ZABZUGU-TATALE

TRAVERSE: D

STATION INTERVAL: 10 m

BEARING: 145°

Distance(m)	Apparent Conductivity (mS/m)		Remarks
	15m depth, HD mode	30m depth, VD mode	
10	12	8	
20	13	10	
30	15	10	
40	15	12	
50	15	11	
60	13	7	
70	12	12	
80	12	14	Potential Drill point
90	11	11	
100	12	10	
110	12	11	
120	12	11	
130	13	14	Potential Drill point
140	12	10	
150	10	12	

SITE NAME: BENATABE EAST

DISTRICT: ZABZUGU-TATALE

TRAVERSE: A

STATION INTERVAL: 10 m

BEARING: 144°

Distance(m)	Apparent Conductivity (mS/m)		Remarks
	15m depth, HD mode	30m depth, VD mode	
10	27	21	
20	27	21	
30	28	17	
40	28	16	
50	28	17	
60	27	18	
70	27	19	
80	24	22	
90	25	22	
100	18	26	Potential Drill point
110	23	18	
120	22	19	
130	23	20	
140	23	20	

SITE NAME: BENATABE EAST

DISTRICT: ZABZUGU-TATALE

TRAVERSE: B

STATION INTERVAL: 10 m

BEARING: 137°

	Apparent Conductivity (mS/m)		
Distance(m)	15m depth, HD mode	30m depth, VD mode	Remarks
10	20	17	
20	22	9	
30	23	18	
40	23	20	
50	23	16	
60	23	16	
70	23	15	
80	23	13	
90	23	20	
100	24	27	Drill Site
110	26	16	
120	28	9	

SITE NAME: GOR KUKANI

DISTRICT: ZABZUGU-TATALE

TRAVERSE: A

STATION INTERVAL: 10 m

BEARING: 184°

Distance(m)	Apparent Conductivity (mS/m)		Remarks
	15m depth, HD mode	30m depth, VD mode	
10	17	14	
20	16	15	
30	16	14	
40	15	14	
50	15	14	
60	14	13	
70	14	13	
80	14	13	
90	14	13	
100	13	13	
110	13	14	Drill point
120	15	13	
130	15	15	
140	16	15	
150	16	13	
160	16	14	
170	23	15	

SITE NAME: GOR KUKANI

DISTRICT: ZABZUGU-TATALE

TRAVERSE: B

STATION INTERVAL: 10 m

BEARING: 084°

Distance(m)	Apparent Conductivity (mS/m)		Remarks
	15m depth, HD mode	30m depth, VD mode	
10	22	12	
20	18	16	
30	17	16	
40	14	19	Anomalous point
50	13	17	Anomalous point
60	13	16	Anomalous point
70	15	14	
80	15	14	

SITE NAME: BATIGMADO

DISTRICT: ZABZUGU-TATALE

TRAVERSE: A

STATION INTERVAL: 10 m

BEARING: 225°

Distance(m)	Apparent Conductivity (mS/m)		Remarks
	15m depth, HD mode	30m depth, VD mode	
10	28	24	
20	28	25	
30	28	23	
40	29	22	
50	27	22	
60	27	22	
70	25	22	
80	24	25	Potential Drill point
90	22	24	
100	22	22	
110	22	24	Potential Drill point
120	22	22	
130	22	22	
140	24	22	
150	26	20	
160	29	19	
170	29	21	

SITE NAME: BATIGMADO

DISTRICT: ZABZUGU-TATALE

TRAVERSE: B

STATION INTERVAL: 10 m

BEARING: 225°

Distance(m)	Apparent Conductivity (mS/m)		Remarks
	15m depth, HD mode	30m depth, VD mode	
10	28	26	
20	29	26	
30	31	27	
40	31	22	
50	30	22	
60	29	24	
70	25	26	Potential Drill point
80	24	26	Potential Drill point
90	22	22	
100	22	21	
110	23	21	
120	23	18	
130	24	19	

SITE NAME: BATIGMADO

DISTRICT: ZABZUGU-TATALE

TRAVERSE: B

STATION INTERVAL: 10 m

BEARING: 225

Distance(m)	Apparent Conductivity (mS/m)		Remarks
	15m depth, HD mode	30m depth, VD mode	
10	26	24	
20	24	29	
30	22	26	
40	22	22	
50	23	23	
60	23	25	
70	22	22	
80	24	22	
90	23	20	

SITE NAME: BIKPANIJIB

DISTRICT: ZABZUGU-TATALE

TRAVERSE: A

STATION INTERVAL: 10 m

BEARING: 171°

Distance(m)	Apparent Conductivity (mS/m)		Remarks
	15m depth, HD mode	30m depth, VD mode	
10	26	26	
20	28	27	
30	28	27	
40	28	29	
50	27	33	Potential Drill point
60	28	28	
70	30	21	
80	32	23	
90	33	28	
100	31	23	
110	28	25	
120	28	27	
130	27	26	
140	26	27	
150	25	29	Potential Drill point
160	25	25	
170	27	22	
180	28	22	
190	28	21	
200	29	22	

SITE NAME: BIKPANIJIB

DISTRICT: ZABZUGU-TATALE

TRAVERSE: B

STATION INTERVAL: 10 m

BEARING: 263°

Distance(m)	Apparent Conductivity (mS/m)		Remarks
	15m depth, HD mode	30m depth, VD mode	
10	25	12	
20	21	16	
30	20	21	Potential Drill Point
40	19	19	
50	20	15	
60	21	13	
70	20	16	
80	21	12	
90	21	14	
100	19	21	Potential Drill Point
110	19	21	
120	20	18	

SITE NAME: BIKPANIJIB

DISTRICT: ZABZUGU-TATALE

TRAVERSE: C

STATION INTERVAL: 10 m

BEARING: 260°

Distance(m)	Apparent Conductivity (mS/m)		Remarks
	15m depth, HD mode	30m depth, VD mode	
10	17	10	
20	16	9	
30	16	8	
40	16	11	
50	16	12	
60	15	11	
70	15	11	
80	17	14	

SITE NAME: BIKPANIJIB

DISTRICT: ZABZUGU-TATALE

TRAVERSE: D

STATION INTERVAL: 10 m

BEARING: 222°

Distance(m)	Apparent Conductivity (mS/m)		Remarks
	15m depth, HD mode	30m depth, VD mode	
10	32	27	
20	30	24	
30	28	23	
40	28	27	
50	28	29	
60	27	29	
70	28	29	
80	29	26	
90	31	24	
100	32	21	
110	28	22	
120	27	24	
130	23	22	
140	22	16	
150	18	8	

